CHAPTER IV

RESULTS

In vitro Evaluation of Mucoadehesive Films

1. Physical characteristics of the mucoadhesive films

The characteristics of mucoadhesive films prepared from casting solution technique were transparent, glossy, flexible, sticky, and easy to peel off from the glass petri dish. The physical appearances of the mucoadhesive films are shown in Table 8 and Figures 26 and 27.

CMC films of various ratios of polymer and drug were not transparent and some precipitated as shown in Figure 26. Increasing the drug content increased the precipitates. Therefore, they were not further investigated. All HPMC E15 and HPMC E4M films were colorless, transparent. easy to peel off from glass petri dish and were not sticky. But HPMC E15 films were more flexible and easier to peel off than HPMC E4M films. HPC-H films were also transparent and glossy. They were highly sticky and difficult to peel off from petri dish. Chitosan films were yellow color. They were translucent and difficult to peel off from petri dish. The films that prepared from the combination of HPMC E15 and HPC-H were flexible and easy to peel off from glass petri dish.

2. Film thickness

The results from the thickness measurement are presented in Appendix C. The average thickness of the prepared mucoadhesive films is given in Table 9. The thickness of the films from Formulas E15 1:1, E4M 1:1 and HPC 1:1 was about 120 μm. The thickness of the films from Formulas E15HPC 1:3, 2:3, 3:3, 3:2 and 3:1 was about 130 μm. The thickness of the films from Formulas E15 1:0.67, E4M 1:0.67 and HPC 1:0.67 was about 110 μm. The thickness of the films from Formulas E15 1:0.5, E4M 1:0.5 and HPC 1:0.5 was about 100 μm. And that from Formulas CS 1:1, CS 1:0.67 and CS 1:0.5 was about 253 μm, 209 μm and 197 μm respectively.

Table 8 Physical characteristics of mucoadhesive films

Formulas	Transparency	Glossiness	Flexibility	Stickiness	Ease of peeling
CMC 1:1	-	-	-	-	+++
CMC 1:0.67	-	-	-	-	+++
CMC 1:0.5	-	-	-	-	++
CMC 0.5:1	-	-	-	-	++
E15 1:1	+++	++	++	-	+++
E15 1:0.67	+++	++	++	-	+++
E15 1:0.5	+++	++	++	-	+++
E4M 1:1	+++	++	+	-	+++
E4M 1:0.67	+++	++	+	-	++
E4M 1:0.5	+++	++	+	-	++
E4M 2:1	+++	++	+	-	++
HPC 1:1	+++	+++	+++	+++	+
HPC 1:0.67	+++	+++	+++	+++	+
HPC 1:0.5	+++	+++	+++	+++	-
CS 1:1	-	+	+	-	+
CS 1:0.67	--	-	+	-	+
CS 1:0.5	---	--	+	-	+
E15HPC 1:3	++	++	++	+	+++
E15HPC 2:3	+++	+	++	+	+++
E15HPC 3:3	+++	+	++	-	+++
E15HPC 3:2	++	-	+	-	+++
E15HPC 3:1	++	-	+	-	+++

The symbols of (+) and (-) showed the appearance and no appearance, respectively.

The number of the symbol of (+) showed a degree of the appearance.

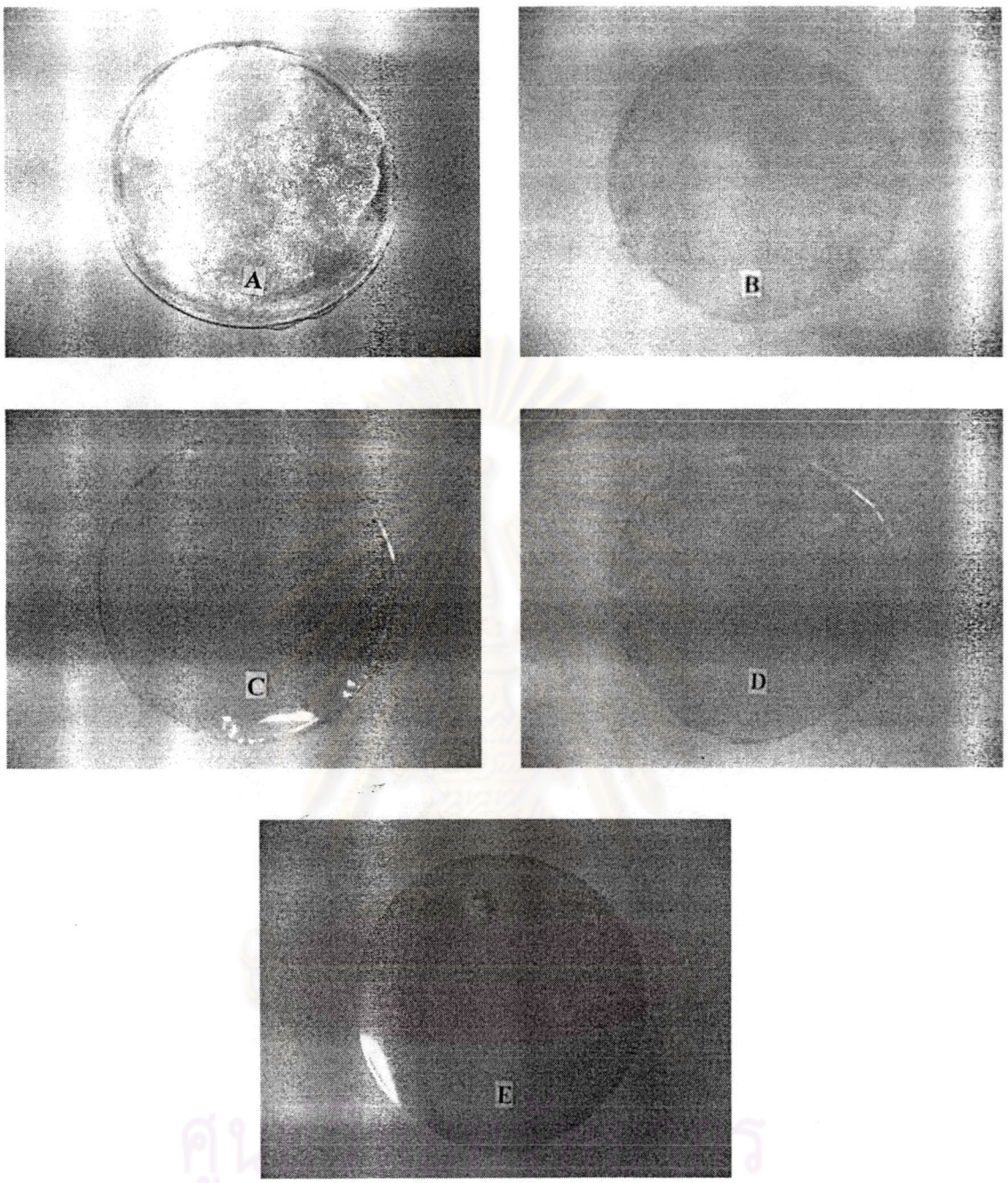

Figure 26 The photographs of the mucoadhesive films: (A) CMC 1:1; (B) E15 1:1; (C) E4M 1:1; (D) HPC 1:1; (E) CS 1:1

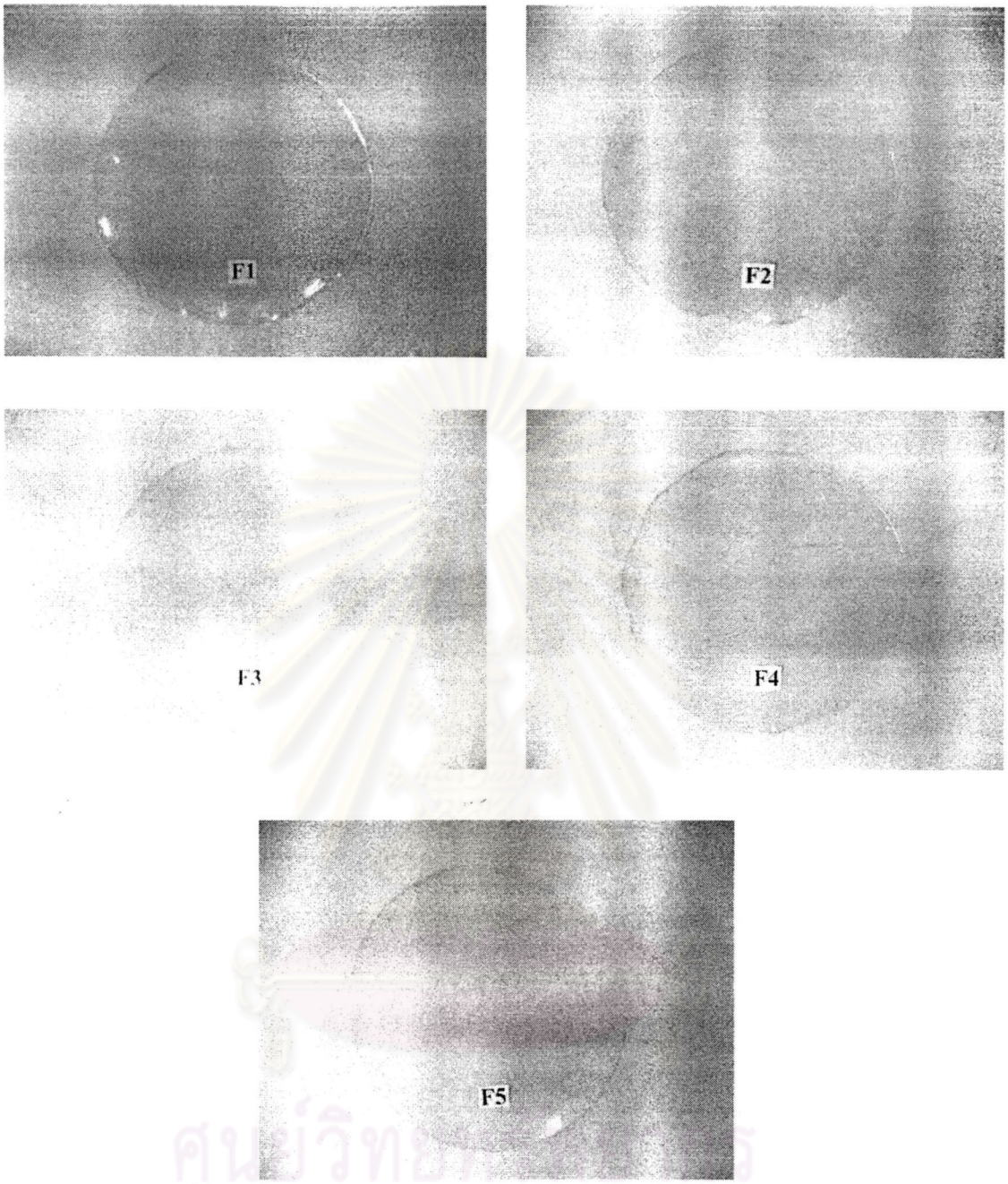

Figure 27 The photographs of the mucoadhesive films: (F1) E15HPC 1:3; (F2) E15HPC 2:3; (F3) E15HPC 3:3; (F4) E15HPC 3:2; (F5) E15HPC 3:1

Table 9 The average thickness of the prepared mucoadhesive films (n=3 each sample was measured at 5 locations)

Formulas	Thickness ± SD (μm)			
	No.1	No. 2	No.3	Mean ± SD
E15 1:1	121.8 ± 6.7	122.0 ± 3.1	121 ± 4.3	121.6 ± 0.5
E15 1:0.67	115.4 ± 4.6	116.4 ± 7.4	110.2 ± 6.9	114.0 ± 3.3
E15 1:0.5	98.8 ± 4.0	106.6 ± 7.1	98.4 ± 6.5	101.3 ± 4.6
E4M 1:1	121.2 ± 3.4	119.0 ± 4.1	121.4 ± 7.6	120.5 ± 1.3
E4M 1:0.67	112.6 ± 5.3	111.2 ± 6.9	109.8 ± 5.9	111.2 ± 1.4
E4M 1:0.5	100.4 ± 3.0	102.0 ± 5.2	104.8 ± 5.3	102.4 ± 2.2
E4M 2:1	204.6 ± 8.3	202.6 ± 7.5	206.0 ± 7.4	204.4 ± 1.7
HPC 1:1	119.8 ± 5.5	121.2 ± 4.3	122.0 ± 5.3	121.0 ± 1.1
HPC 1:0.67	112.8 ± 4.1	111.4 ± 4.1	110.6 ± 4.6	111.6 ± 1.1
HPC 1:0.5	100.4 ± 2.6	99.0 ± 3.2	98.8 ± 1.6	99.4 ± 0.9
CS 1:1	255.4 ± 6.5	251.8 ± 7.2	252.8 ± 6.5	253.3 ± 1.9
CS 1:0.67	208.2 ± 6.9	210.6 ± 7.6	208.8 ± 8.1	209.2 ± 1.2
CS 1:0.5	194.6 ± 8.6	197.6 ± 7.1	198.6 ± 8.3	196.9 ± 2.1
E15HPC 1:3	130.6 ± 3.6	129.8 ± 3.0	131.0 ± 3.4	130.5 ± 0.6
E15HPC 2:3	127.6 ± 4.0	129.4 ± 4.2	127.6 ± 4.8	128.2 ± 1.0
E15HPC 3:3	130.4 ± 4.2	131.2 ± 2.9	132.4 ± 5.8	131.3 ± 1.0
E15HPC 3:2	129.6 ± 4.6	128.0 ± 4.6	128.8 ± 4.8	128.8 ± 0.8
E15HPC 3:1	128.8 ± 4.4	129.4 ± 5.7	126.4 ± 4.4	128.2 ± 1.6

3. Content uniformity

The results of content uniformity are presented in Appendix C. It was seen in Table 10 that the concentration of all test films was within the limit as 95-105% label amount with low %CV.

Table 10 The average of the percent content of lidocaine HCl in the prepared mucoadhesive films

Formula	%Content	%CV
E15 1:1	99.74	2.03
E15 1:0.67	102.24	2.14
E15 1:0.5	98.03	1.62
E4M 1:1	98.82	1.98
E4M 1:0.67	100.12	1.57
E4M 1:0.5	98.51	2.37
E4M 2:1	101.12	2.95
HPC 1:1	98.96	2.75
HPC 1:0.67	98.70	1.83
HPC 1:0.5	101.19	2.46
CS 1:1	99.03	2.62
CS 1:0.67	102.31	1.52
CS 1:0.5	101.40	1.99
E15HPC 1:3	101.96	2.29
E15HPC 2:3	98.67	1.98
E15HPC 3:3	101.89	2.48
E15HPC 3:2	100.89	2.11
E15HPC 3:1	101.13	2.09

4. Surface topography

Scanning electron photomicrographs showing the surface topography of HPMC E15 mucoadhesive films as seen in Figure 28. The smooth surface without any pore in HPMC E15 free film is depicted in Figure 28A. The photomicrographs of surface of HPMC E15 films containing lidocaine HCl and additives of drug to polymer of 1:1 and 1:0.67 exhibited the smooth surface and homogeneous films. The photomicrographs of cross-sectional area of HPMC E15 films, drug to polymer ratio of 1:1 and 1:0.67 exhibited dense, smooth and homogeneous texture. Texture of HPMC E15 film which drug to polymer ratio was 1:0.5 revealed that the film had aggregation of particles, rough surface and some cracks.

The surface topography of HPMC E4M mucoadhesive films shown in scanning electron photomicrographs as depicted in Figure 29. Rather smooth surface without any pore of HPMC E4M free film is shown in Figure 29A. The photomicrographs of HPMC E4M films containing lidocaine HCl and additives with various drug and polymer ratio are depicted in Figures 29B, 29C and 29D. They exhibited smooth and homogeneous surface without any pore. Some cracks could be seen. Increasing the amount of drug markedly increased the particle aggregation.

Figure 30 displays the scanning electron photomicrographs showing the surface topography of HPC mucoadhesive films. Rather smooth surface without any pore of HPC free film as shown in Figure 30A. Scanning electron photomicrographs of HPC film containing the drug and additives are depicted in Figures 30B, 30C and 30D. They were smooth and had many small void spaces within cross-section area of film. The surface photomicrographs of mucoadhesive films prepared from various drug to polymer ratios did not show any differences.

Scanning electron photomicrographs showing the surface topography of chitosan mucoadhesive films are illustrated in Figure 31. The smooth but unhomogeneous surface of chitosan free film is shown in Figure 31A. The drug loaded films were rough as demonstrated in Figure 31 and had void spaces within

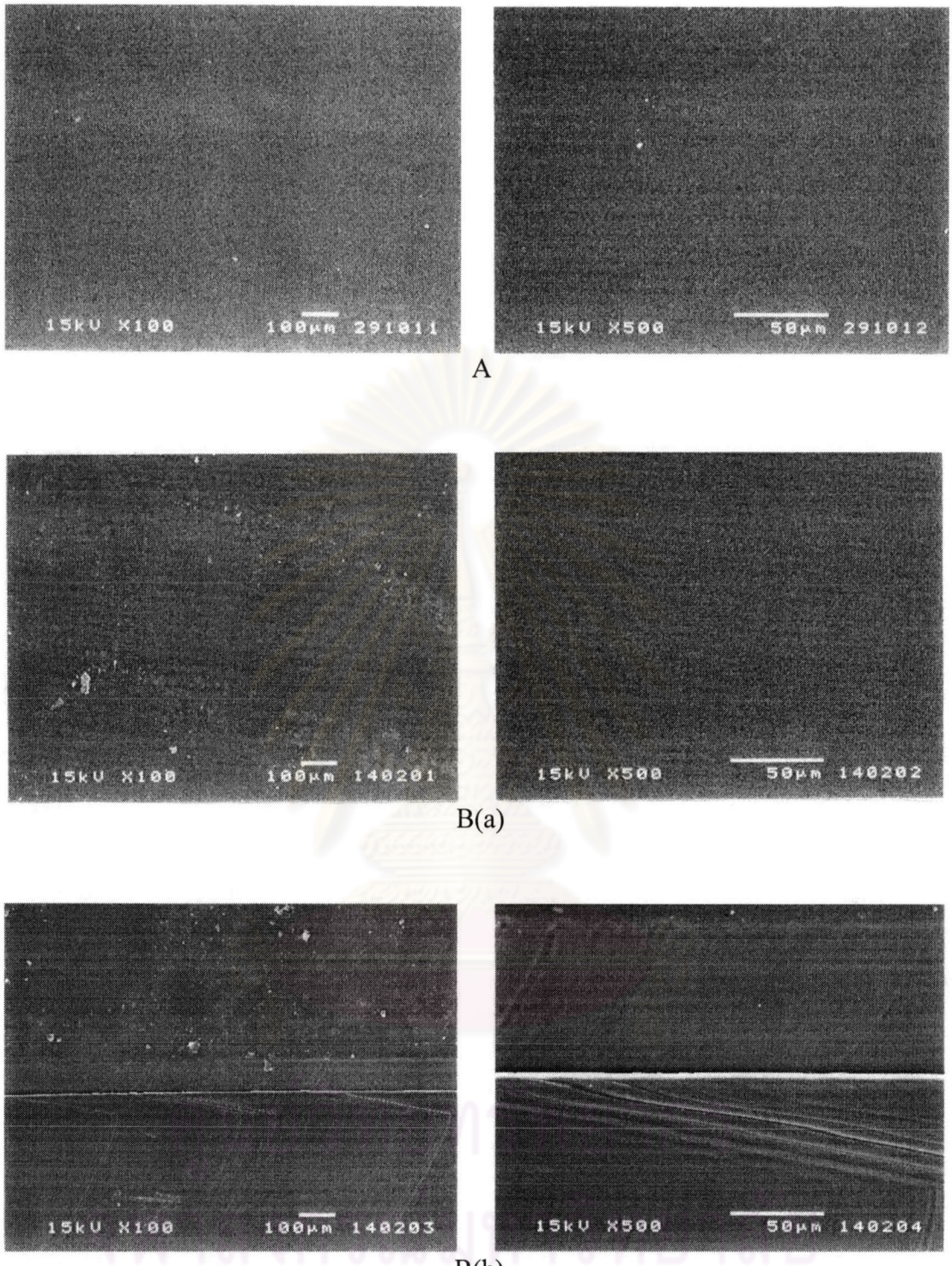

Figure 28 Scanning electron photomicrograph of (A) HPMC E15 free film; (B) E15 1:1 drug loaded film; (C) E15 1:0.67 drug loaded film; (D) E15 1:0.5 drug loaded film (a = surface, b = cross-section)

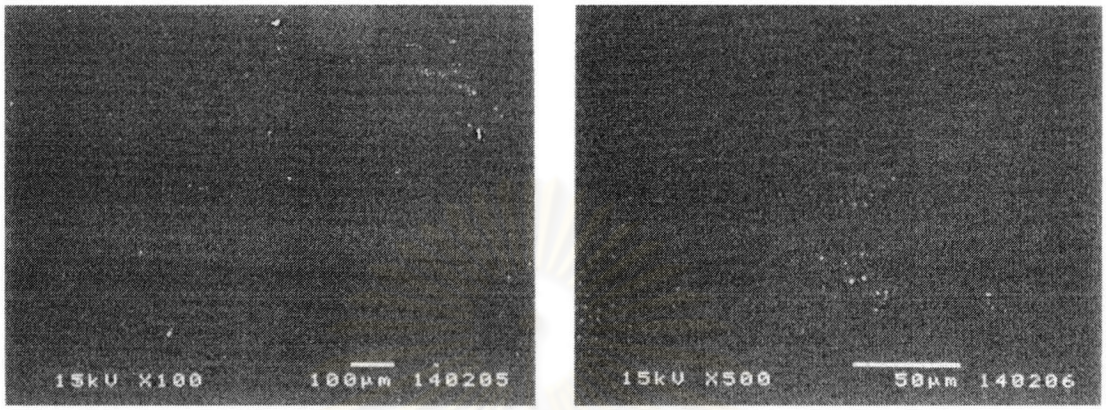

C(a)

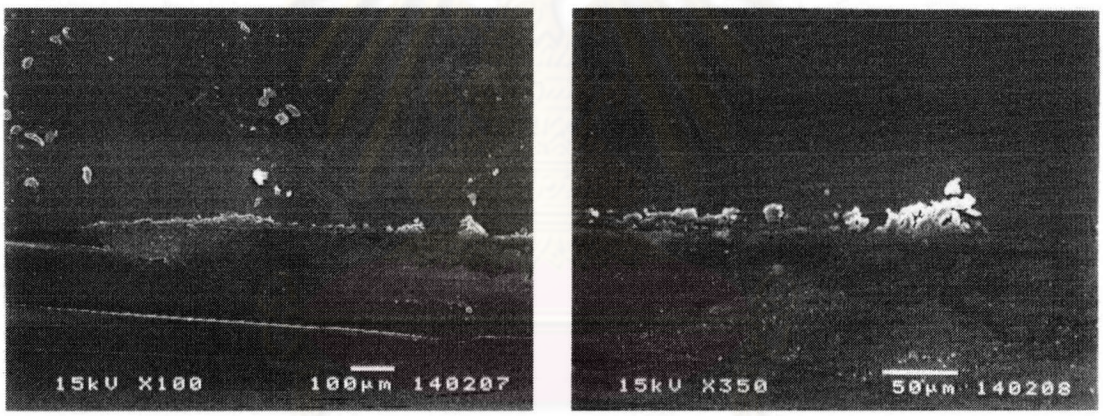

C(b)

Figure 28 Scanning electron photomicrograph of (A) HPMC E15 free film; (B) E15 1:1 drug loaded film; (C) E15 1:0.67 drug loaded film; (D) E15 1:0.5 drug loaded film (a = surface, b = cross-section) (Cont.)

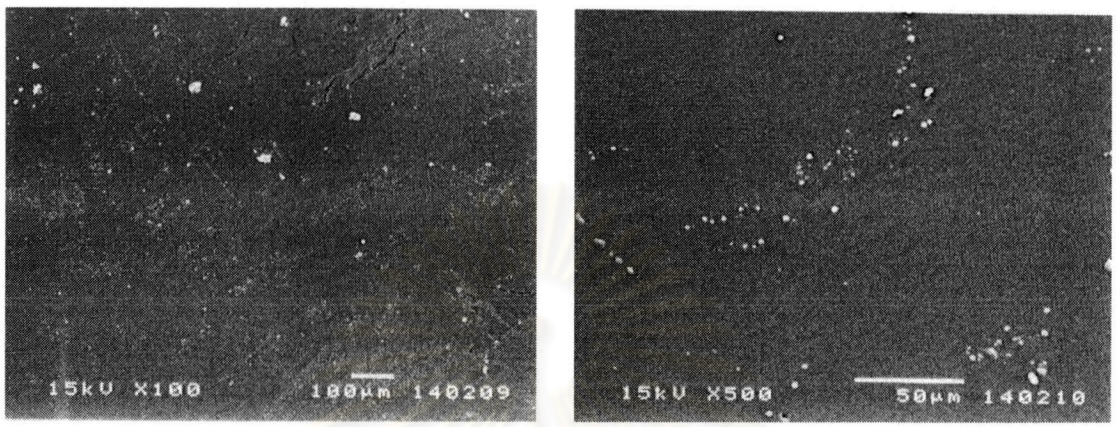

D(a)

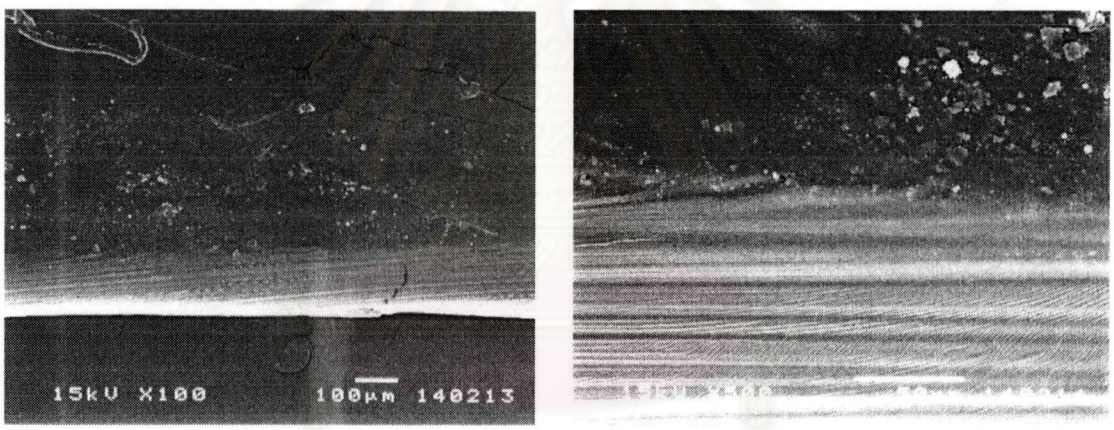

D(b)

Figure 28 Scanning electron photomicrograph of (A) HPMC E15 free film; (B) E15 1:1 drug loaded film; (C) E15 1:0.67 drug loaded film; (D) E15 1:0.5 drug loaded film (a = surface, b = cross-section) (Cont.)

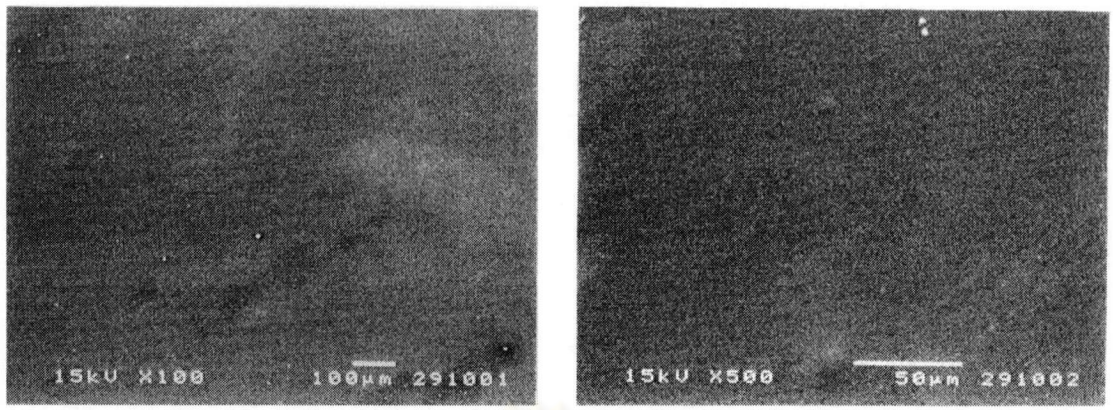

A

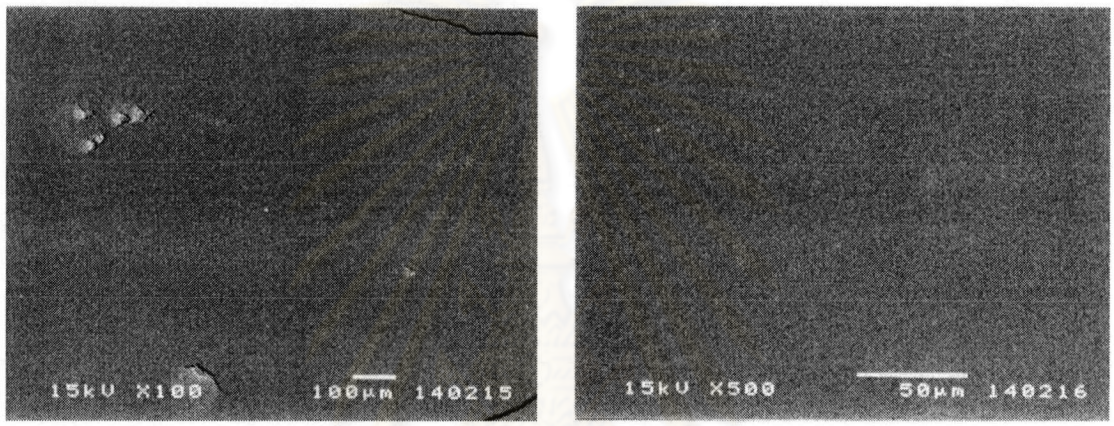

B(a)

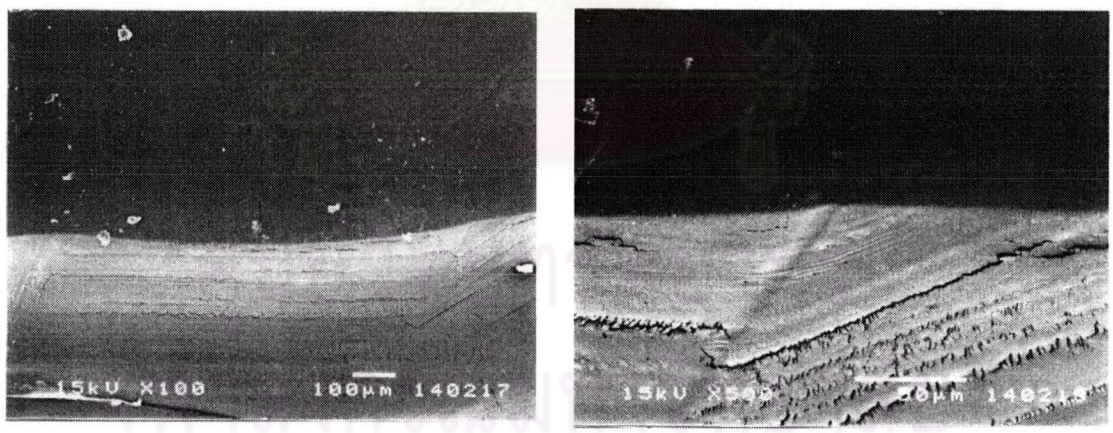

B(b)

Figure 29 Scanning electron photomicrograph of (A) HPMC E4M free film; (B) E4M 1:1 drug loaded film; (C) E4M 1:0.67 drug loaded film; (D) E4M 1:0.5 drug loaded film (a = surface, b = cross-section)

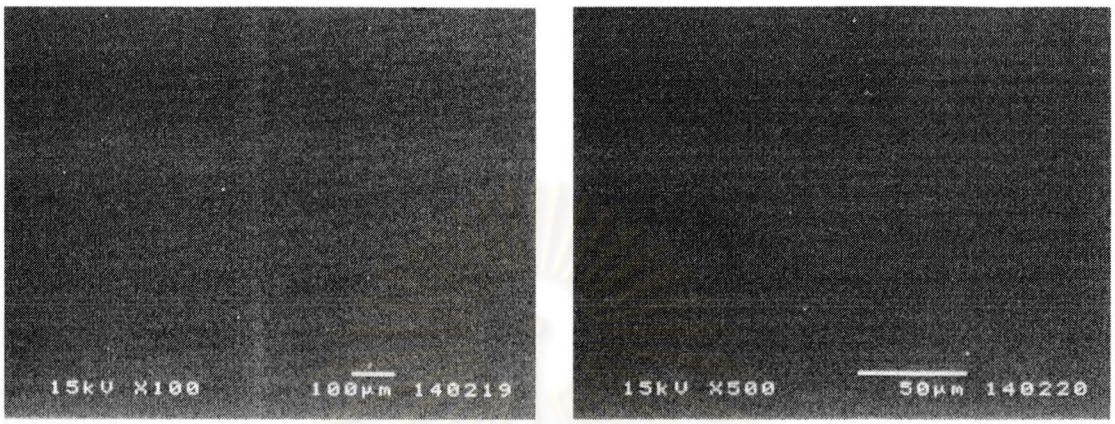

C(a)

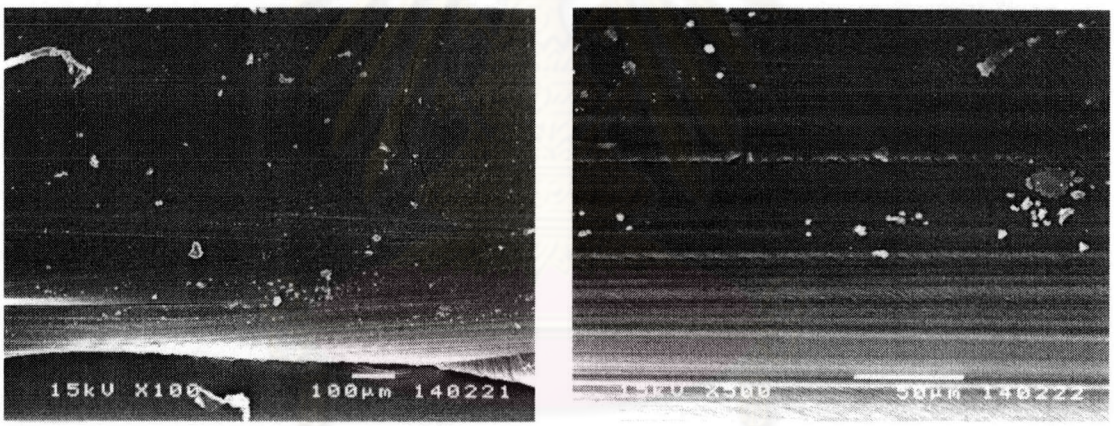

C(b)

Figure 29 Scanning electron photomicrograph of (A) HPMC E4M free film; (B) E4M 1:1 drug loaded film; (C) E4M 1:0.67 drug loaded film; (D) E4M 1:0.5 drug loaded film (a = surface, b = cross-section) (Cont.)

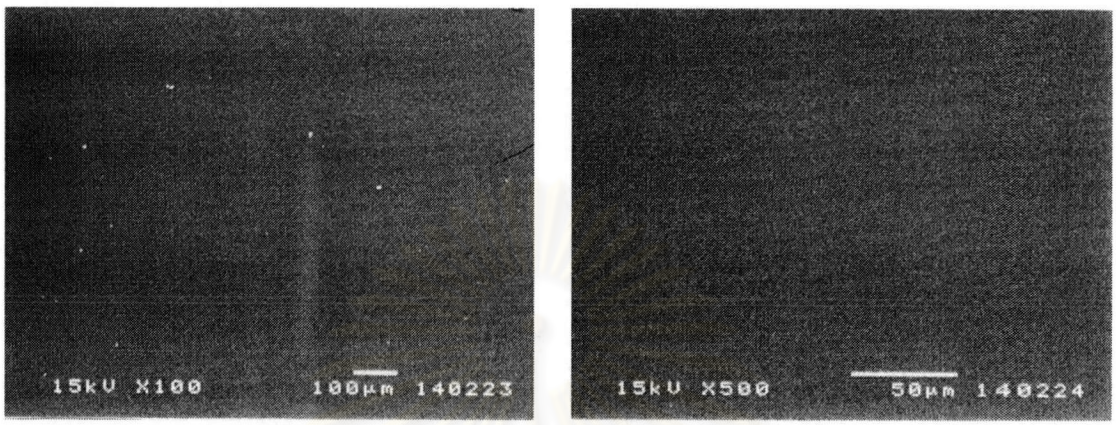

D(a)

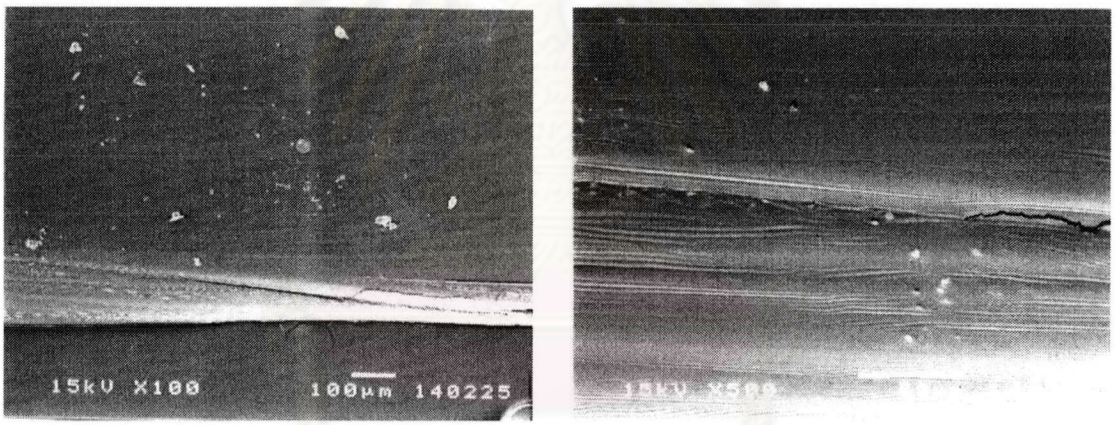

D(b)

Figure 29 Scanning electron photomicrograph of (A) HPMC E4M free film; (B) E4M 1:1 drug loaded film; (C) E4M 1:0.67 drug loaded film; (D) E4M 1:0.5 drug loaded film (a = surface, b = cross-section) (Cont.)

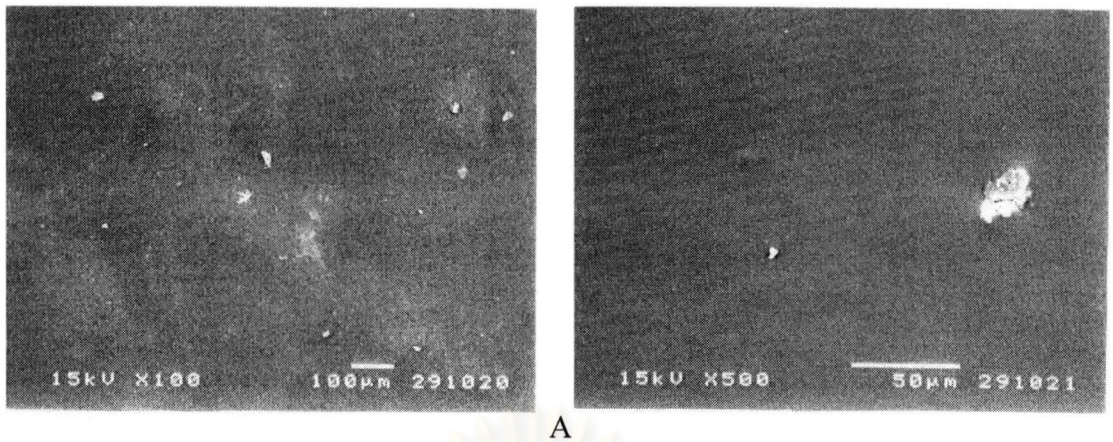

A

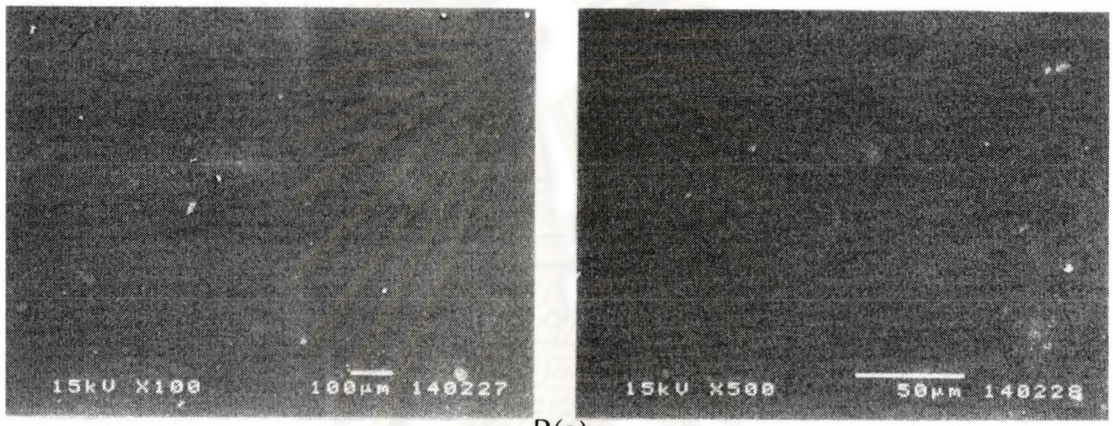

B(a)

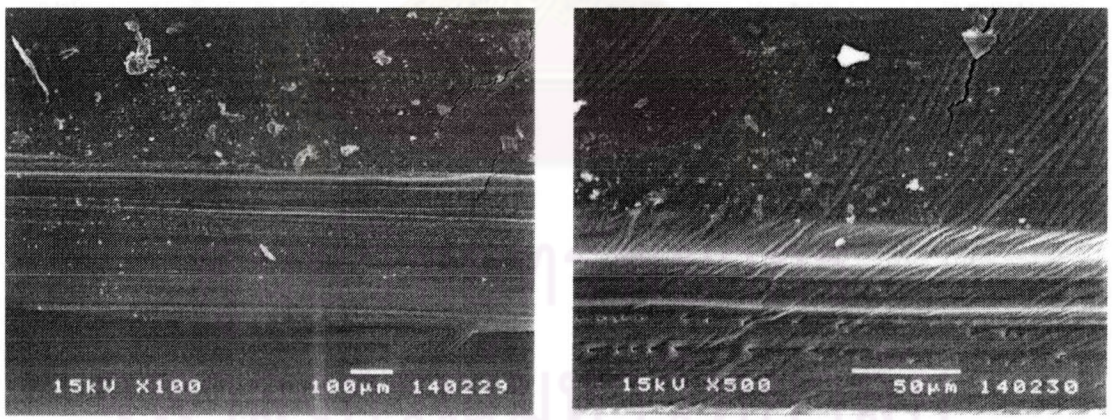

B(b)

Figure 30 Scanning electron photomicrograph of (A) HPC free film; (B) HPC 1:1 drug loaded film; (C) HPC 1:0.67 drug loaded film; (D) HPC 1:0.5 drug loaded film (a = surface, b = cross-section)

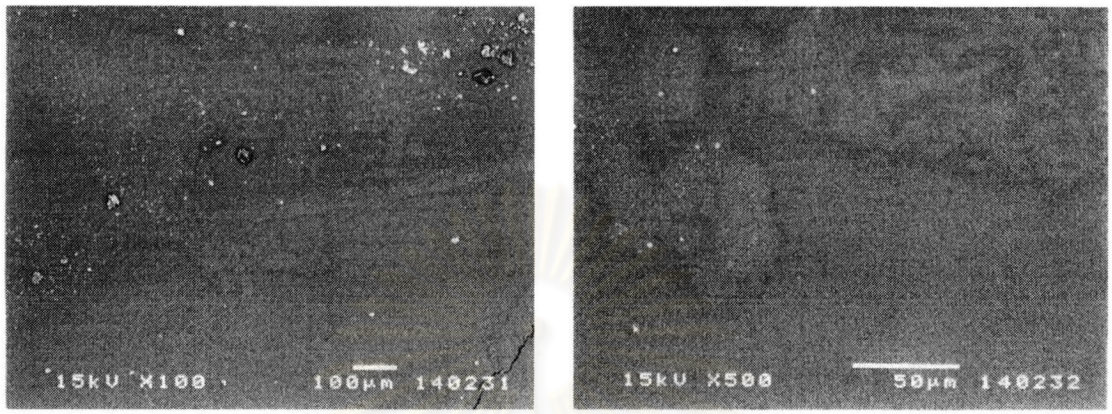

C(a)

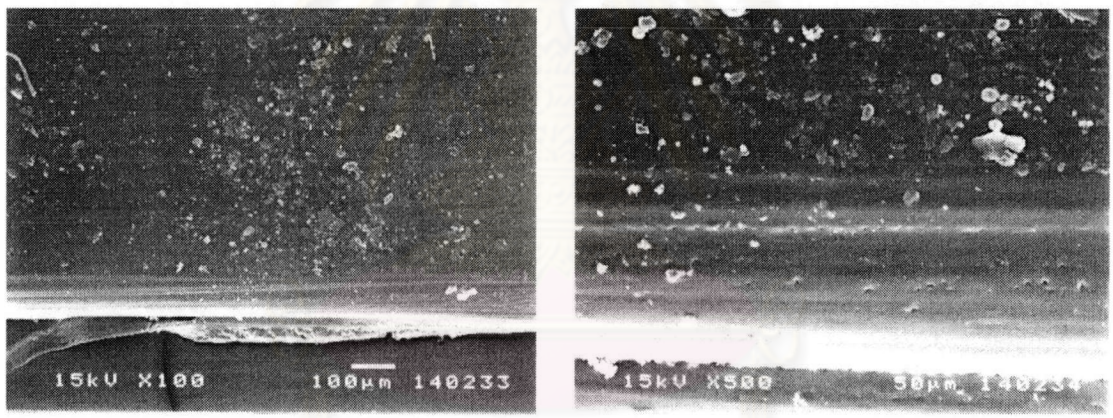

C(b)

Figure 30 Scanning electron photomicrograph of (A) HPC free film; (B) HPC 1:1 drug loaded film; (C) HPC 1:0.67 drug loaded film; (D) HPC 1:0.5 drug loaded film (a = surface, b = cross-section) (Cont.)

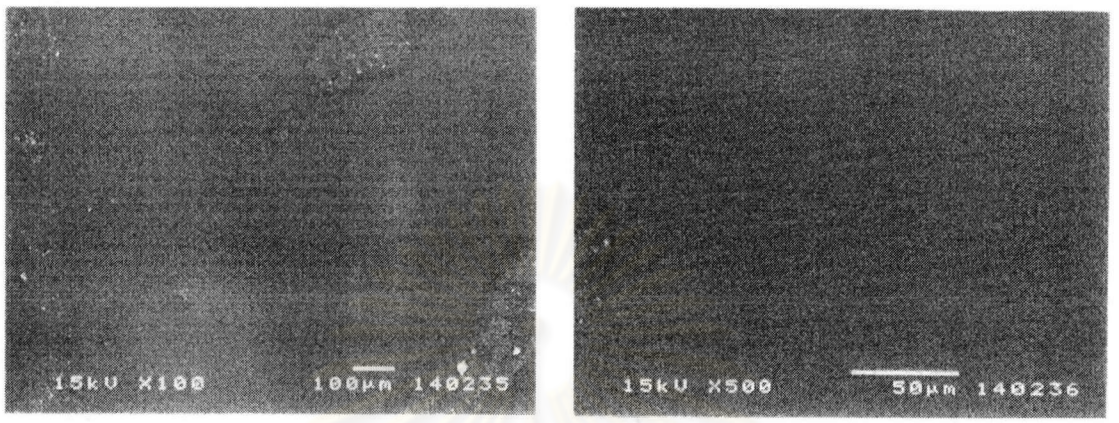

D(a)

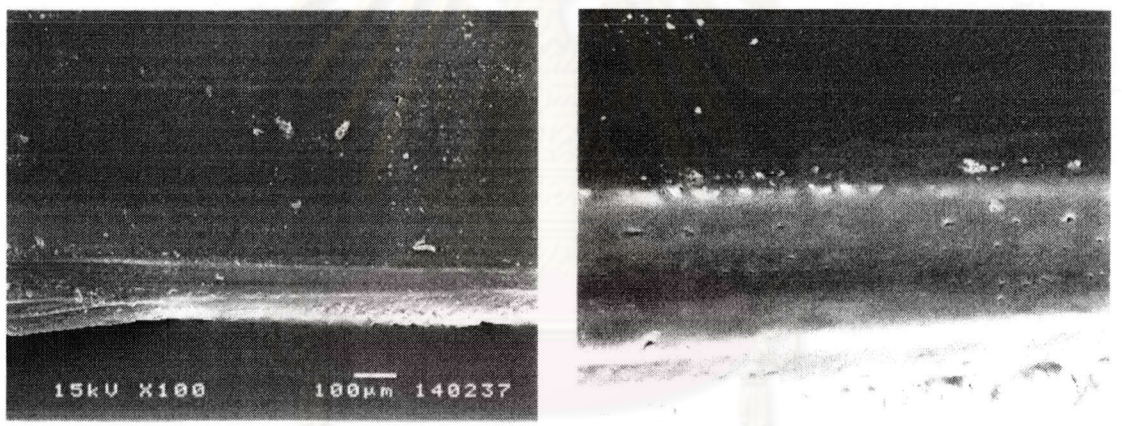

D(b)

Figure 30 Scanning electron photomicrograph of (A) HPC free film; (B) HPC 1:1 drug loaded film; (C) HPC 1:0.67 drug loaded film; (D) HPC 1:0.5 drug loaded film (a = surface, b = cross-section) (Cont.)

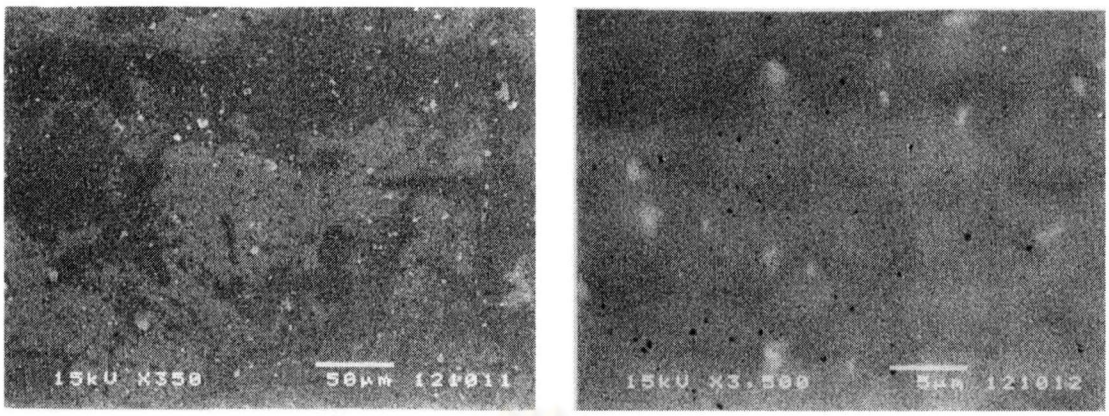

A

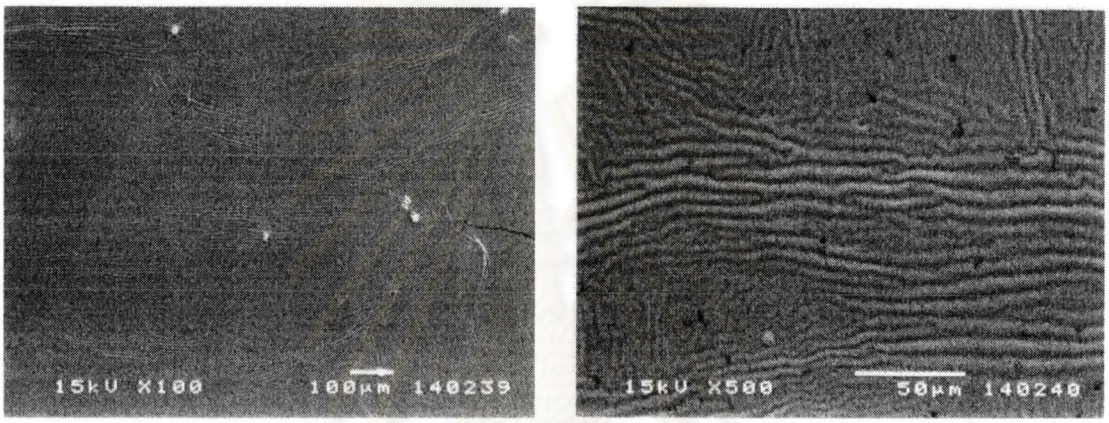

B(a)

B(b)

Figure 31 Scanning electron photomicrograph of (A) chitosan free film; (B) CS 1:1 drug loaded film; (C) CS 1:0.67 drug loaded film; (D) CS 1:0.5 drug loaded film (a = surface, b = cross-section)

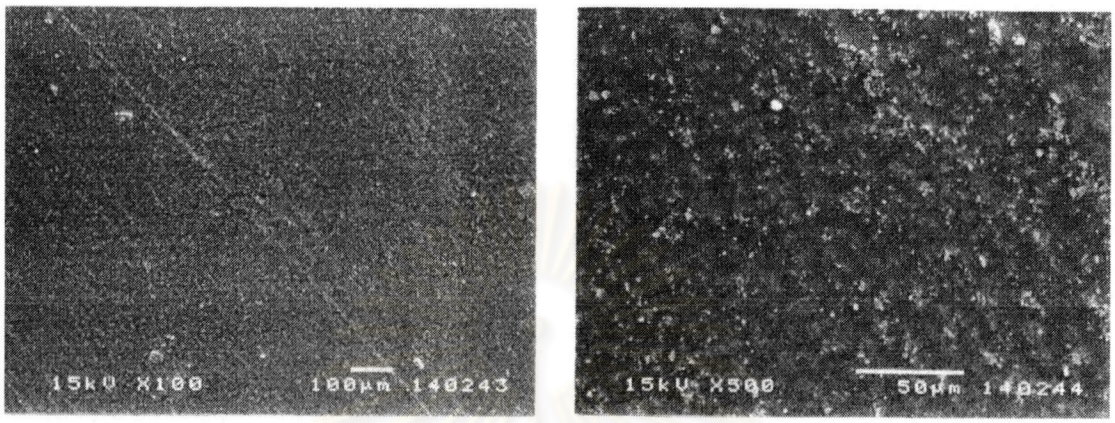

C(a)

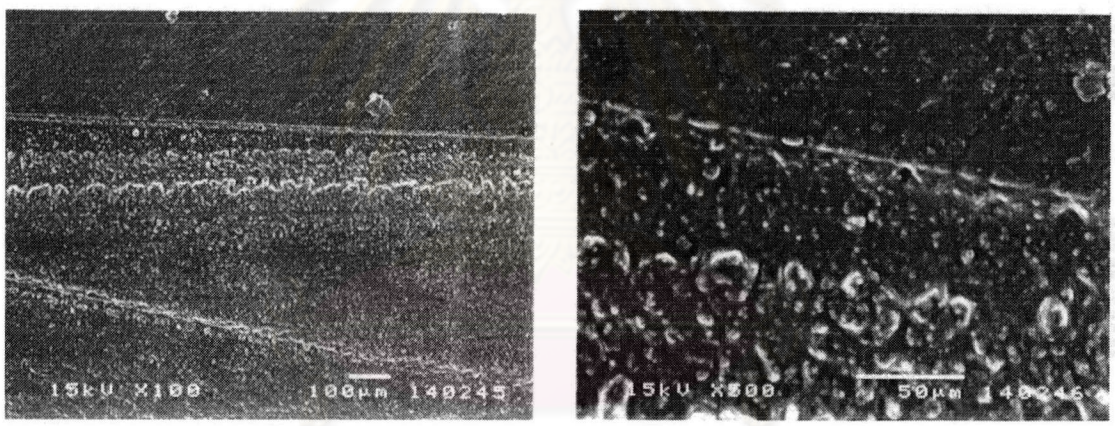

C(b)

Figure 31 Scanning electron photomicrograph of (A) chitosan free film; (B) CS 1:1 drug loaded film; (C) CS 1:0.67 drug loaded film; (D) CS 1:0.5 drug loaded film (a = surface, b = cross-section) (Cont.)

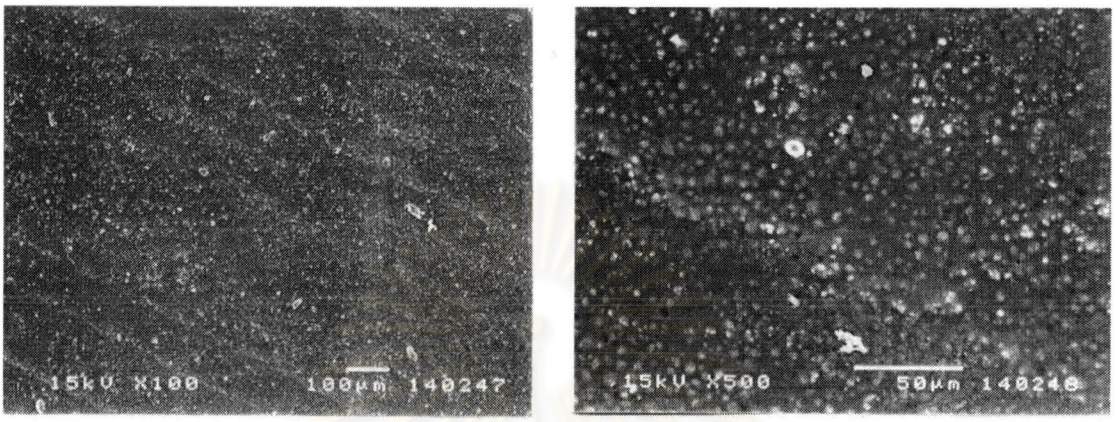

D(a)

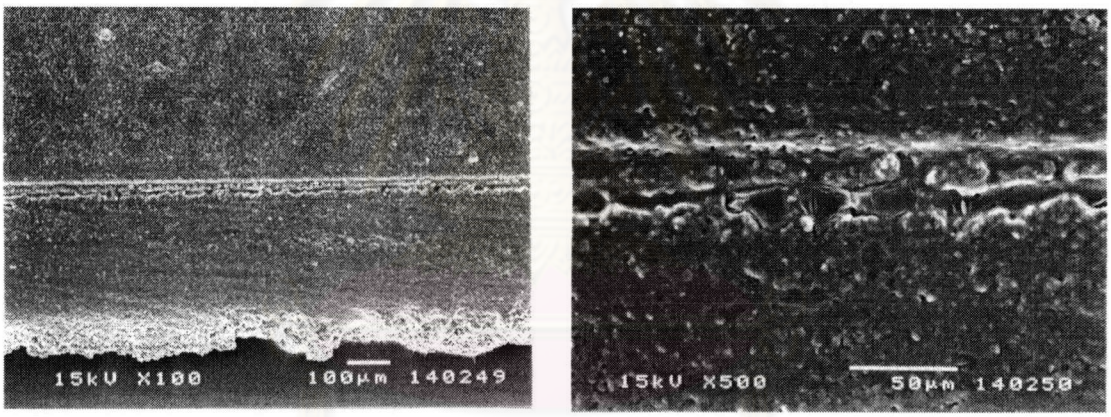

D(b)

Figure 31 Scanning electron photomicrograph of (A) chitosan free film; (B) CS 1:1 drug loaded film; (C) CS 1:0.67 drug loaded film; (D) CS 1:0.5 drug loaded film (a = surface, b = cross-section) (Cont.)

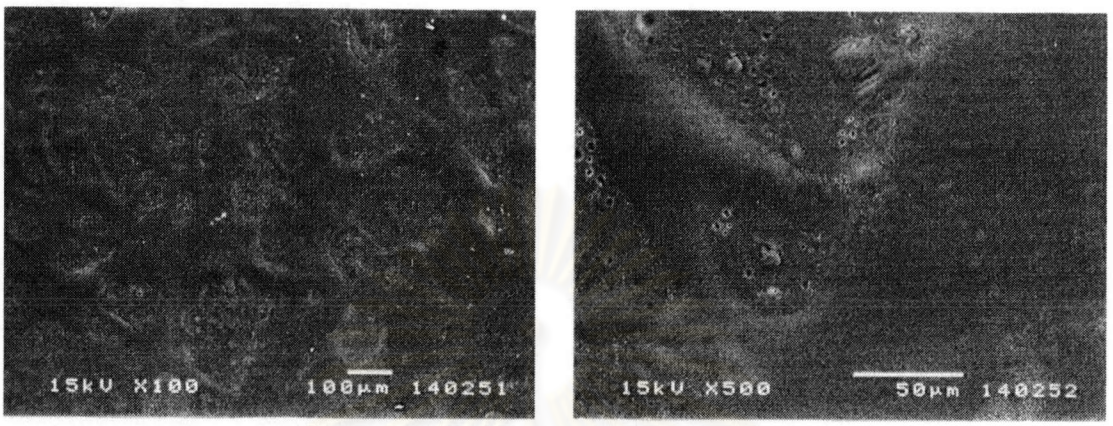

A(a)

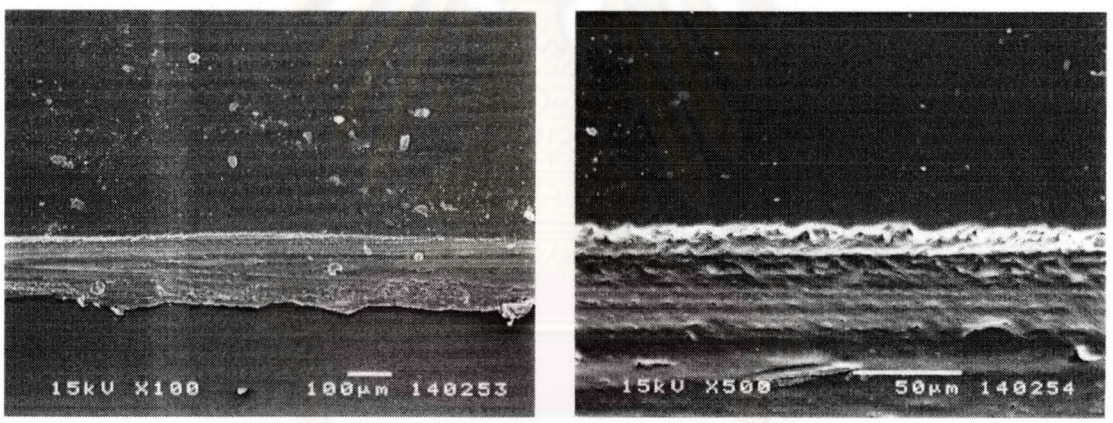

A(b)

Figure 32 Scanning electron photomicrograph of (A) E15HPC 1:3 drug loaded film; (B) E15HPC 2:3 drug loaded film; (C) E15HPC 3:3 drug loaded film; (D) E15HPC 3:2 drug loaded film; (E) and E15HPC 3:1 drug loaded film (a = surface, b = cross-section)

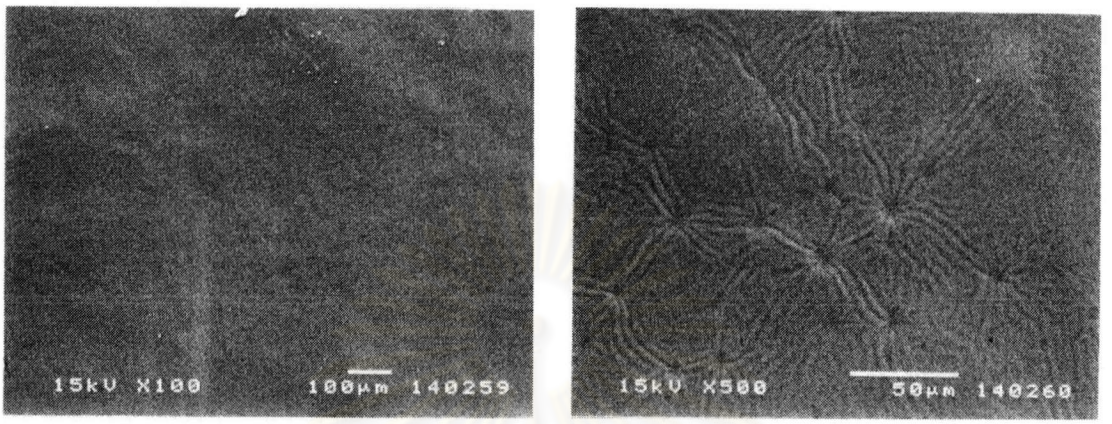

B(a)

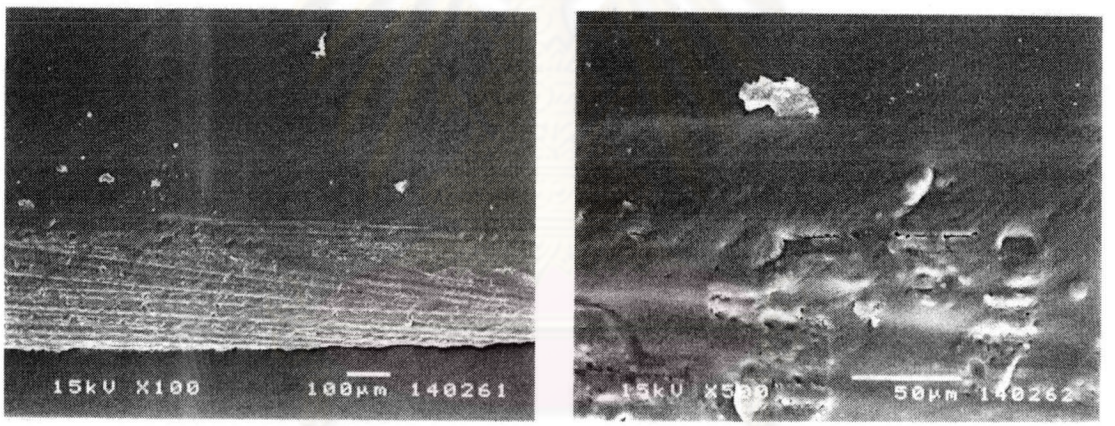

B(b)

Figure 32 Scanning electron photomicrograph of (A) E15HPC 1:3 drug loaded film; (B) E15HPC 2:3 drug loaded film; (C) E15HPC 3:3 drug loaded film; (D) E15HPC 3:2 drug loaded film; (E) and E15HPC 3:1 drug loaded film (a = surface, b = cross-section) (Cont.)

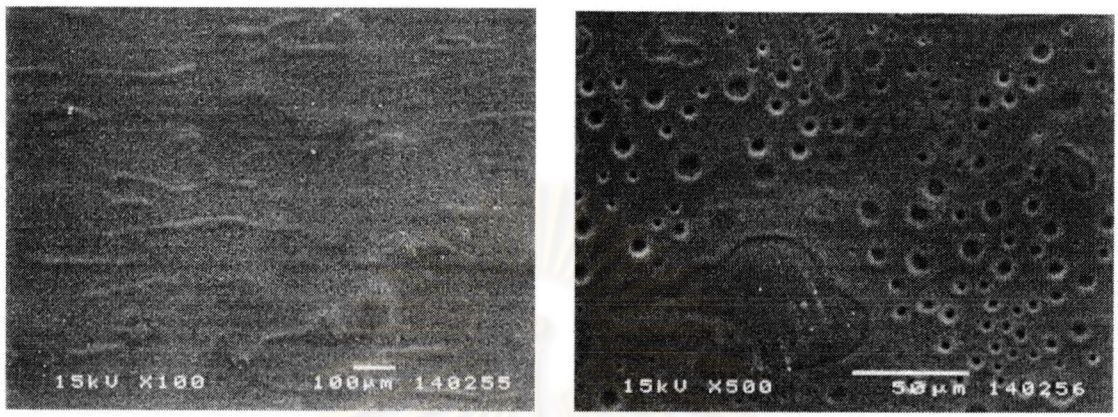

C(a)

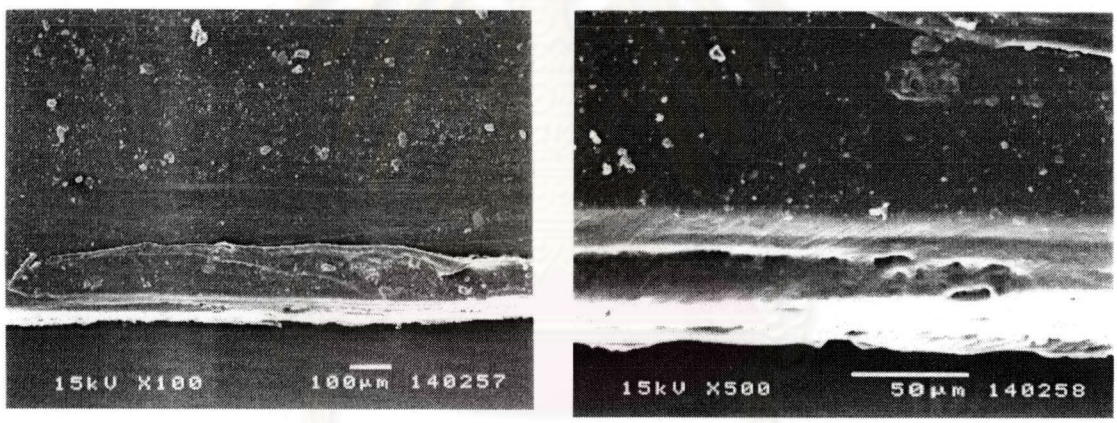

C(b)

Figure 32 Scanning electron photomicrograph of (A) E15HPC 1:3 drug loaded film; (B) E15HPC 2:3 drug loaded film; (C) E15HPC 3:3 drug loaded film; (D) E15HPC 3:2 drug loaded film; (E) and E15HPC 3:1 drug loaded film (a = surface, b = cross-section) (Cont.)

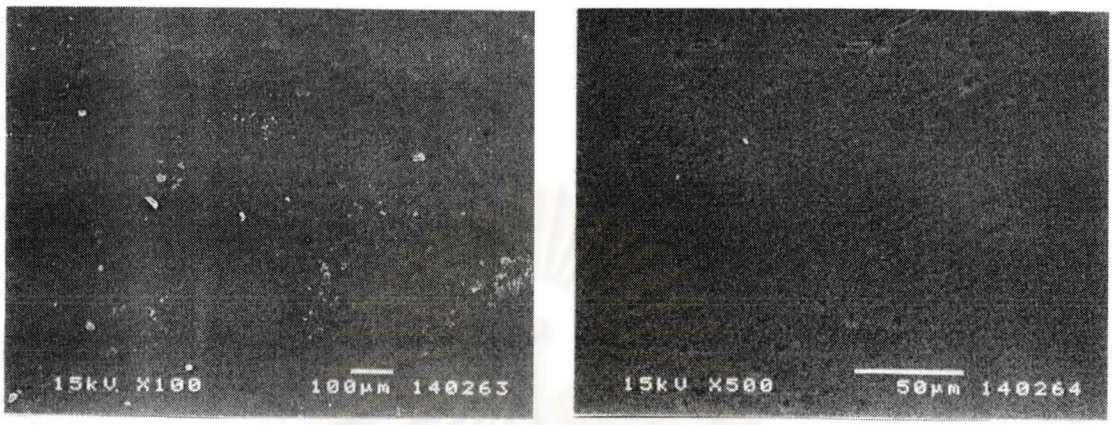

D(a)

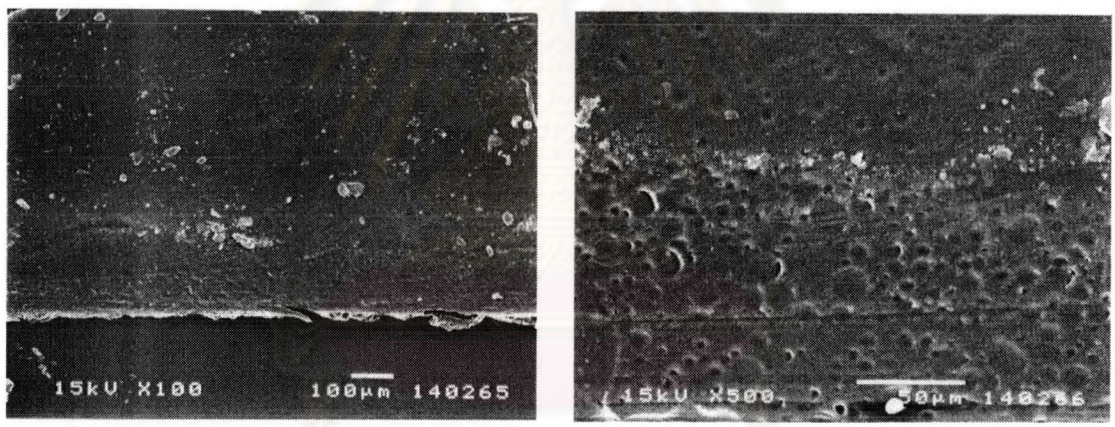

D(b)

Figure 32 Scanning electron photomicrograph of (A) E15HPC 1:3 drug loaded film; (B) E15HPC 2:3 drug loaded film; (C) E15HPC 3:3 drug loaded film; (D) E15HPC 3:2 drug loaded film; (E) and E15HPC 3:1 drug loaded film (a = surface, b = cross-section) (Cont.)

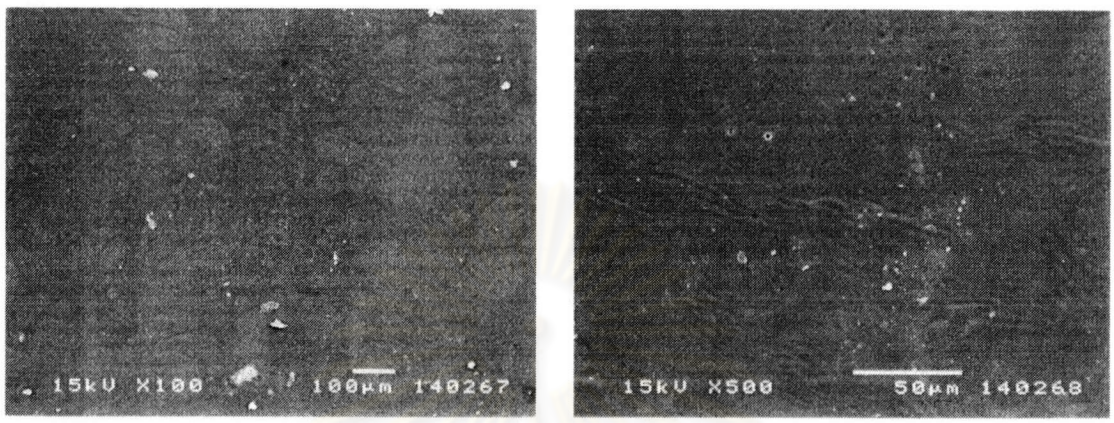

E(a)

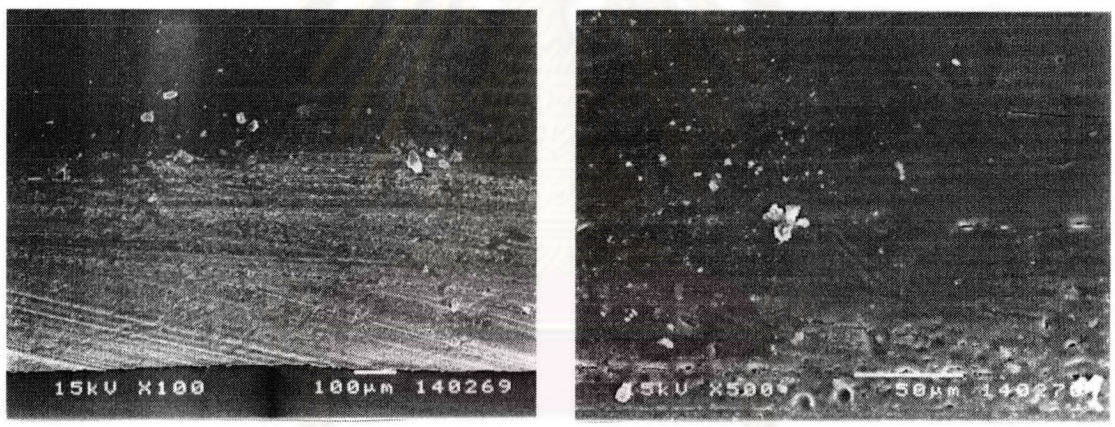

E(b)

Figure 32 Scanning electron photomicrograph of (A) E15HPC 1:3 drug loaded film; (B) E15HPC 2:3 drug loaded film; (C) E15HPC 3:3 drug loaded film; (D) E15HPC 3:2 drug loaded film; (E) and E15HPC 3:1 drug loaded film (a = surface, b = cross-section) (Cont.)

the cross-sectional area of film texture. Increasing the proportion of drug, increased the rough surface and the void spaces.

The scanning electron photomicrograph of the combination of HPMC E15 and HPC are illustrated in Figure 32. They had rough surfaces with pores. And the cross-sectioned textures of the mixed polymer films were rough. The rather rough pores on the surface of the film was observed in Formula E15HPC 1:3. The cross-sectional surface of the film was dense and had aggregate of particles as depicted in Figure 32B. The large and homogeneously distributed pores were observed in Formula E15HPC 3:3.

5. Surface area determination

The results of the specific surface area of the mucoadhesive films are shown in Table 11. Comparison between the combination films, the maximum specific surface area was obtained from E15HPC 1:3. Increasing in proportion of HPMC E15 decreased the specific surface areas. E4M 1:1 exhibited higher specific surface area than E15 1:1. For HPC 1:1 film, the specific surface area could not be measured due to its stickiness.

Table 11 Specific surface area of mucoadhesive films

Formula	Specific surface area (m^2/g)
E15 1:1	0.3623
E4M 1:1	0.4252
HPC 1:1*	-
CS 1:1	0.2353
CS 1:0.67	0.0846
CS 1:0.5	0.2138
E15HPC 1:3	0.6022
E15HPC 2:3	0.5306
E15HPC 3:3	0.4173
E15HPC 3:2	0.2283
E15HPC 3:1	0.0650

* can not be measured

6. The physicochemical characterization

6.1 Infrared spectrometry

FT-IR spectrum of lidocaine HCl powder in Figure 33 showed the peak at 1658 cm^{-1} indicating C=C cyclic stretching overlapped with the C=O stretching (amide I band) at 1673 cm^{-1}. The peak at 1545 cm^{-1} was N-H stretching (amide II band). The peak at 3459 cm^{-1}, 3388 cm^{-1} and 3040 cm^{-1} indicated N-H stretching bands, the peak at 2981 was C-H stretching band and the peak at 1275cm^{-1} was C-N stretching band.

The FT-IR spectra of CMC mucoadhesive film containing drug (Formula CMC 1:1), pure drug and CMC powder are illustrated in Figure 34. The spectrum of film containing drug was different from that of pure drug. The C=O stretching band was shifted from 1673 cm^{-1} to 1689 cm^{-1}. The N-H stretching band was shifted from 1545 cm^{-1} to 1541 cm^{-1}. The C=C stretching band was shifted from 1658 cm^{-1} to 1605 cm^{-1} and 1478 cm^{-1} to 1474 cm^{-1} and this peak intensity was regressed. No new peak was observed from this spectrum.

The FT-IR spectra of HPMC E15 mucoadhesive film containing drug (Formula E15 1:1), pure drug, citric acid, menthol and HPMC E15 powder are illustrated in Figure 35. The spectrum of Formula E15 1:1 showed the peak at 1735 cm^{-1} and 1691 cm^{-1} that were the peak of C=O stretching of the drug and citric acid overlap to the peak of C=C stretching of the drug. The peak intensity of amide II band was reduced and slightly shifted from 1545 cm^{-1} to 1542 cm^{-1}. The C=C stretching band was shifted from 1478 cm^{-1} to 1474 cm^{-1} and this peak intensity was regressed. No new peak was observed from this spectrum.

The FT-IR spectra of HPMC E4M mucoadhesive film containing drug (Formula E4M 1:1), pure drug, citric acid, menthol and HPMC E4M powder are depicted in Figure 36. The drug-loaded film showed the spectrum similarly to that of HPMC E15 film.

The FT-IR spectra of HPC mucoadhesive containing drug (Formula HPC 1:1), pure drug, citric acid, menthol and HPC powder are showed in Figure 37. The result was similarly to that of HPMCs films (Formula E15 1:1 and E4M 1:1).

However it was slightly different from HPMCs films at the amide II band (C-N stretching) that was slightly shifted from 1542 cm^{-1} to 1543 cm^{-1}.

The FT-IR spectra of chitosan mucoadhesive containing drug (Formula CS 1:1), pure drug, citric acid, menthol, PEG400 and chitosan powder are presented in Figure 38. The peak at 1733 cm^{-1} was C=O stretching of the drug and citric acid, overlap to the peaks of C=O stretching of PEG and N-H stretching of the drug and chitosan. And the other peaks that were integration of peaks of the drug, polymer, PEG, citric acid and menthol which were slightly shifted or regression of the peaks. No new peak was observed from this spectrum.

The FT-IR spectra of mixed of HPMC E15 and HPC film in ratio of 1:1 with drug loading (Formula E15HPC 3:3), pure drug, citric acid, menthol and HPC powder are presented in Figure 39. The spectrum of the film was similar to the case of HPMC E15 and HPC. However it was slightly different from that of HPMC E15 film that amide II band was shifted from 1542 cm^{-1} to 1541 cm^{-1}.

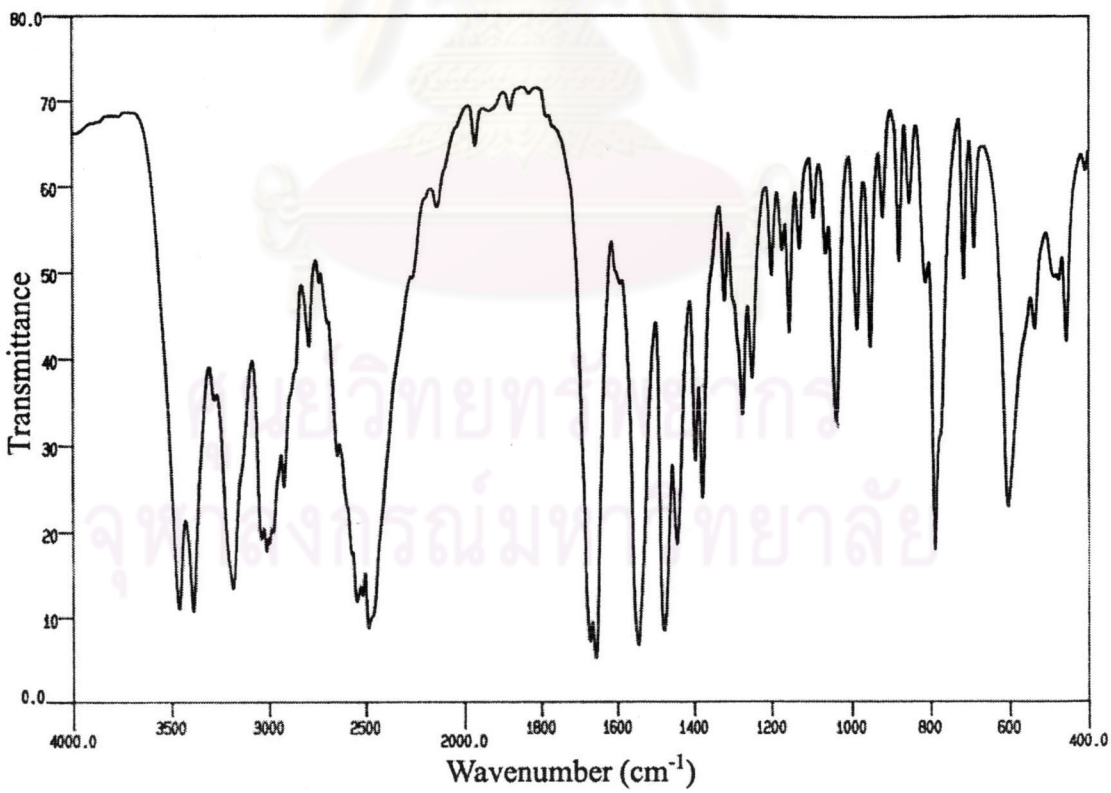

Figure 33 FT-IR spectra of lidocaine HCl

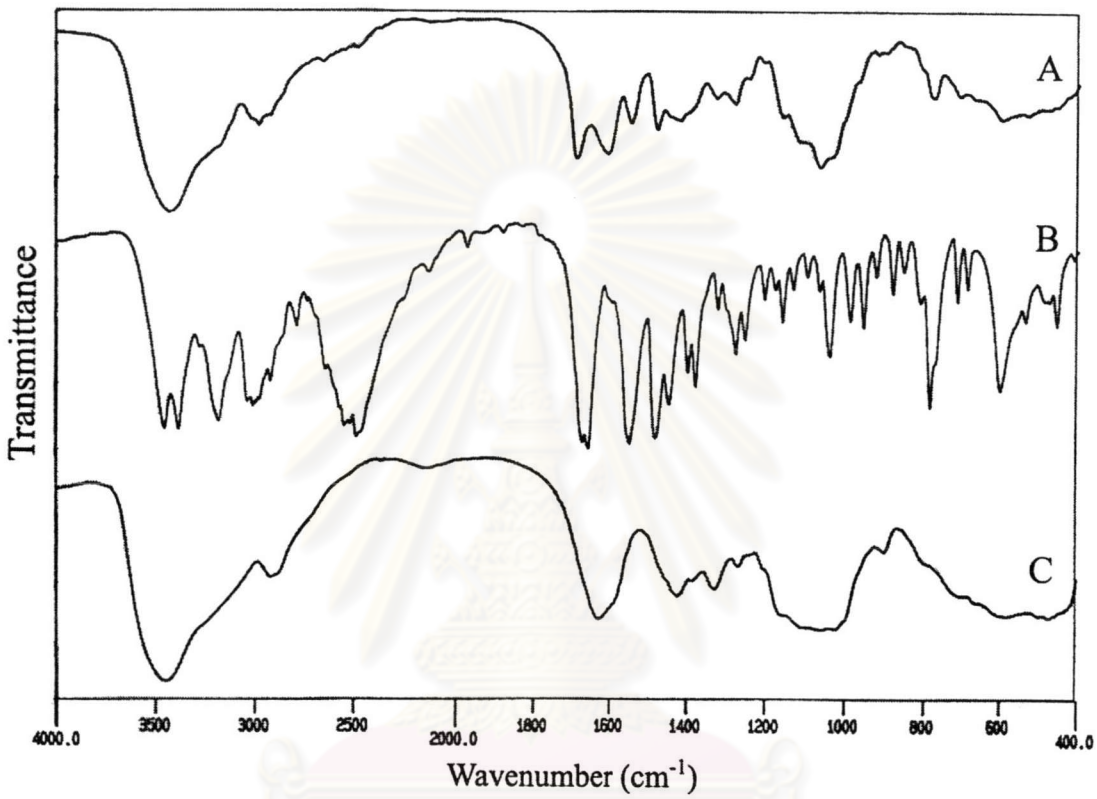

Figure 34 FT-IR spectra of (A) mucoadhesive film of CMC 1:1; (B) lidocaine HCl; (C) CMC powder

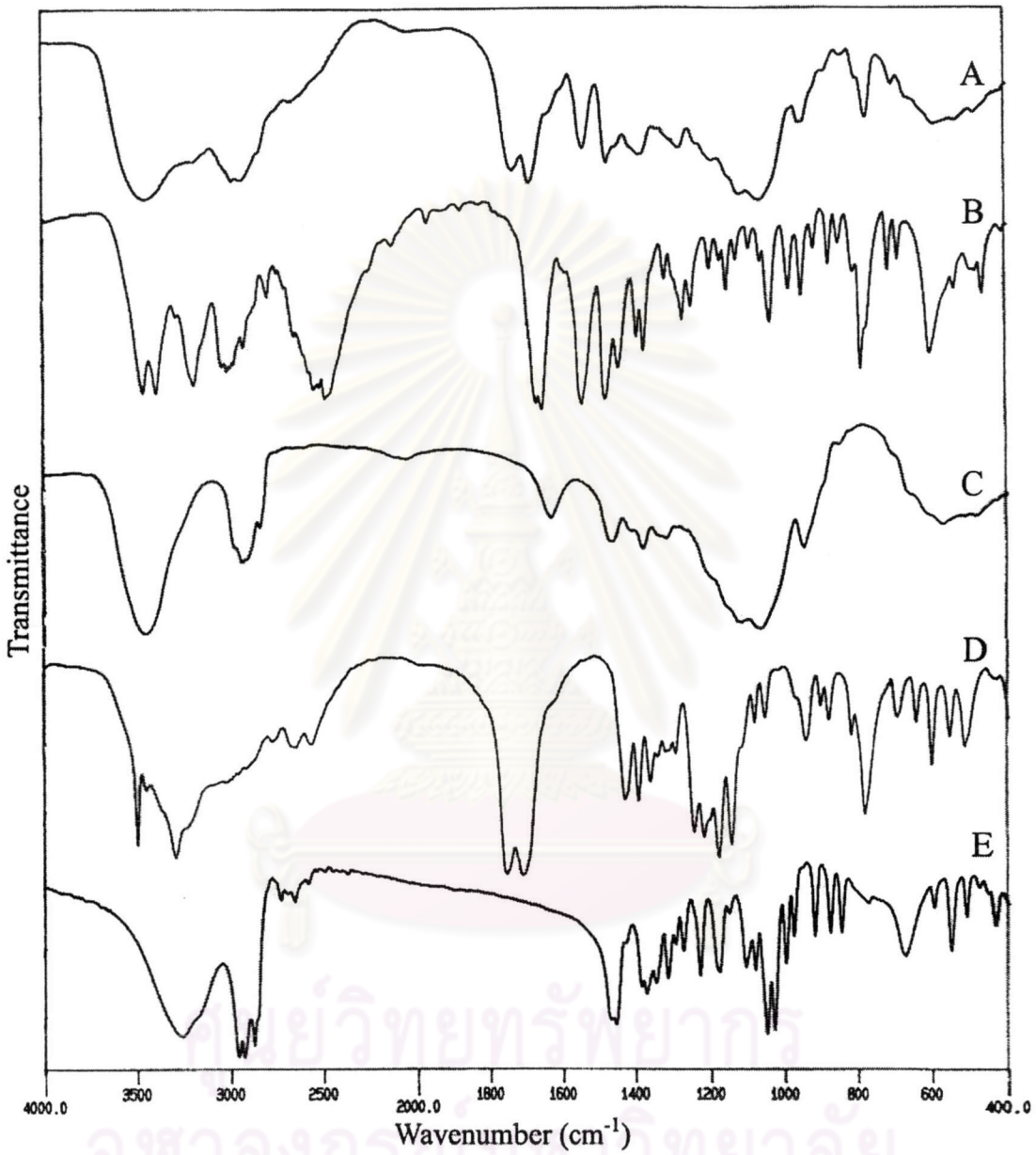

Figure 35 FT-IR spectra of (A) mucoadhesive film of E15 1:1; (B) lidocaine HCl; (C) HPMC E15 powder; (D) citric acid; (E) menthol

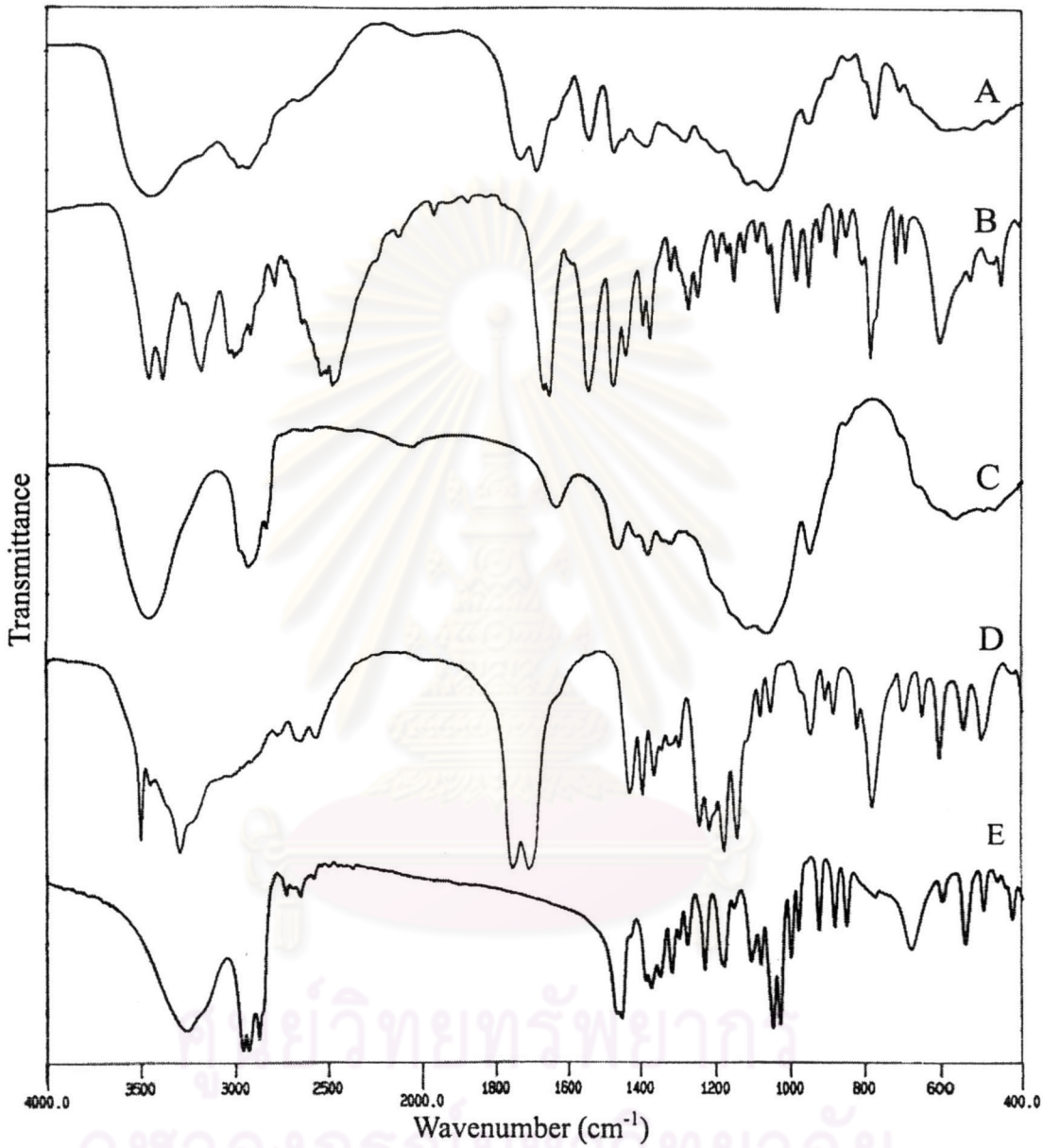

Figure 36 FT-IR spectra of (A) mucoadhesive film of E4M 1:1; (B) lidocaine HCl; (C) HPMC E4M powder; (D) citric acid; (E) menthol

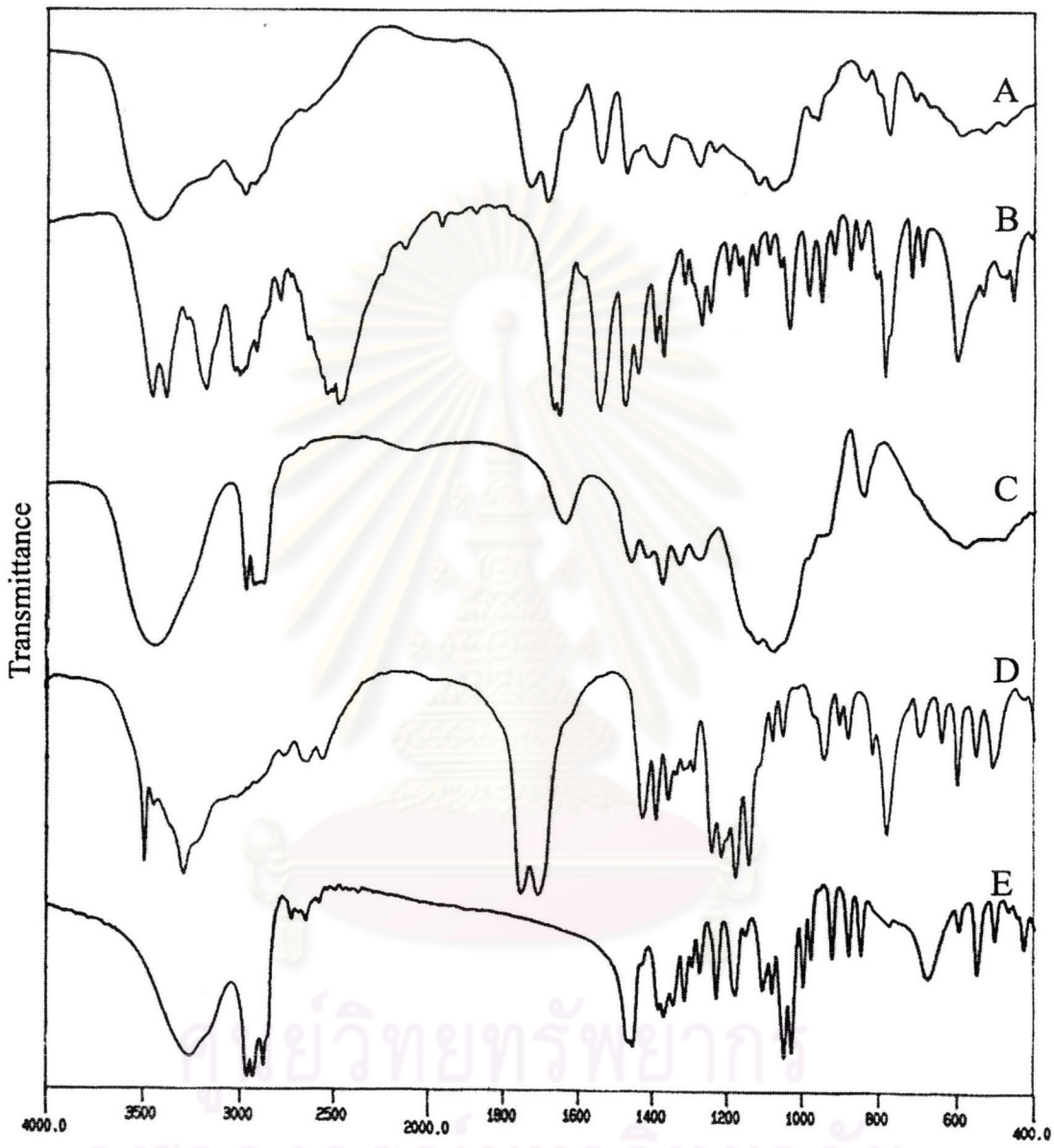

Figure 37 FT-IR spectra of (A) mucoadhesive film of HPC 1:1); (B) lidocaine HCl; (C) HPC powder; (D) citric acid; (E) menthol

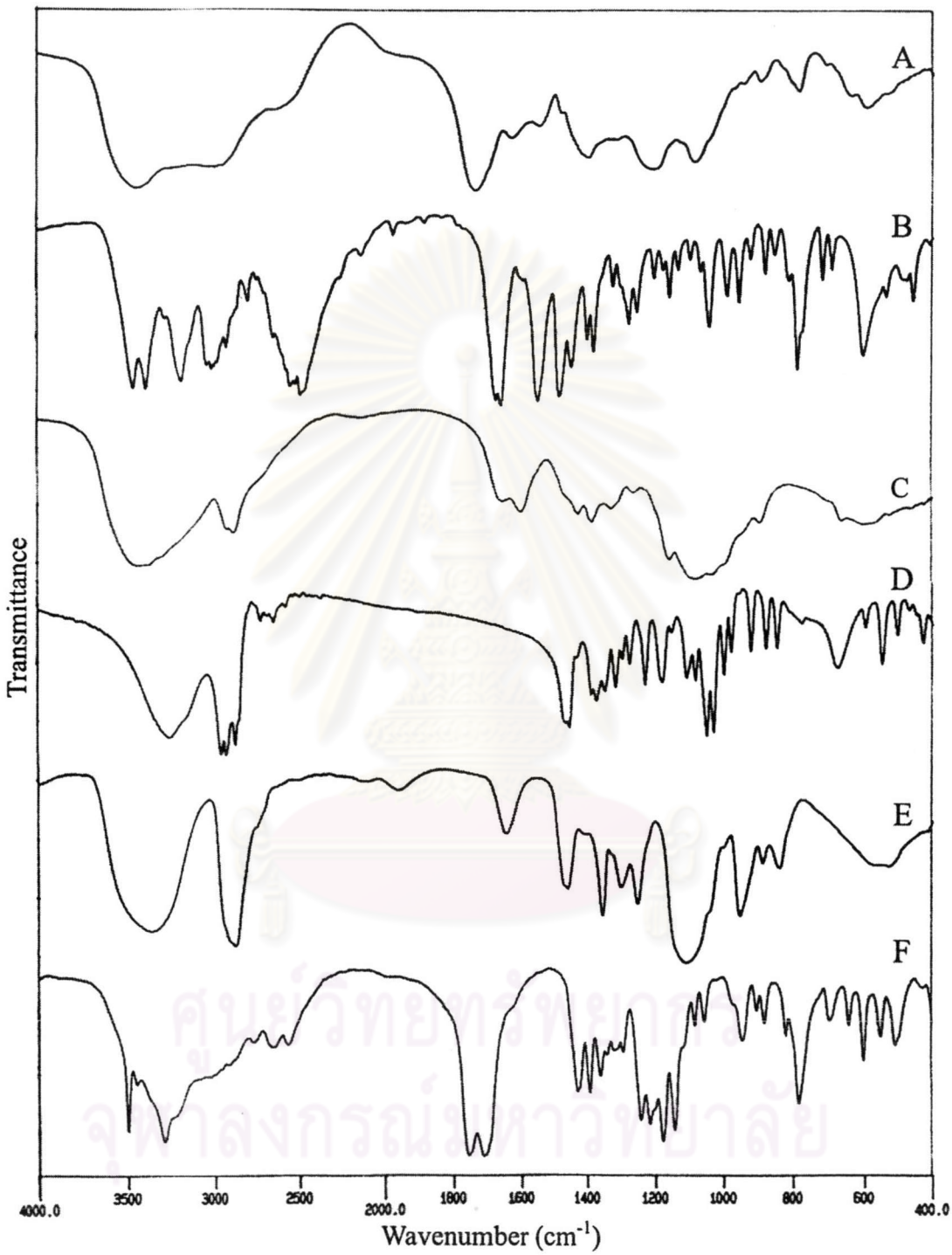

Figure 38 FT-IR spectra of (A) mucoadhesive film of CS 1:1; (B) lidocaine HCl; (C) chitosan powder; (D) menthol; (E) PEG 400; (F) citric acid

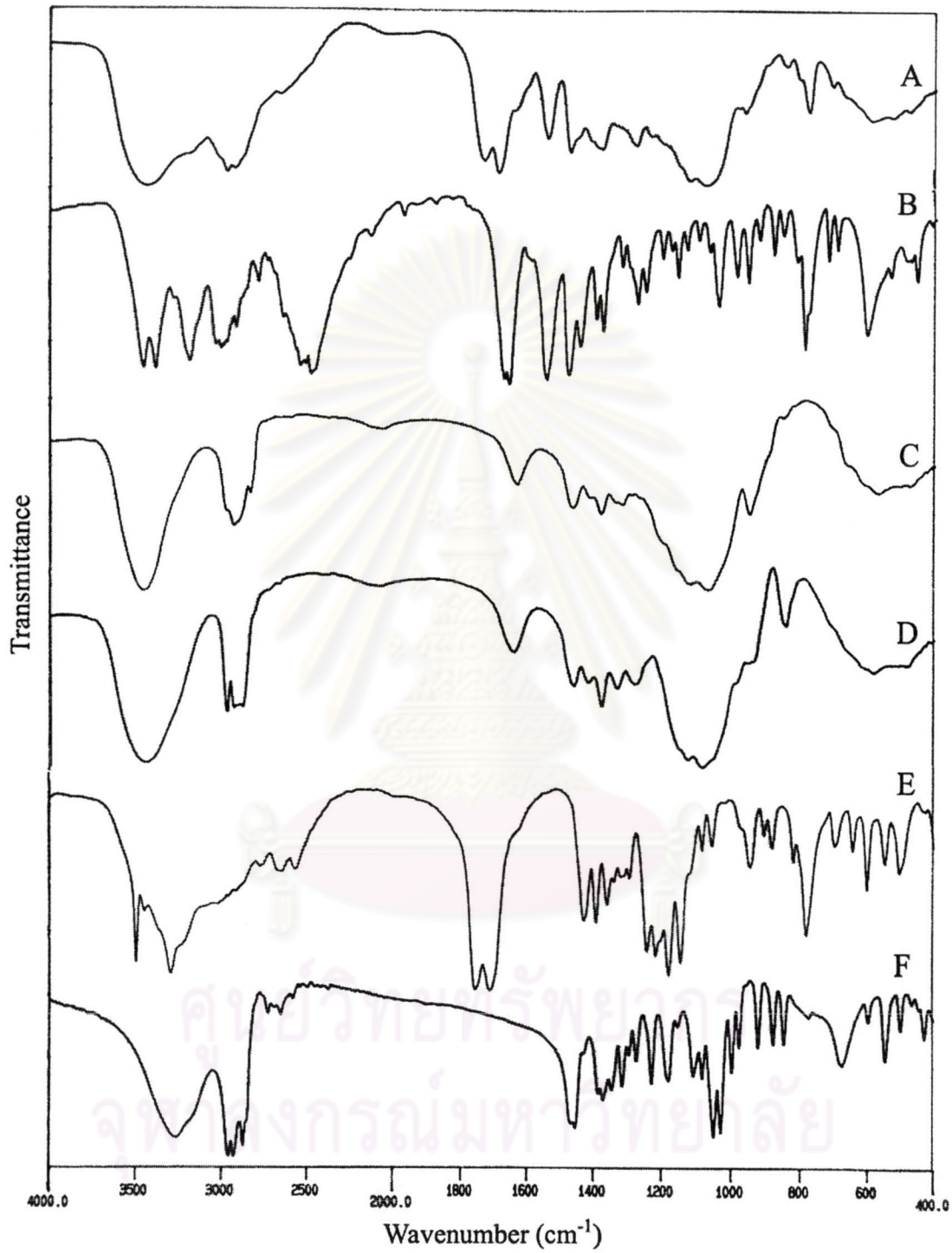

Figure 39 FT-IR spectra of (A) mucoadhesive film of E15HPC 3:3; (B) lidocaine HCl; (C) HPMC E15 powder; (D) HPC powder; (E) citric acid; (F) menthol

6.2 Powder X-ray diffraction

The power X-ray diffraction pattern of citric acid and menthol are illustrated in Figures 40 and 41 respectively. Citric acid was crystalline which had major peaks at 15.24°, 18.20°, 22.36°, 23.08° and 26.04° 2θ, and the small peaks between 10° to 48° 2θ. Menthol was crystalline and showed high peaks at 8.20°, 9.44°, 12.52°, 14.16°, 16.40°, 16.68°, 17.32°, 19.16°, 20.28° and 21.72° 2θ, and the small peaks between 15° to 47° 2θ. The X-ray diffraction patterns of the lidocaine HCl in original powder and in mucoadhesive films are shown in Figures 37-42. Lidocaine HCl was crystalline and showed high peaks at 12.93°, 14.13° 16.61°, 25.05°, 25.73°, and the small peaks between 6° to 53°.

By comparison, the diffractogram of mucoadhesive film of CMC 1:1 was different from that of CMC powder and lidocaine HCl powder as presented in Figure 42. The CMC powder did not show any dominant peaks indicating amorphous form while lidocaine HCl powder was crystalline. The mucoadhesive film containing drug showed the combination signal peak of two compounds consisting of 12.84°, 14.08°, 16.52°, 20.08°, 25.00°, 25.88° and 26.92° 2θ. However the peaks of lidocaine HCl in the films were notably regressed.

By comparison, the diffractogram of mucoadhesive film of E15 1:1 was different from that of HPMC E15 powder and lidocaine HCl powder as presented in Figure 43. Lidocaine HCl had many dominant peaks. The intensity of the dominant peaks of crystalline was reduced after casting, indicating that the drug and other ingredients have changed to amorphous state or molecular dispersion. However obtained film showed small peaks at 9.28° and 28.48° 2θ.

The X-ray diffraction of mucoadhesive film of E4M 1:1 was different from that of pure ingredients as depicted in Figure 44. Lidocaine HCl film showed small peaks at 9.40° and 28.56° 2θ. The result was similar to the case of HPMC E15 1:1 film.

The X-ray diffraction pattern of HPC powder did not show any dominant peaks. While from lidocaine HCl mucoadhesive film of HPC 1:1, all peaks

disappeared as shown in Figure 45. This result suggested that all ingredients existed as molecular dispersion or as amorphous state.

The powder X-ray diffractogram of chitosan powder did not show any dominant peaks. No apparent dominant sharp peak appeared in diffractogram of mucoadhesive film of CS 1:1 as illustrated in Figure 46 indicating that lidocaine HCl and other ingredients were existed as molecular dispersion or as amorphous state.

The X-ray diffraction of mucoadhesive film of E15HPC 3:3 is shown in Figure 47. There were two small peaks at 9.38° and 28.56° 2θ. The other dominant peaks disappeared indicating that the crystallinity of lidocaine HCl and other ingredient were reduced after casting.

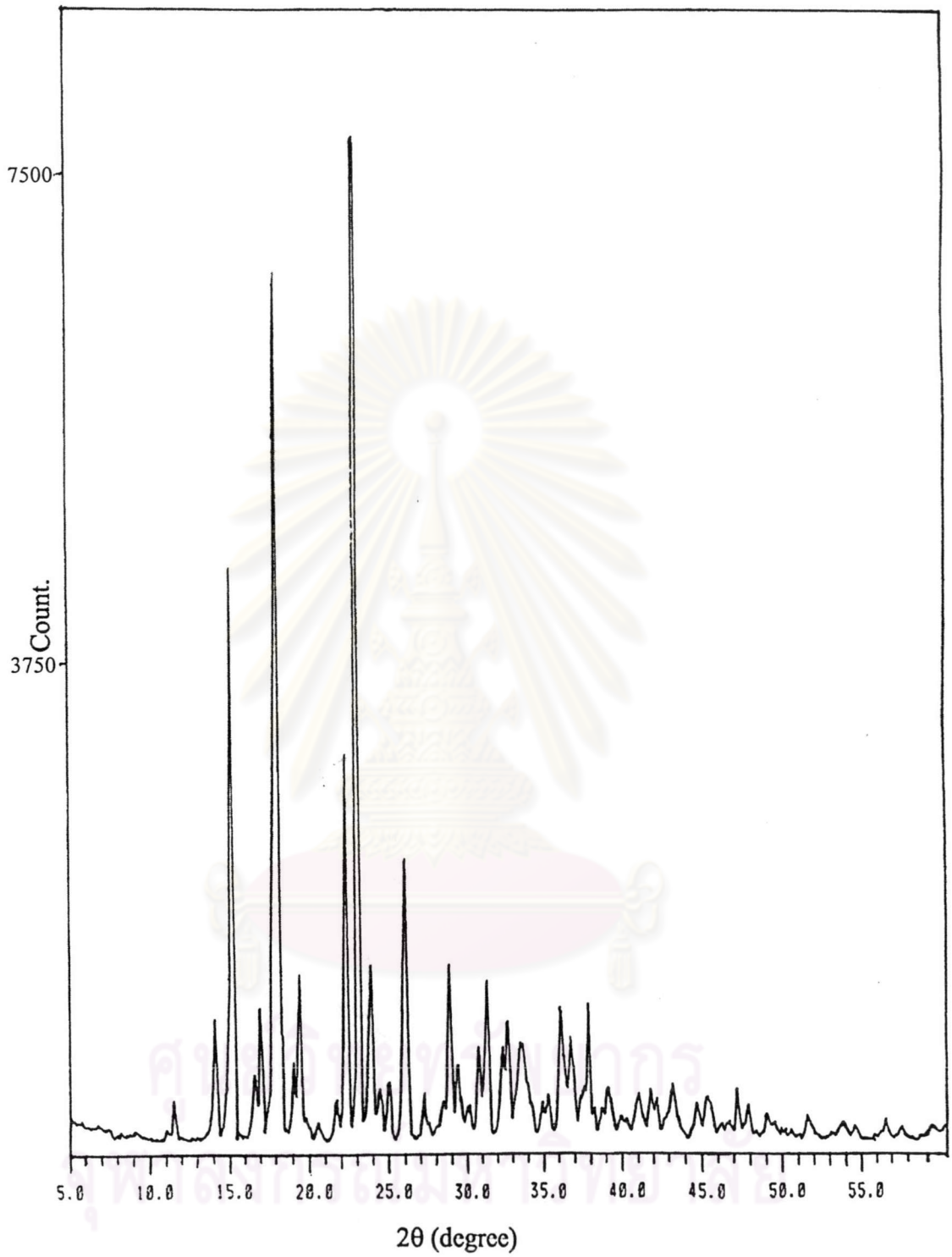

Figure 40 X-ray diffractogram of citric acid

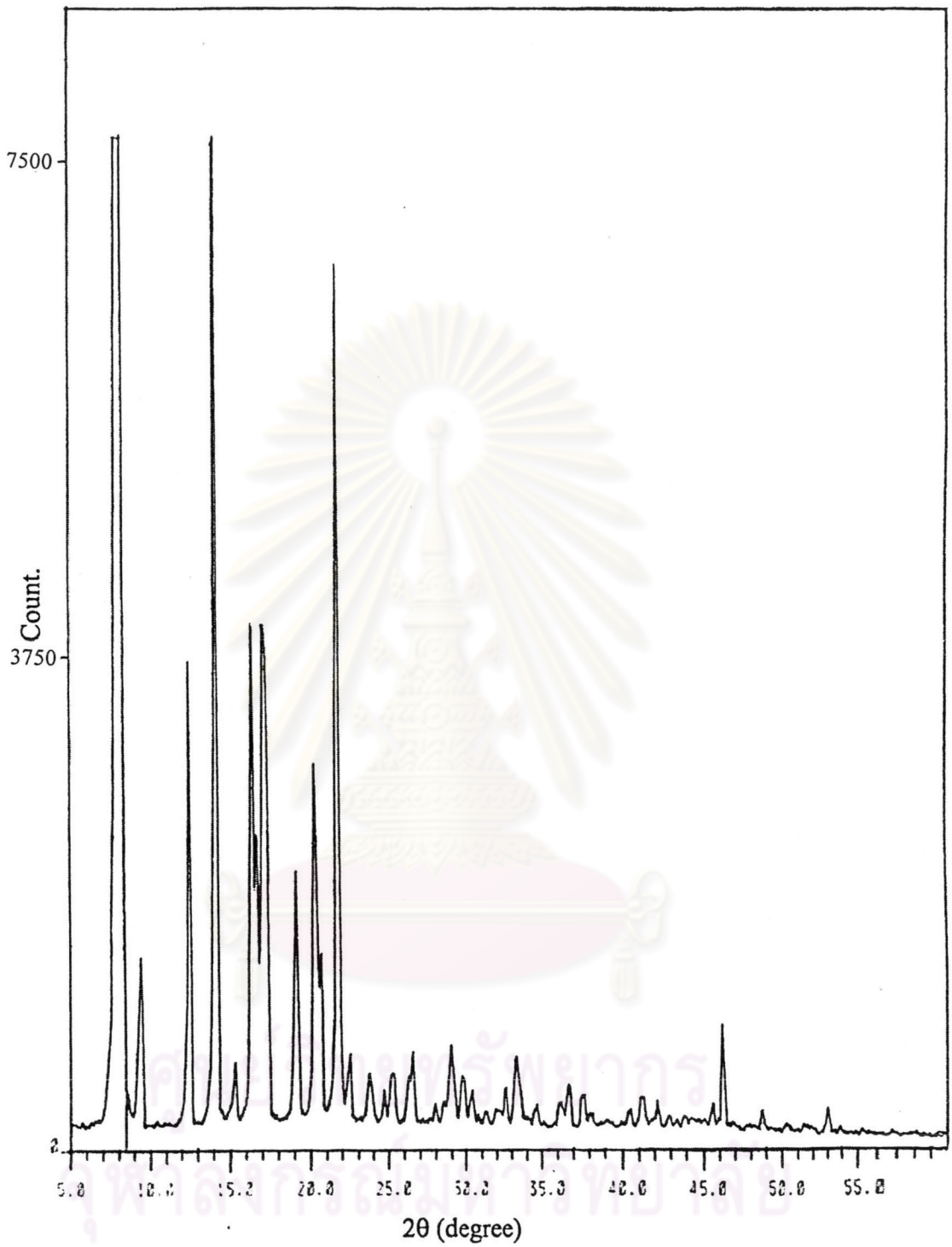

Figure 41 X-ray diffractogram of menthol

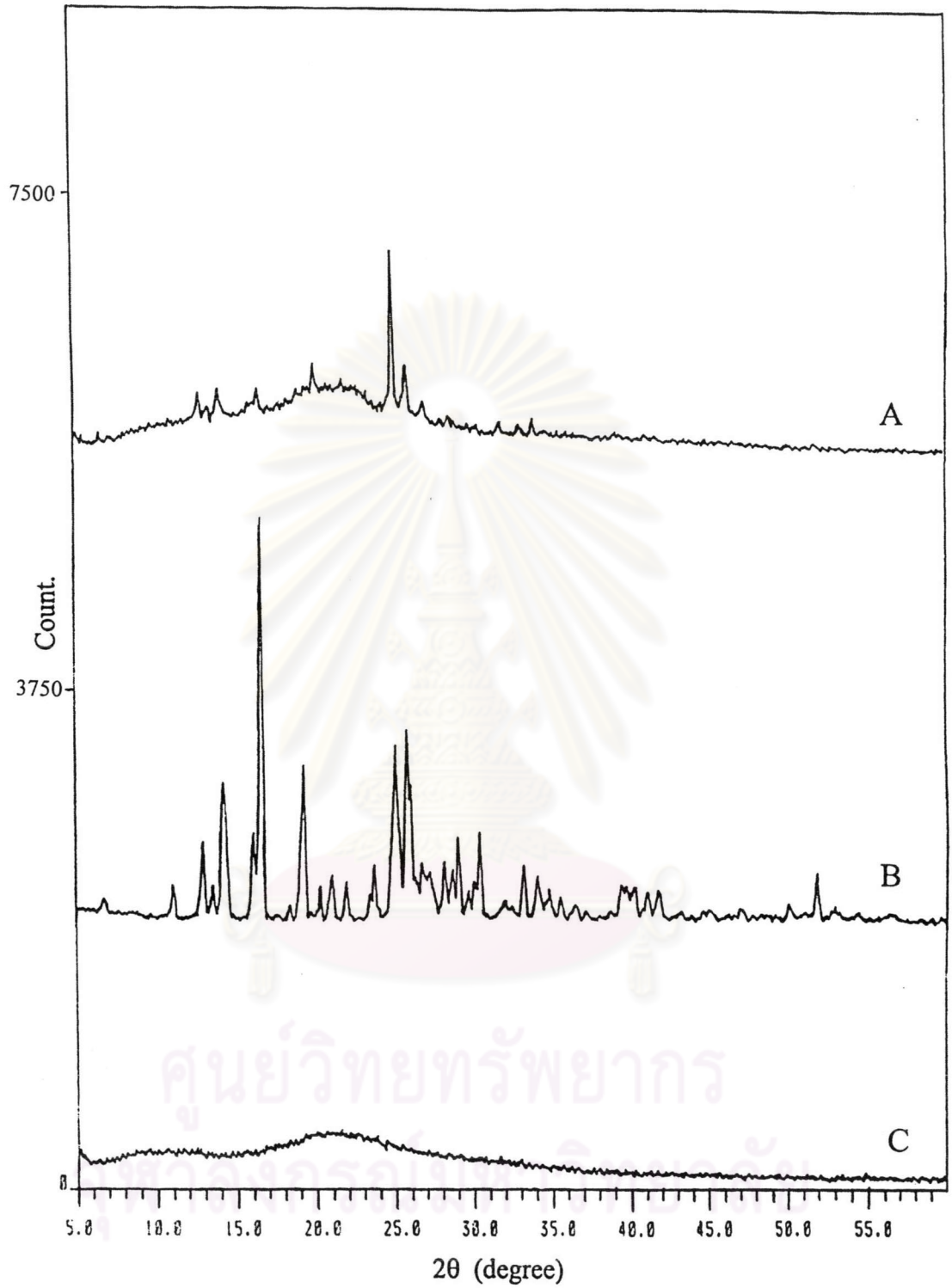

Figure 42 X-ray diffractograms of (A) mucoadhesive film of CMC 1:1; (B) lidocaine HCl; (C) CMC powder

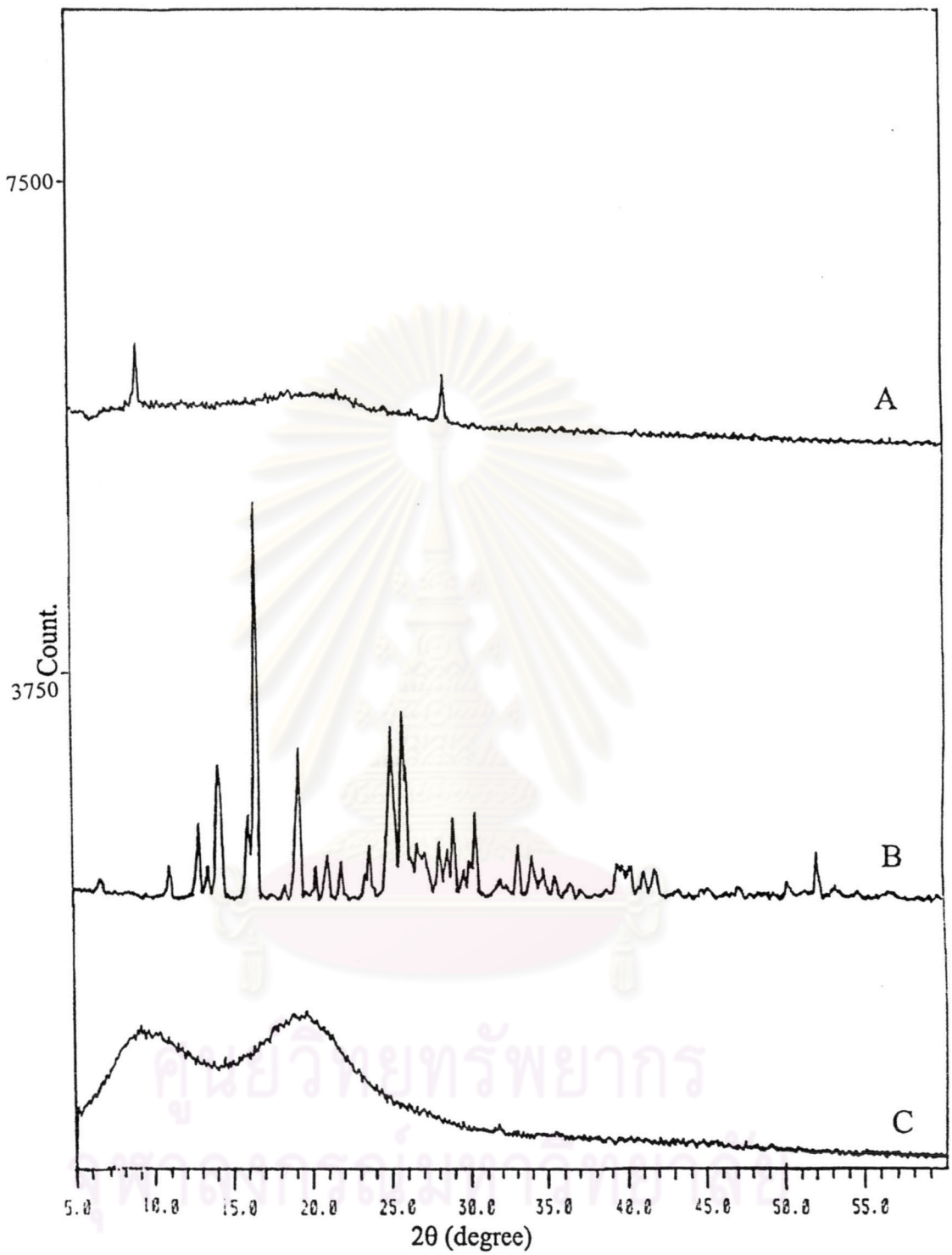

Figure 43 X-ray diffractograms of (A) mucoadhesive film of E15 1:1; (B) lidocaine HCl; (C) HPMC E15 powder

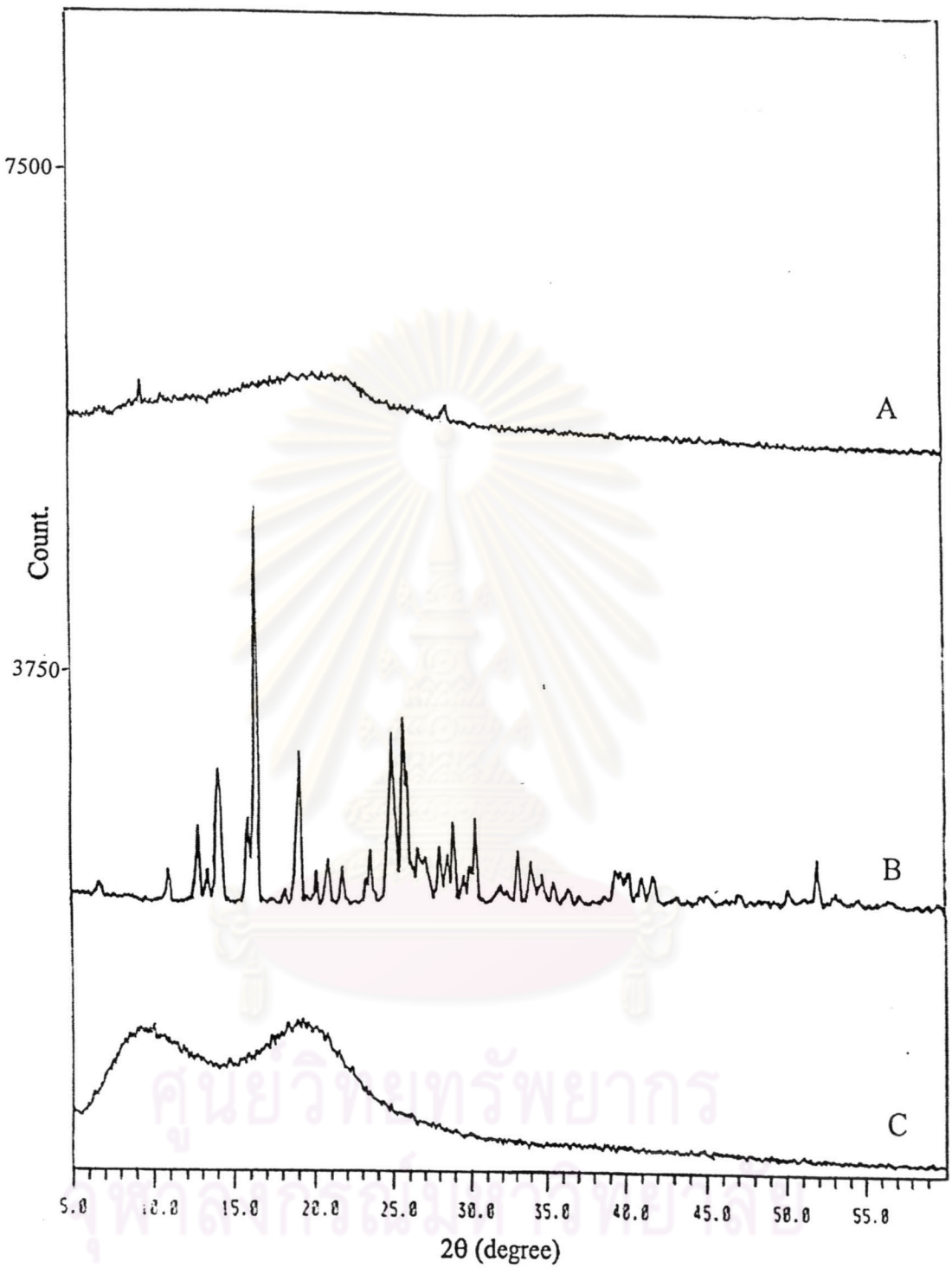

Figure 44 X-ray diffractograms of (A) mucoadhesive film of E4M 1:1; (B) lidocaine HCl; (C) HPMC E4M powder

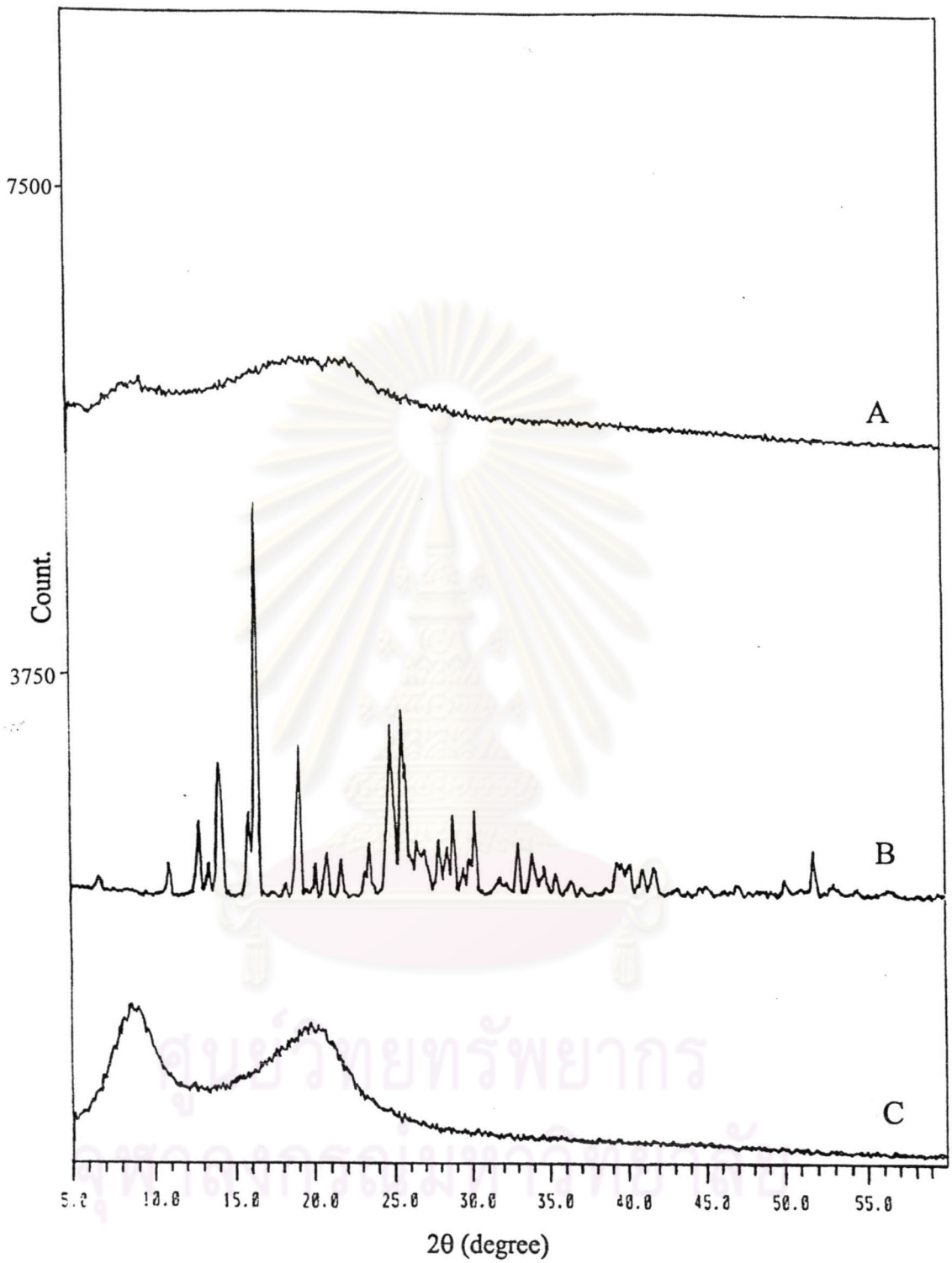

Figure 45 X-ray diffractograms of (A) mucoadhesive film of HPC 1:1; (B) lidocaine HCl; (C) HPC powder

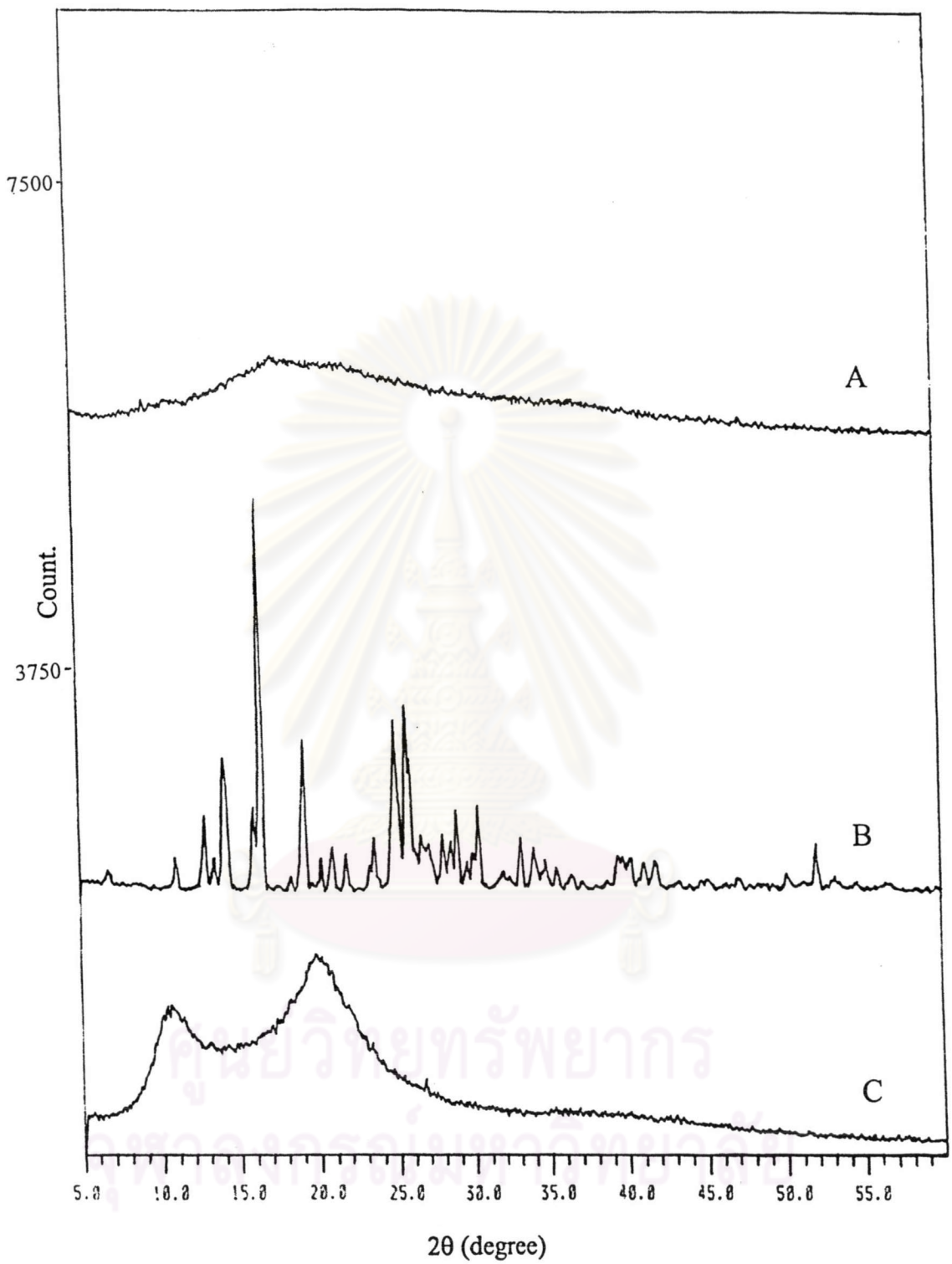

Figure 46 X-ray diffractograms of (A) mucoadhesive film of CS 1:1; (B) lidocaine HCl; (C) chitosan powder

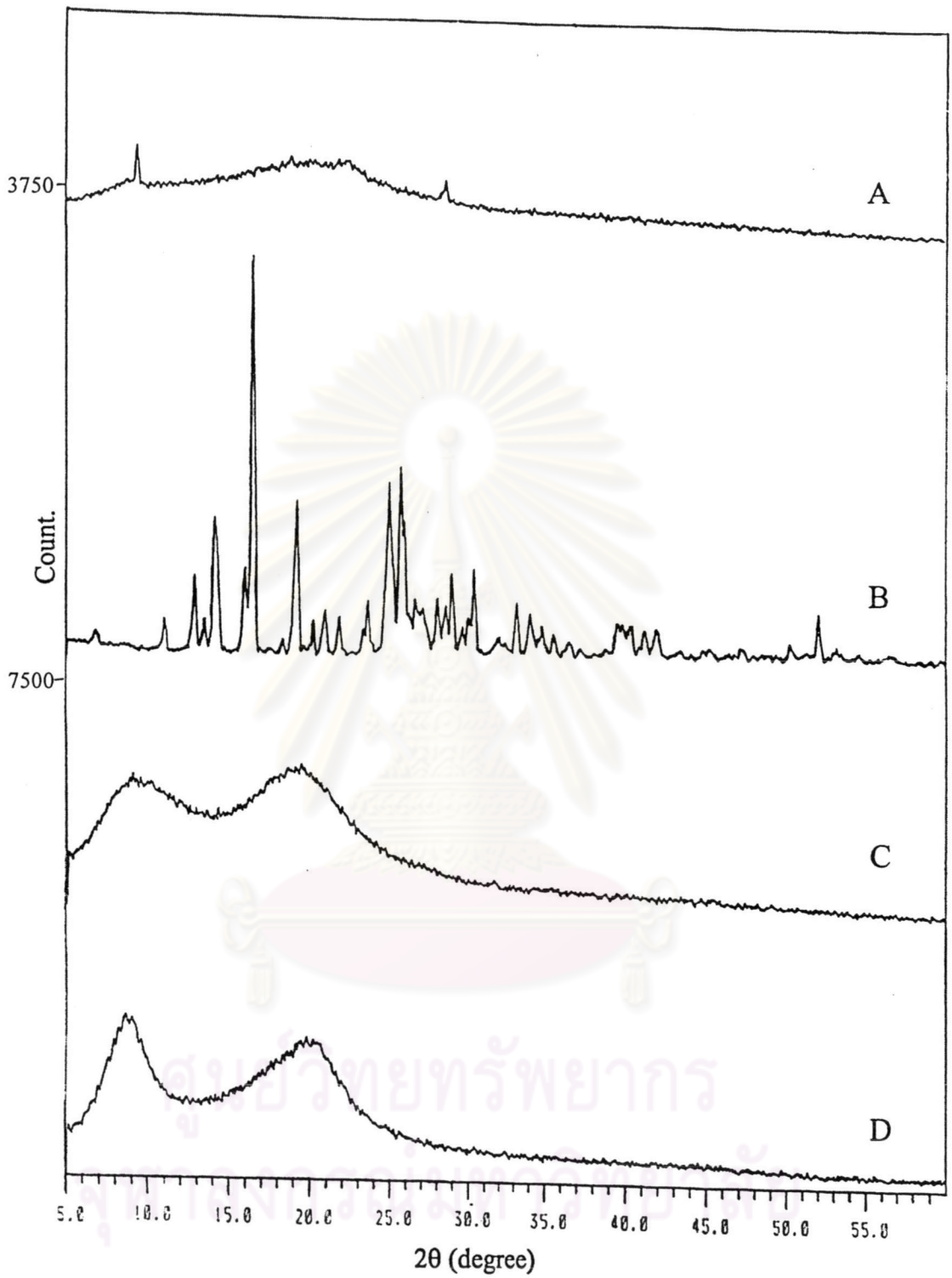

Figure 47 X-ray diffractograms of (A) mucoadhesive film of E15HPC 3:3; (B) lidocaine HCl; (C) HPMC E15 powder; (D) HPC powder

6.3 Differential thermal analysis

Figures 48-53 presents the DSC thermograms of the mucoadhesive ingredients consisting of lidocaine HCl, citric acid, menthol, polymers and lidocaine mucoadhesive films. The DSC thermogram of lidocaine HCl displayed its endothermic peak at 79.3°C due to the melting of crystalline form. The melting point of lidocaine HCl was 74°C to 79°C (Lund, 1994). The DSC thermogram of menthol and citric acid showed endothermic peak at 42.7°C and 158.4°C, respectively. However, no peaks were found in the lidocaine HCl mucoadhesive films. These results indicated that lidocaine HCl and other ingredients changed to either molecular dispersed or amorphous form. Nevertheless CMC film with lidocaine HCl exhibited the very small peak at 67.7°C.

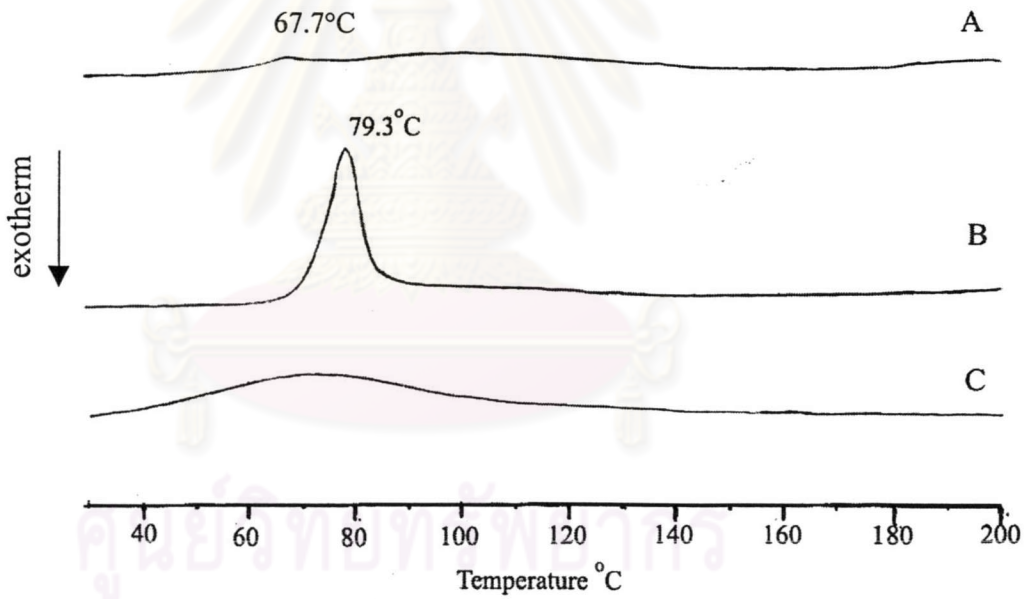

Figure 48 DSC thermograms of (A) mucoadhesive film of CMC 1:1; (B) lidocaine HCl; (C) CMC powder

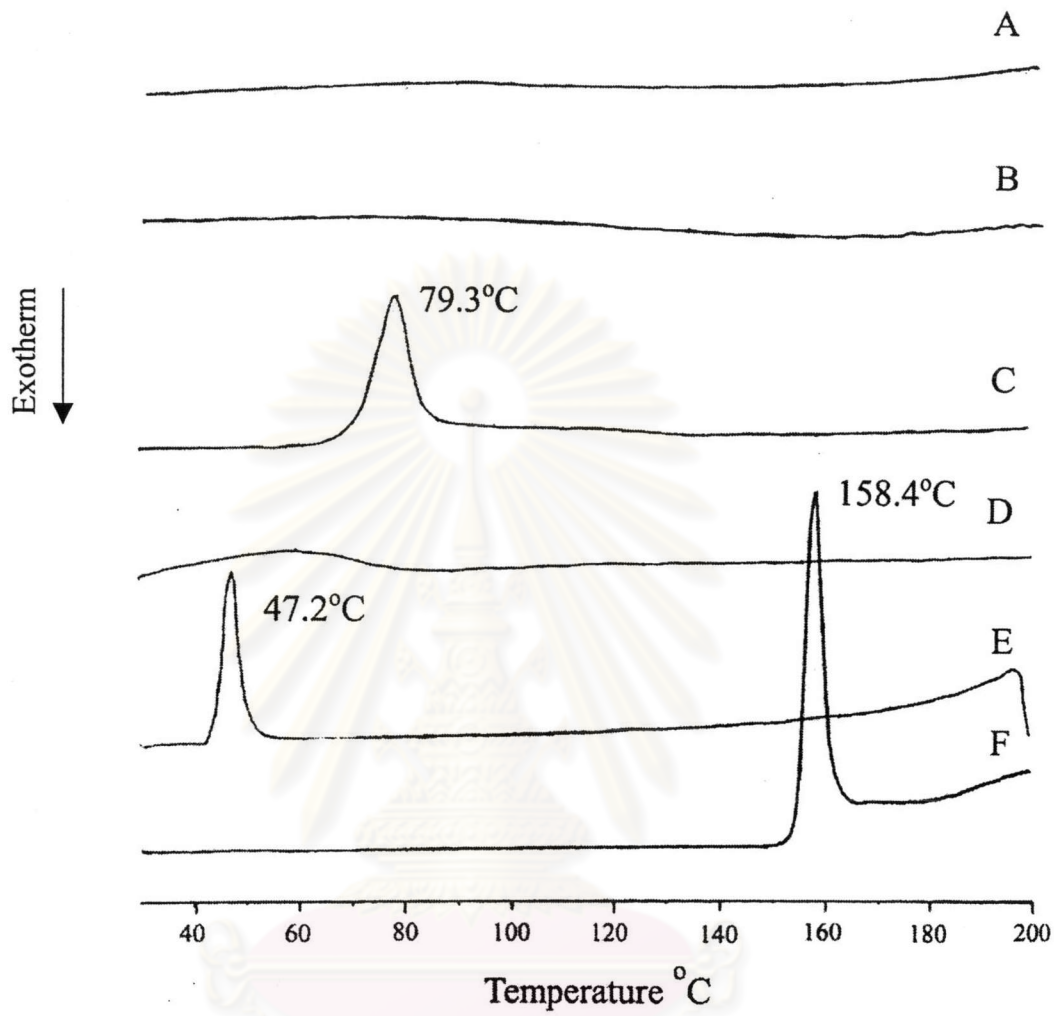

Figure 49 DSC thermograms of (A) mucoadhesive film of E15 1:1; (B) mucoadhesive film of E15 1:0.5; (C) lidocaine HCl; (D) HPMC E15; (E) menthol; (F) citric acid

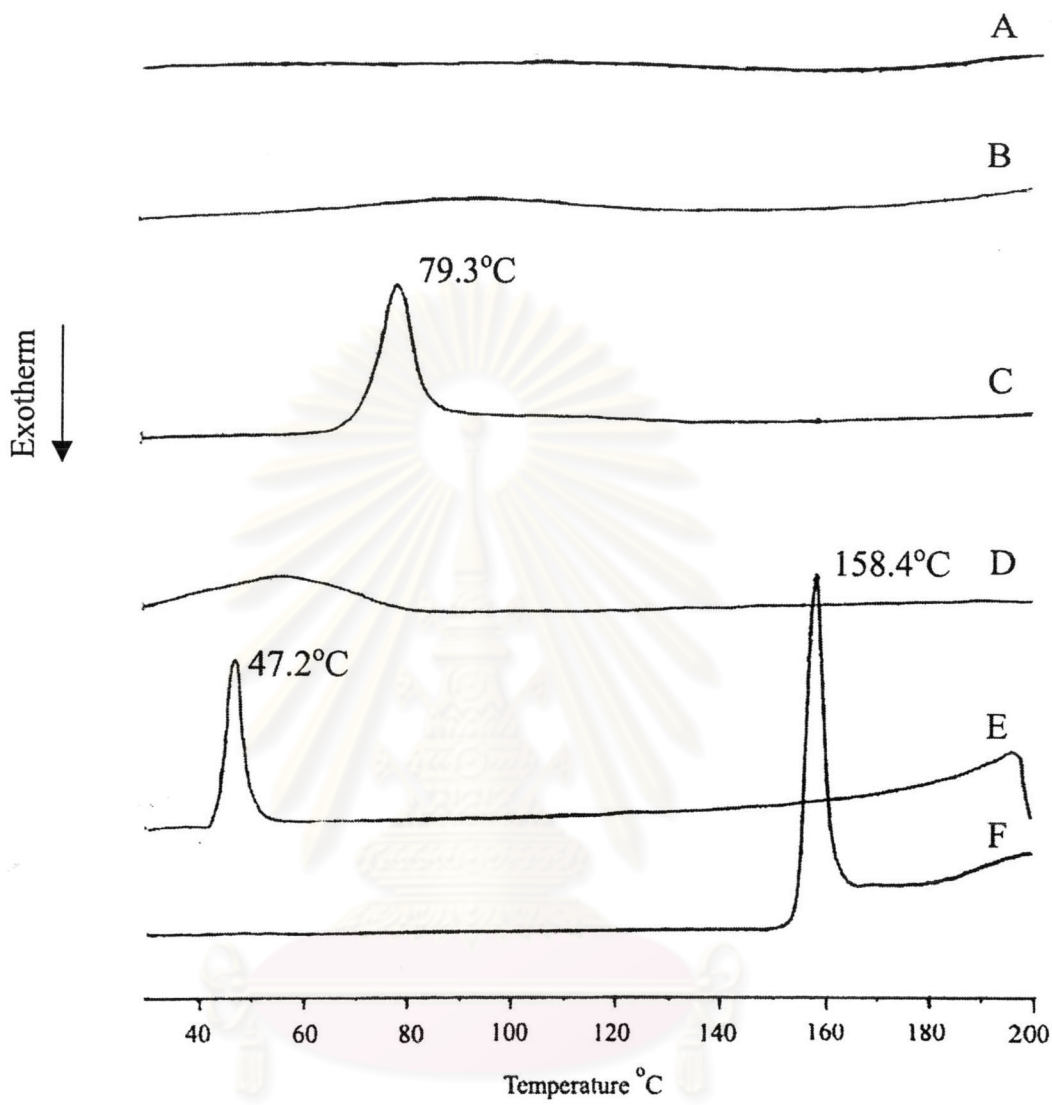

Figure 50 DSC thermograms of (A) mucoadhesive film of E4M 1:1; (B) mucoadhesive film of E4M 1:0.5; (C) lidocaine HCl; (D) HPMC E4M; (E) menthol; (F) citric acid

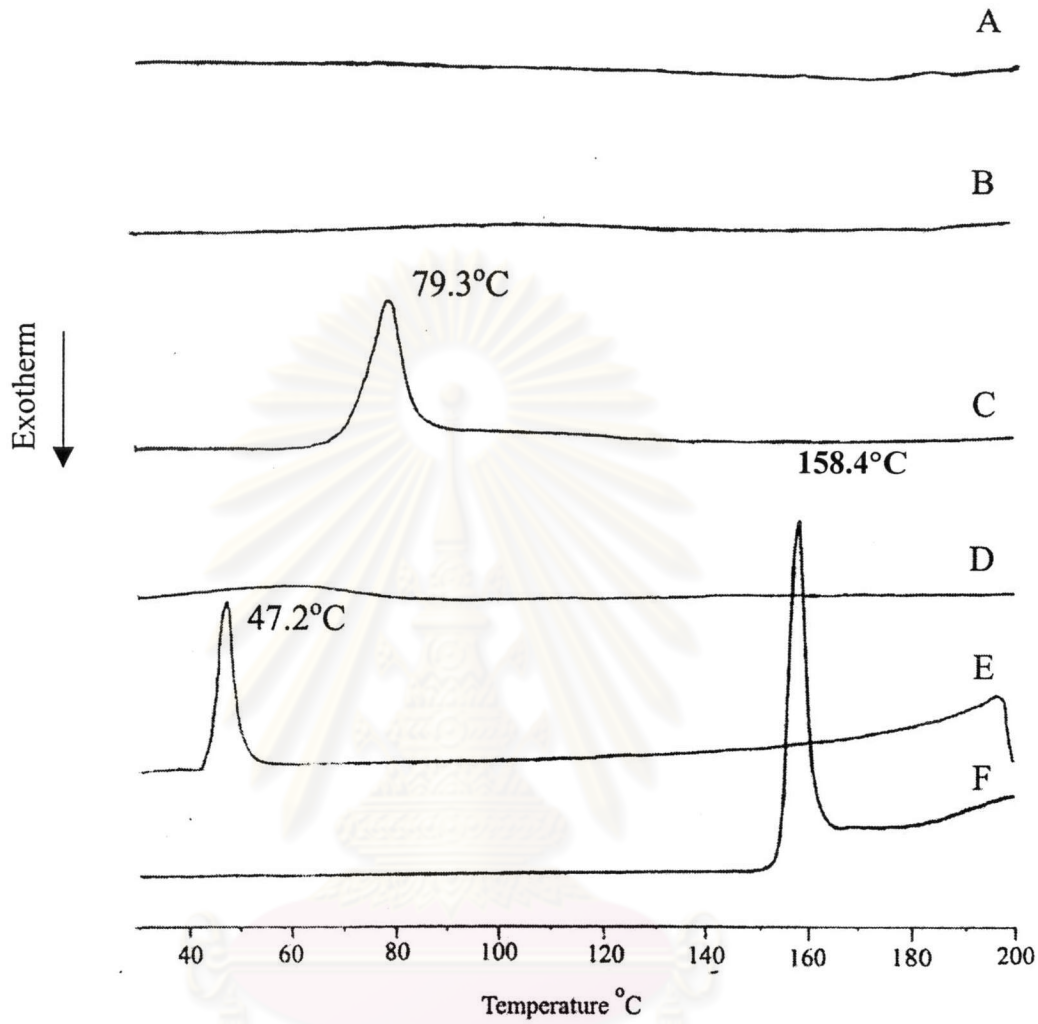

Figure 51 DSC thermograms of (A) mucoadhesive film of HPC 1:1; (B) mucoadhesive film of HPC 1:0.5; (C) lidocaine HCl; (D) HPC; (E) menthol; (F) citric acid

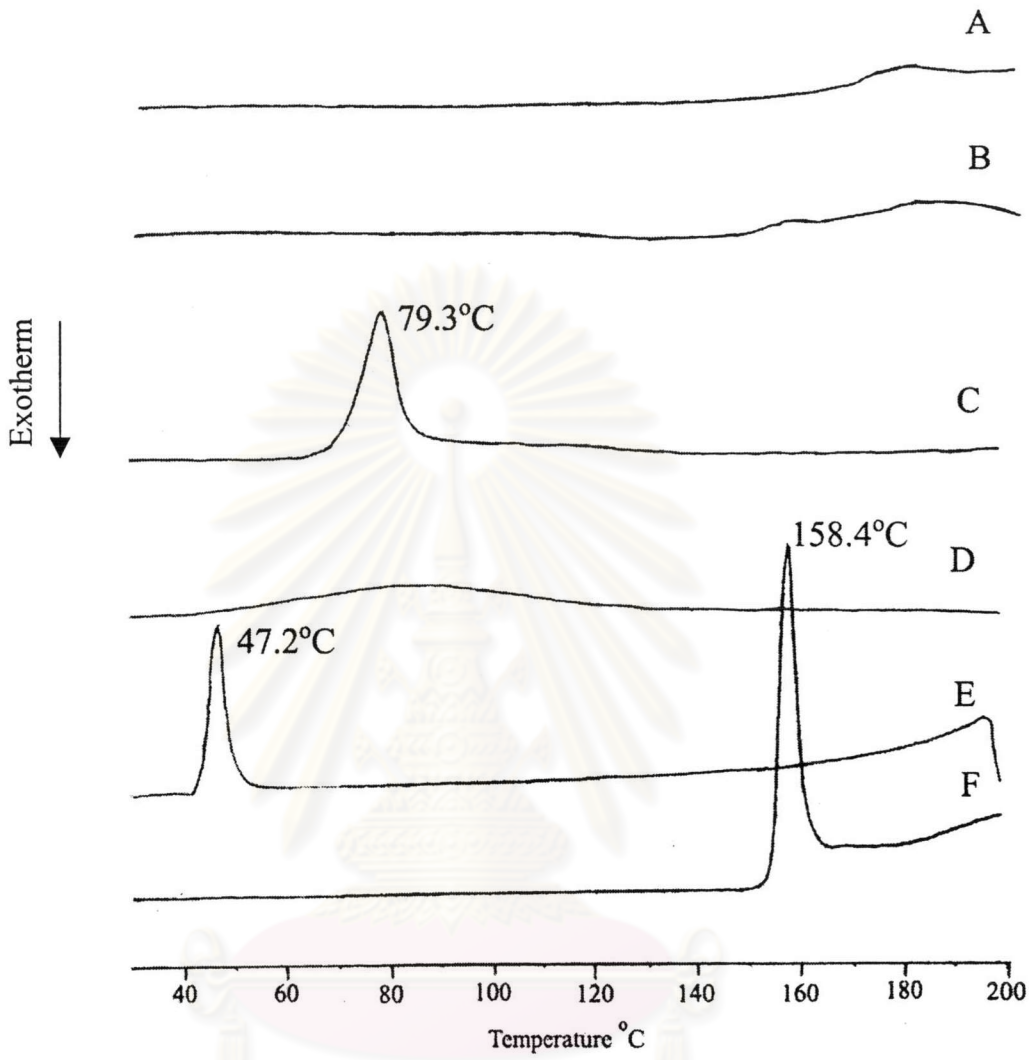

Figure 52 DSC thermograms of (A) mucoadhesive film of CS 1:1; (B) mucoadhesive film of CS 1:0.5; (C) lidocaine HCl; (D) chitosan; (E) menthol; (F) citric acid

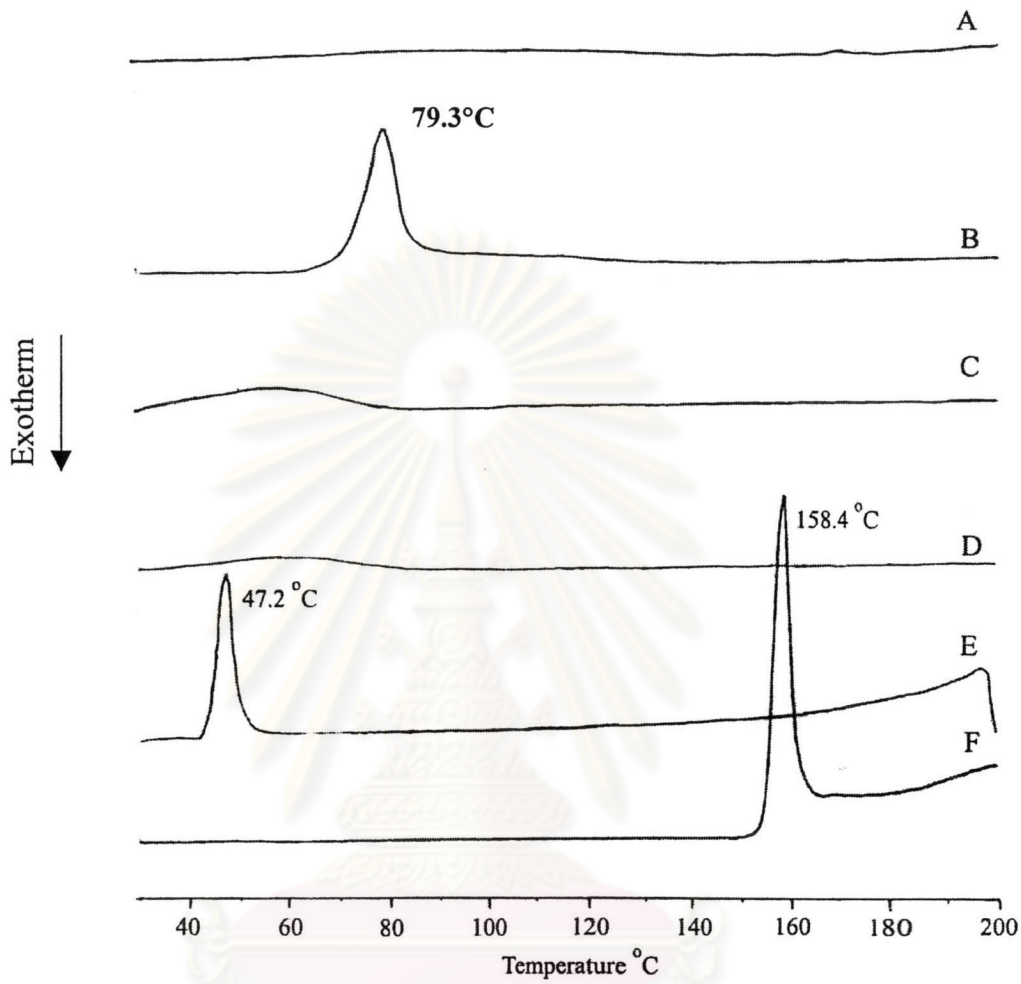

Figure 53 DSC thermograms of (A) mucoadhesive film of E15HPC 3:3; (B) lidocaine HCl; (C) HPMC E15; (D) HPC; (E) menthol; (F) citric acid

7. Tensile properties

Tensile properties including, percent strain at point of break, Young's modulus and ultimate tensile strength are presented in Table 11 and Figures 54-59. Focused on percent strain at point of break as shown in Figures 54 and 55, HPC films had the highest percent strain when compared to films from other polymers within drug to polymer ratio of 1:0.67. There is no significant difference between HPC and HPMC E15 films when compared within drug to polymer ratios of 1:1 and 1:0.5, upon test with one-way ANOVA. The lowest percent strain at point of break was observed in chitosan films for all drug to polymer ratios. For the combination of polymers, Formula E15 1:1 (HPMC E15:HPC, 3:0) and HPC 1:1 (HPMC E15:HPC, 0:3) had the highest percent strain. Increasing the proportion of HPMC E15 decreased the percent strains at point of break.

Focused on Young's modulus, HPC films had the lowest value of Young's modulus for all drug to polymer ratios as shown in Figure 56. Chitosan films had the highest value of Young's modulus at drug to polymer ratio of 1:0.67 and 1:0.5. At drug to polymer ratio of 1:1, HPMC E4M film had the highest value of Young's modulus. For combination of polymers, decrease in proportion of HPMC E15 likely decrease the Young' modulus as shown in Figure 57.

Focused on tensile strength as shown in Figure 58, HPMC E4M films exhibited the highest value of tensile strength for all drug to polymer ratios as shown in Figure 58, whereas HPC films had the lowest value. The comparison of the tensile strength values of the mucoadhesive combined polymeric films are shown in Figure 59. Increasing HPMC E15 content increased the tensile strength of the films.

Comparison in viscosity grades of HPMC, HPMC E15 (15 cps) and HPMC E4M (4000 cps), HPMC of higher viscosity grade exhibited higher Young's modulus and tensile strength but lower percent strain at point of break.

Table 12 Tensile properties of lidocaine HCl mucoadhesive films

Formula	% Strain at point of break ± SD (%)	Young's modulus ± SD (Mpa)	Ultimate tensile strength ± SD (Mpa)
E15 1:1	180.503 ± 5.691	164.509 ± 9.633	31.357 ± 1.807
E15 1:0.67	155.644 ± 8.737	96.951 ± 7.850	21.360 ± 1.413
E15 1:0.5	138.480 ± 5.184	16.415 ± 3.724	5.818 ± 0.219
E4M 1:1	18.354 ± 1.411	312.189 ± 14.070	33.666 ± 1.138
E4M 1:0.67	104.940 ± 5.917	188.432 ± 44.165	30.029 ± 1.915
E4M 1:0.5	179.699 ± 18.123	93.749 ± 8.445	19.221 ± 1.712
HPC 1:1	183.584 ± 9.200	4.984 ± 0.604	4.731 ± 0.564
HPC 1:0.67	236.394 ± 62.011	8.099 ± 2.118	11.728 ± 2.220
HPC 1:0.5	168.420 ± 31.359	7.656 ± 2.133	6.645 ± 1.440
CS 1:1	135.503 ± 2.231	248.800 ± 36.729	18.678 ± 0.654
CS 1:0.67	13.895 ± 1.410	294.517 ± 13.066	20.103 ± 0.972
CS 1:0.5	5.998 ± 0.942	218.400 ± 12.376	8.404 ± 0.375
E15HPC 1:3	152.419 ± 15.270	10.376 ± 0.756	7.008 ± 0.622
E15HPC 2:3	130.421 ± 4.335	27.054 ± 3.522	7.238 ± 0.853
E15HPC 3:3	64.255 ± 8.831	92.189 ± 9.101	11.044 ± 0.228
E15HPC 3:2	61.310 ± 4.038	138.853 ± 21.966	12.891 ± 0.634
E15HPC 3:1	59.536 ± 6.239	166.895 ± 28.561	18.293 ± 1.497

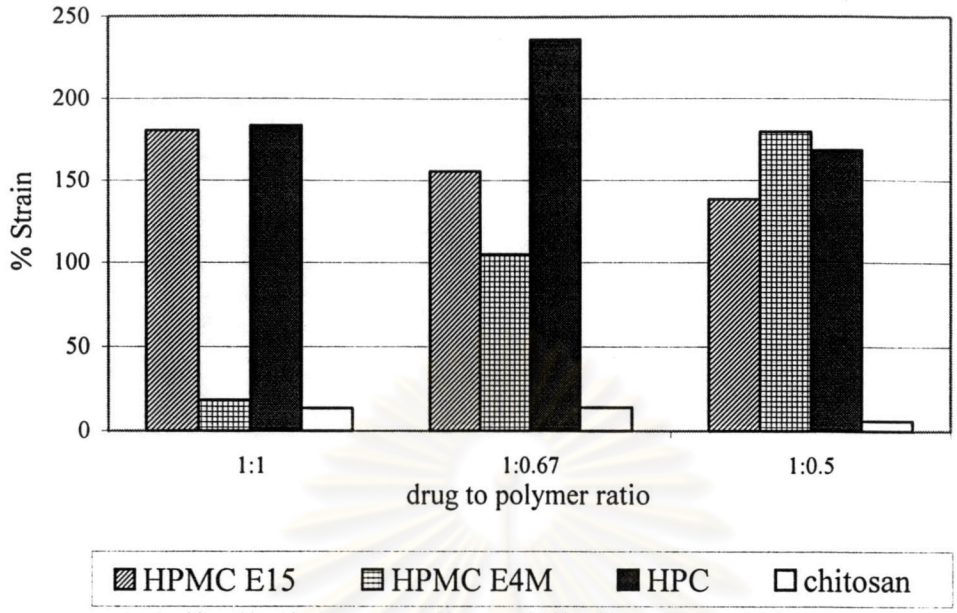

Figure 54 Percent strain at point of break of lidocaine HCl mucoadhesive films

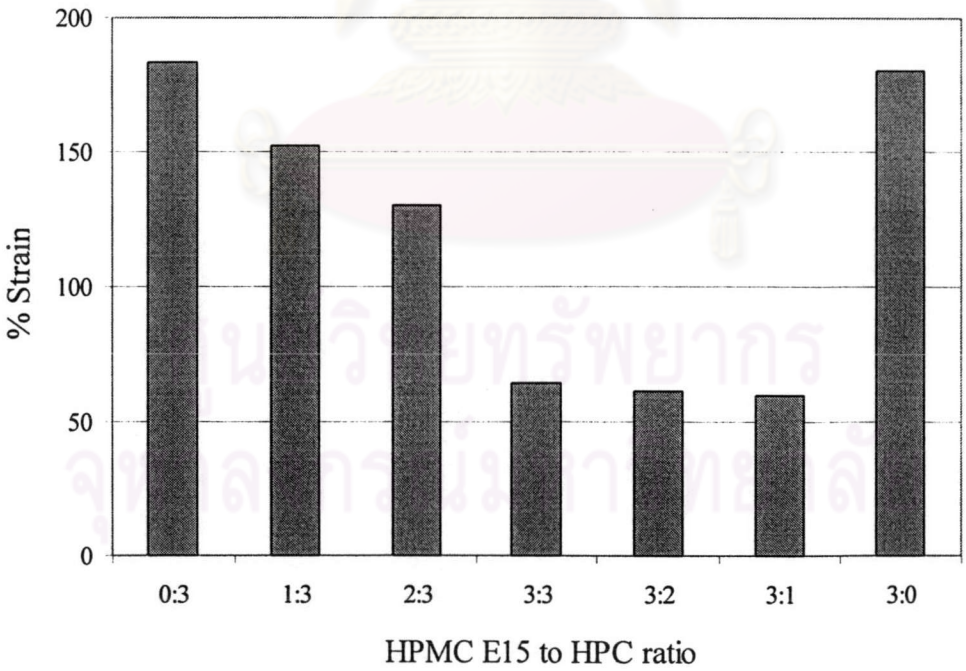

Figure 55 Percent strain at point of break of lidocaine HCl mucoadhesive films from combination of HPMC E15 and HPC with drug to polymer ratio of 1:1

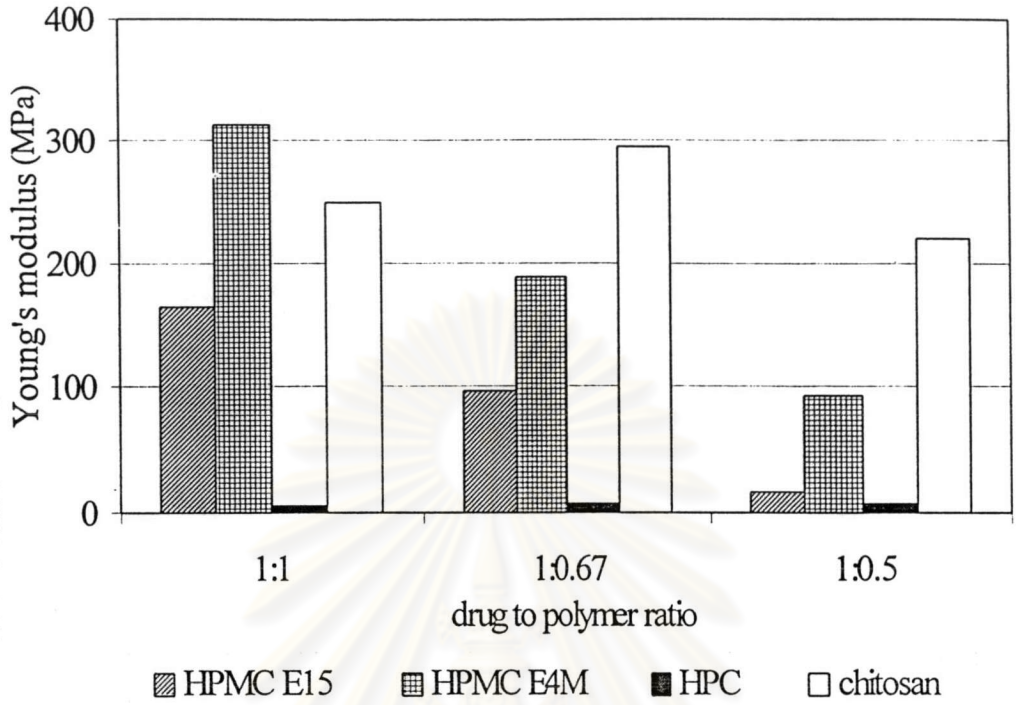

Figure 56 Young's modulus of lidocaine HCl mucoadhesive films

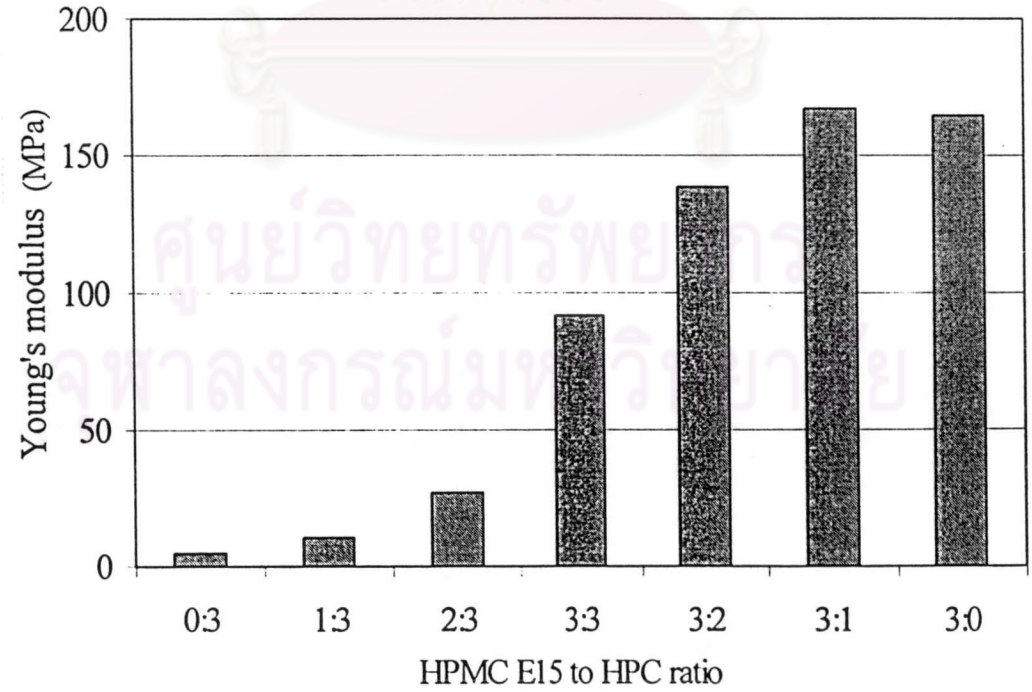

Figure 57 Young's modulus of lidocaine HCl mucoadhesive films from combination of HPMC E15 and HPC at drug to polymer ratio of 1:1

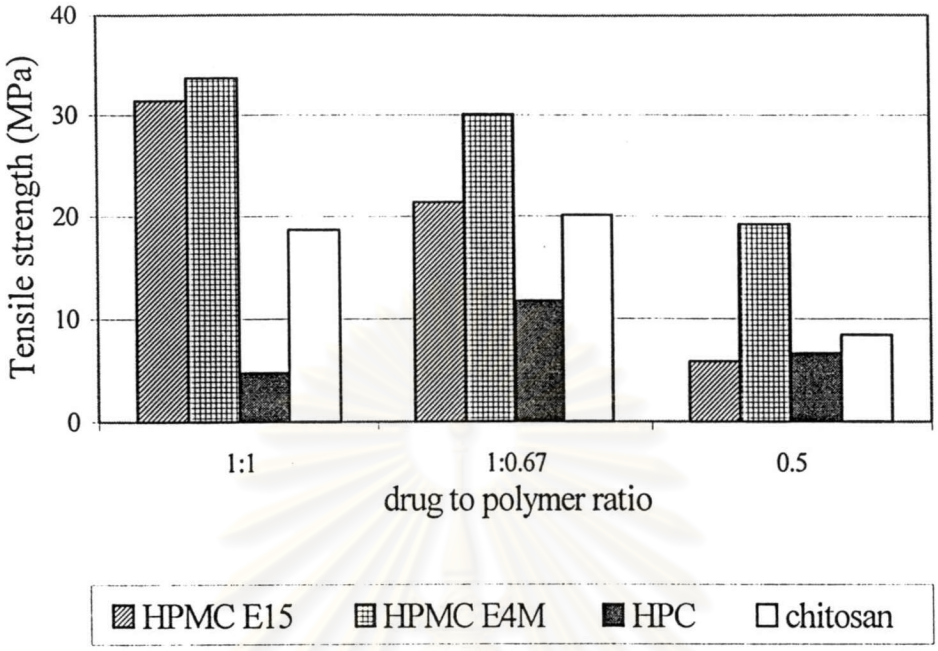

Figure 58 Ultimate tensile strength of lidocaine HCl mucoadhesive films

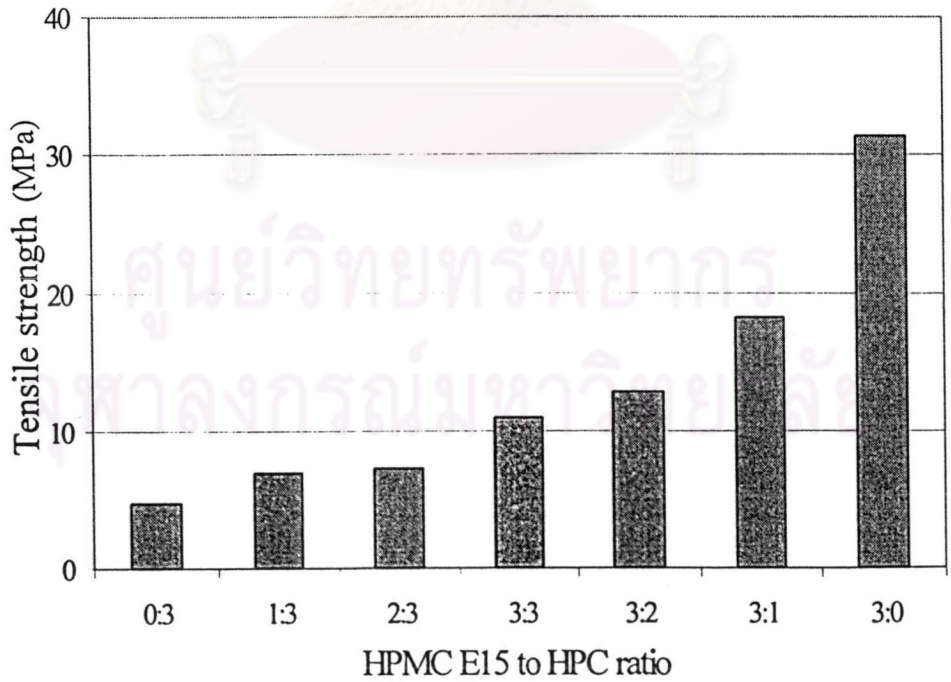

Figure 59 Ultimate tensile strength of lidocaine HCl mucoadhesive films from combination of HPMC E15 and HPC at drug to polymer ratio of 1:1

8. Moisture sorption and swelling property

8.1 Moisture sorption study

As shown in Figures 60-63, the moisture sorption of various mucoadhesive films showed an increase in moisture sorption with an increase of relative humidity. Focused on drug to polymer ratio of 1:1, chitosan provided the films that could absorbed more moisture than other polymers, while HPC films could absorbed the least. At 53%, 75% and 84%RH, the moisture sorptions of all polymers were at equilibrium within 24 hours after exposure to the moisture except those of chitosan films. The latter films continually showed an increase in moisture sorption with an increase of time. At the lower relative humidity (53%RH), no statistical difference was observed between HPMCs and HPC but in higher relative humidity HPMCs could absorb more moisture. When tested with one-way ANOVA, both HPMC E15 (15 cps) and HPMC E4M (4000 cps) showed no statistically significant difference in moisture sorption at the same time and the same relative humidity. The effect of HPMC E15 to HPC ratios on the moisture sorption of the mucoadhesive films was also observed. At 53%RH, combination of both polymers showed no significant difference when compared to either Formula E15 1:1 or Formula HPC 1:1, while significant difference was observed at higher relative humidity.

Focused on higher drug to polymer ratios of 1:0.67 and 1:0.5, as shown in Figures 61 and 62, the results of moisture sorption were similar to those obtained from the films of the lower ratio of 1:1.

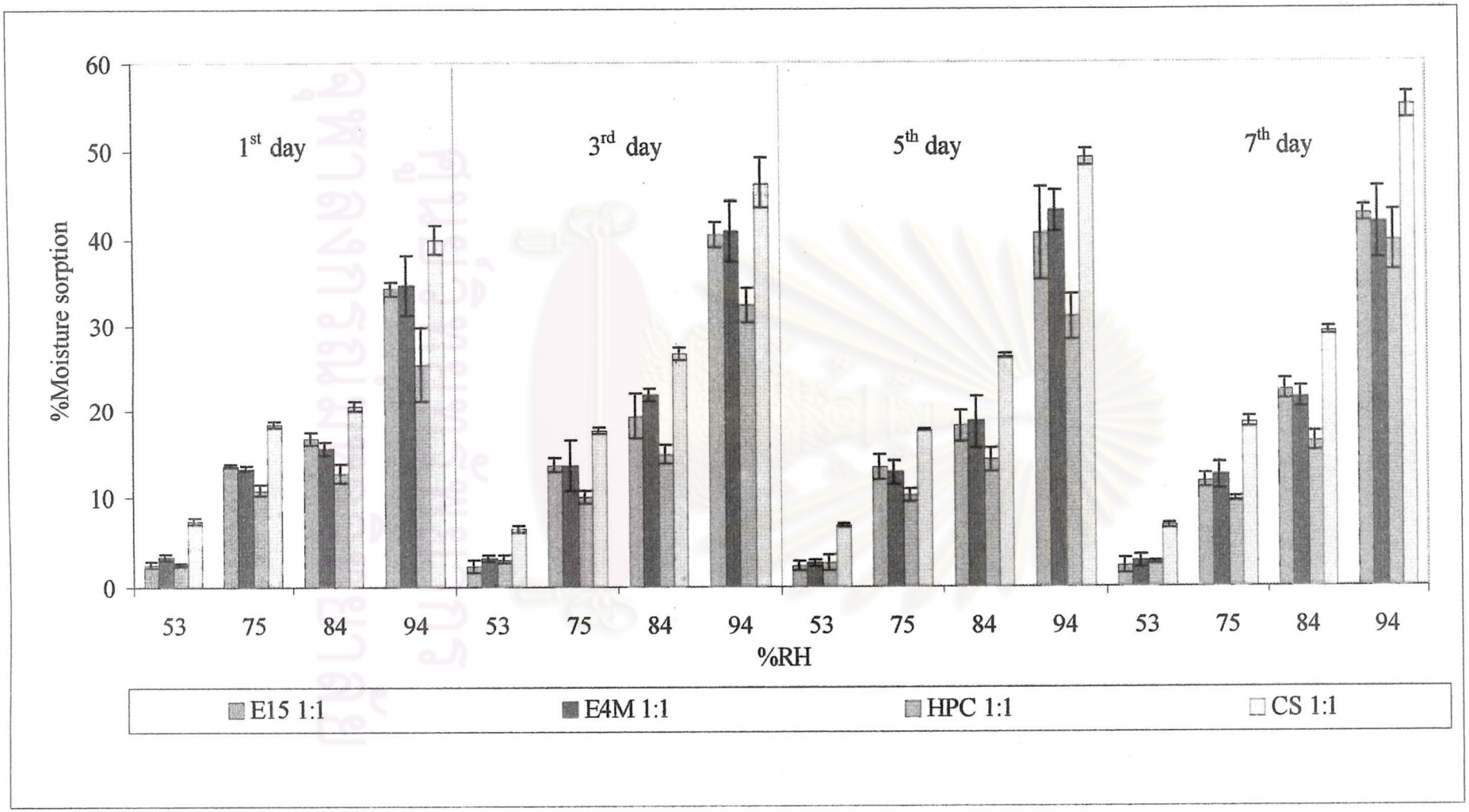

Figure 60 Percentage of moisture sorption of mucoadhesive films prepared from various polymers with drug to polymer ratio of 1:1

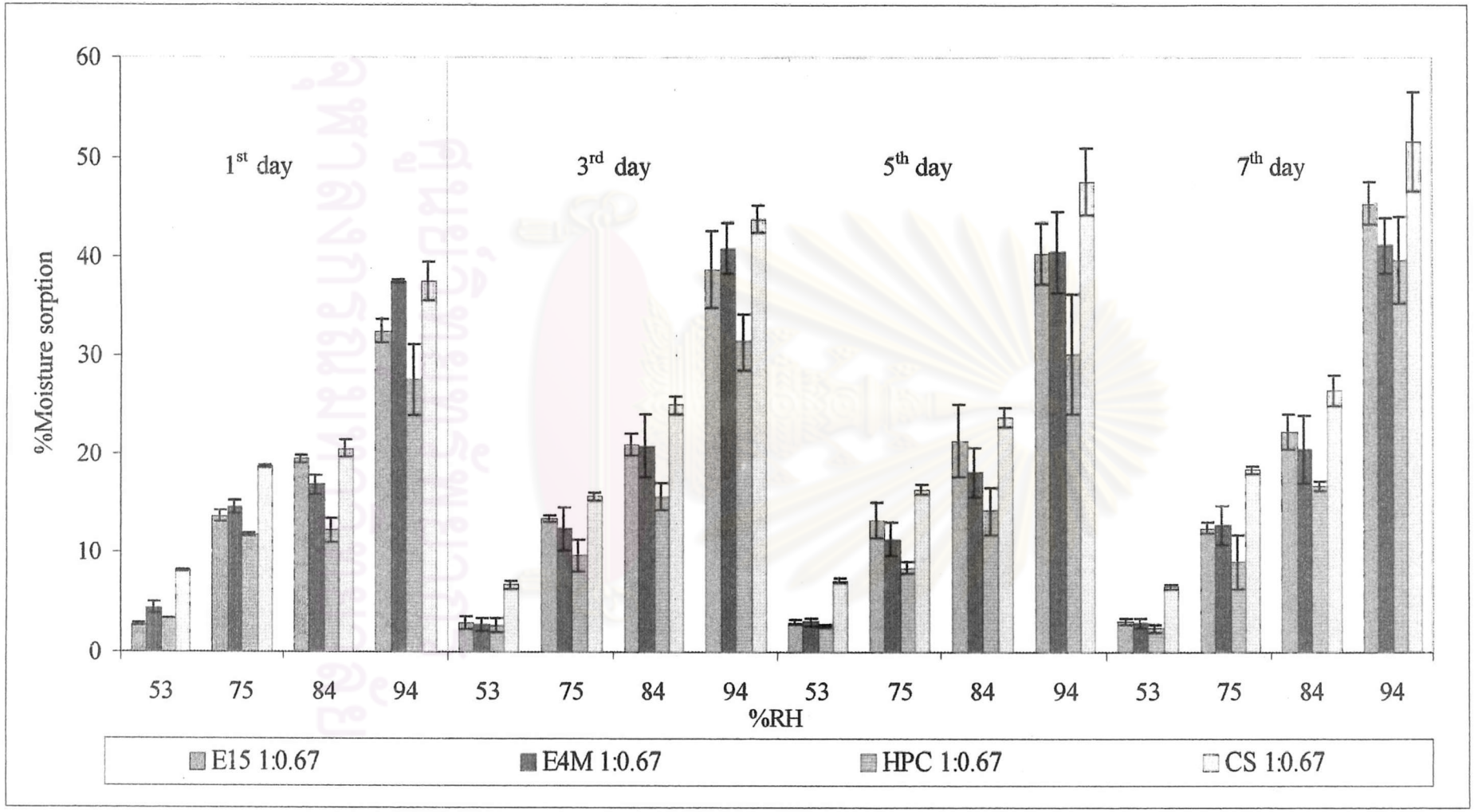

Figure 61 Percentage of moisture sorption of mucoadhesive films prepared from various polymers with drug to polymer ratio of 1:0.67

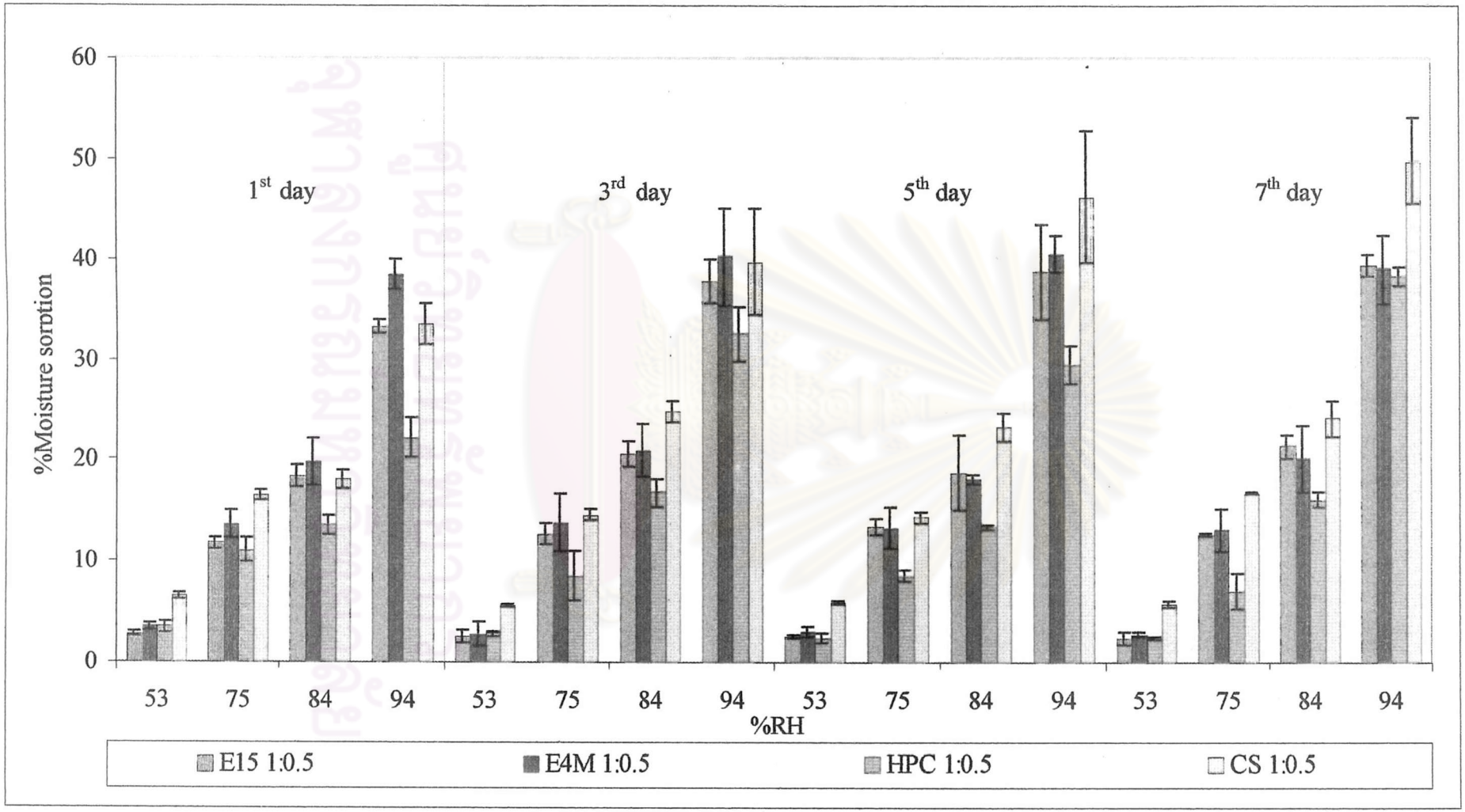

Figure 62 Percentage of moisture sorption of mucoadhesive films prepared from various polymers with drug to polymer ratio of 1:0.5

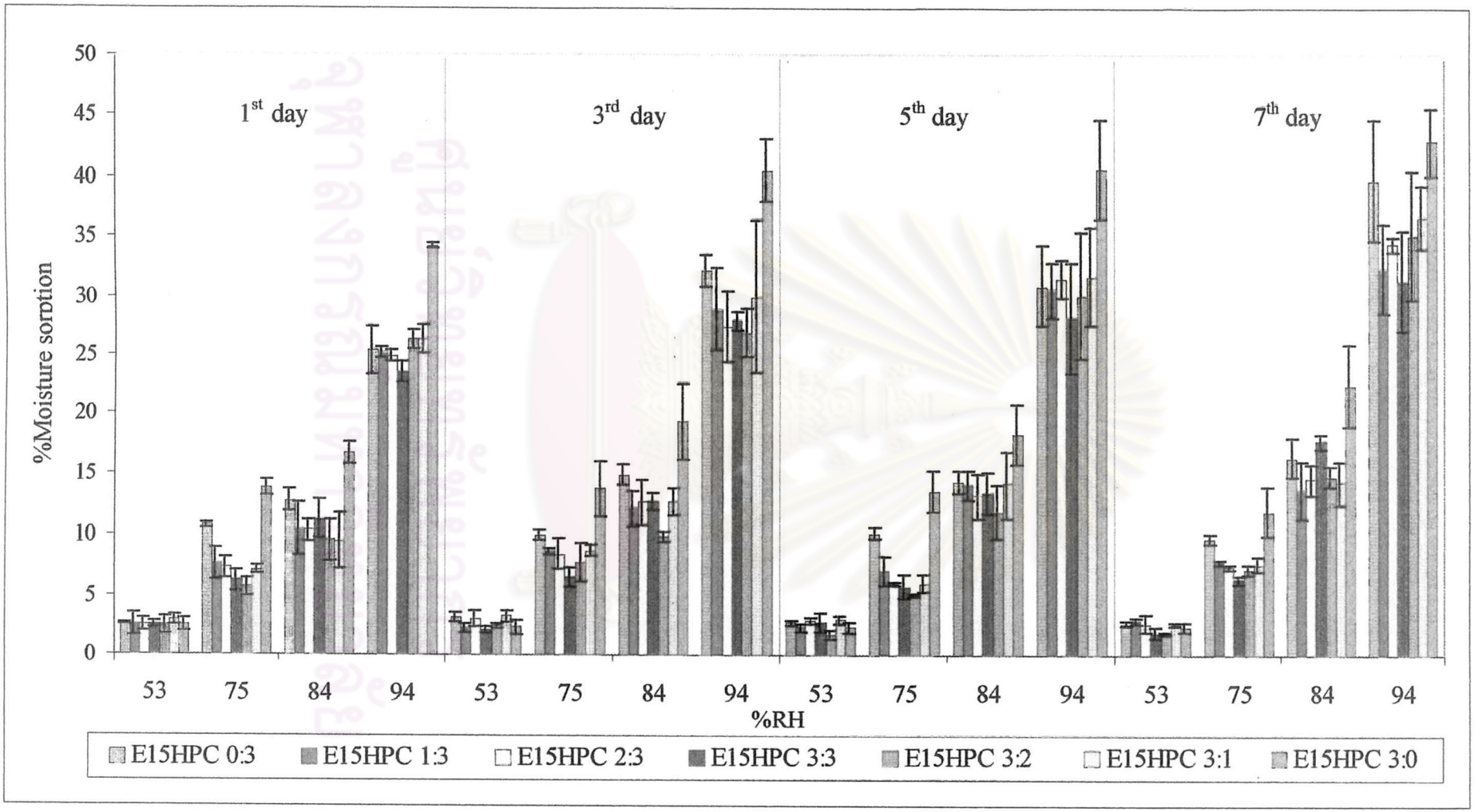

Figure 63 Percentage of moisture sorption of mucoadhesive films prepared from combination of HPMC E15 and HPC with drug to polymer ratio of 1:1

8.2 Swelling property of mucoadhesive films

As shown in Figures 64-67, the swelling of mucoadhesive films increased with the increasing relative humidity. At drug to polymer ratio of 1:1 and 75%RH and 84%RH, HPMC E15 films showed higher value of swelling than HPMC E4M, as shown in Figure 64. But when tested with one-way ANOVA, statistically significant difference were not observed for all relative humidities. At 53% RH chitosan films could swell less than other polymeric film. Although chitosan films could swell more than other polymers at higher relative humidity (84% and 94%RH), chitosan films had slower swelling rate than other polymers. Comparison between HPC and other polymers, although HPC films exhibited slower swelling rate than HPMC E15 at 75% and 84% RH, no significant difference was observed at the 7^{th} day for all relative humidities except it could swell less than chitosan film at 84% and 94%RH.

At drug to polymer ratio of 1:0.67 and 53%RH, HPMC E4M showed the highest swelling after the 5^{th} day. HPMC E15 had the highest swelling at 94%RH in the 1^{st} day. But at the 7^{th} day, no significant difference was observed. The results indicated that HPMC E15 rapidly swelled at high relative humidity.

At drug to polymer ratio of 1:0.5, the results of the swelling of the films were similar to the results of films containing drug to polymer ratio of 1:0.67.

Focused on the combination polymer of HPMC E15 and HPC, the ratio of 3:1 had the maximum swelling at the high relative humidity (84% and 94%RH). But at lower relative humidity (53% and 75%RH), HPC could swell less than HPMC E15 film which had the maximum swelling.

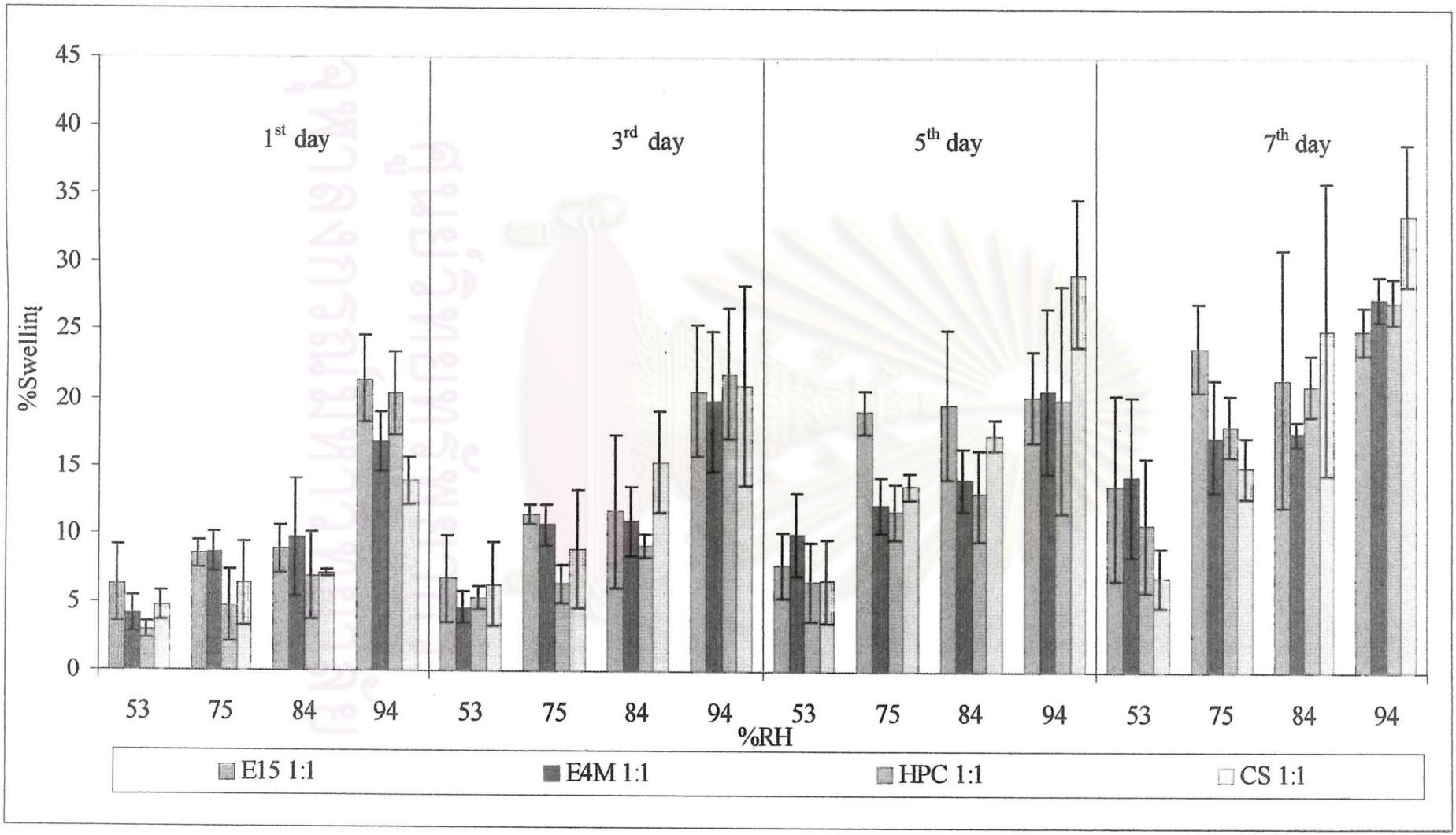

Figure 64 Percentage swelling of mucoadhesive films containing various polymers with drug to polymer ratio of 1:1

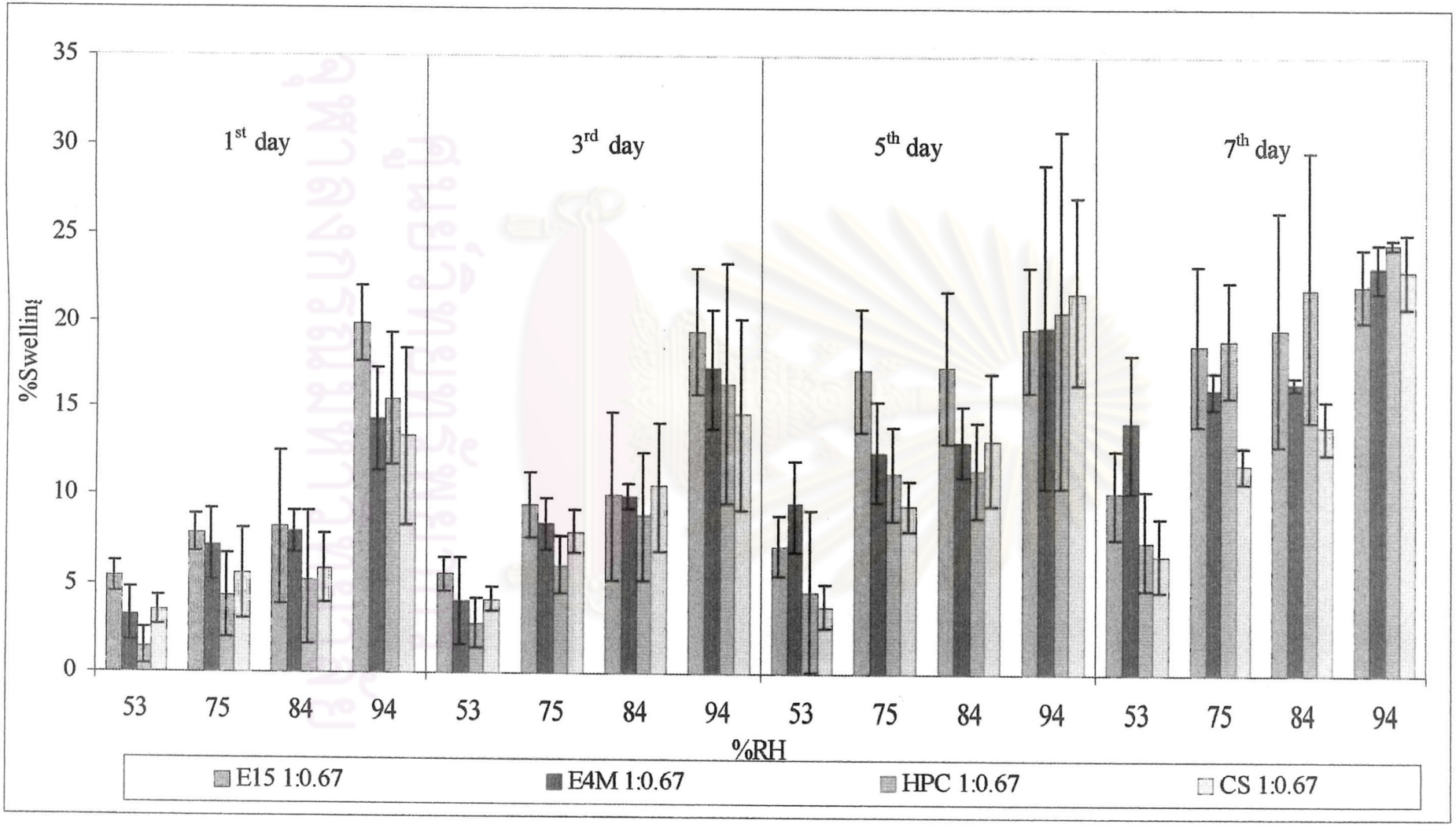

Figure 65 Percentage swelling of mucoadhesive films containing various polymers with drug to polymer ratio of 1:0.67

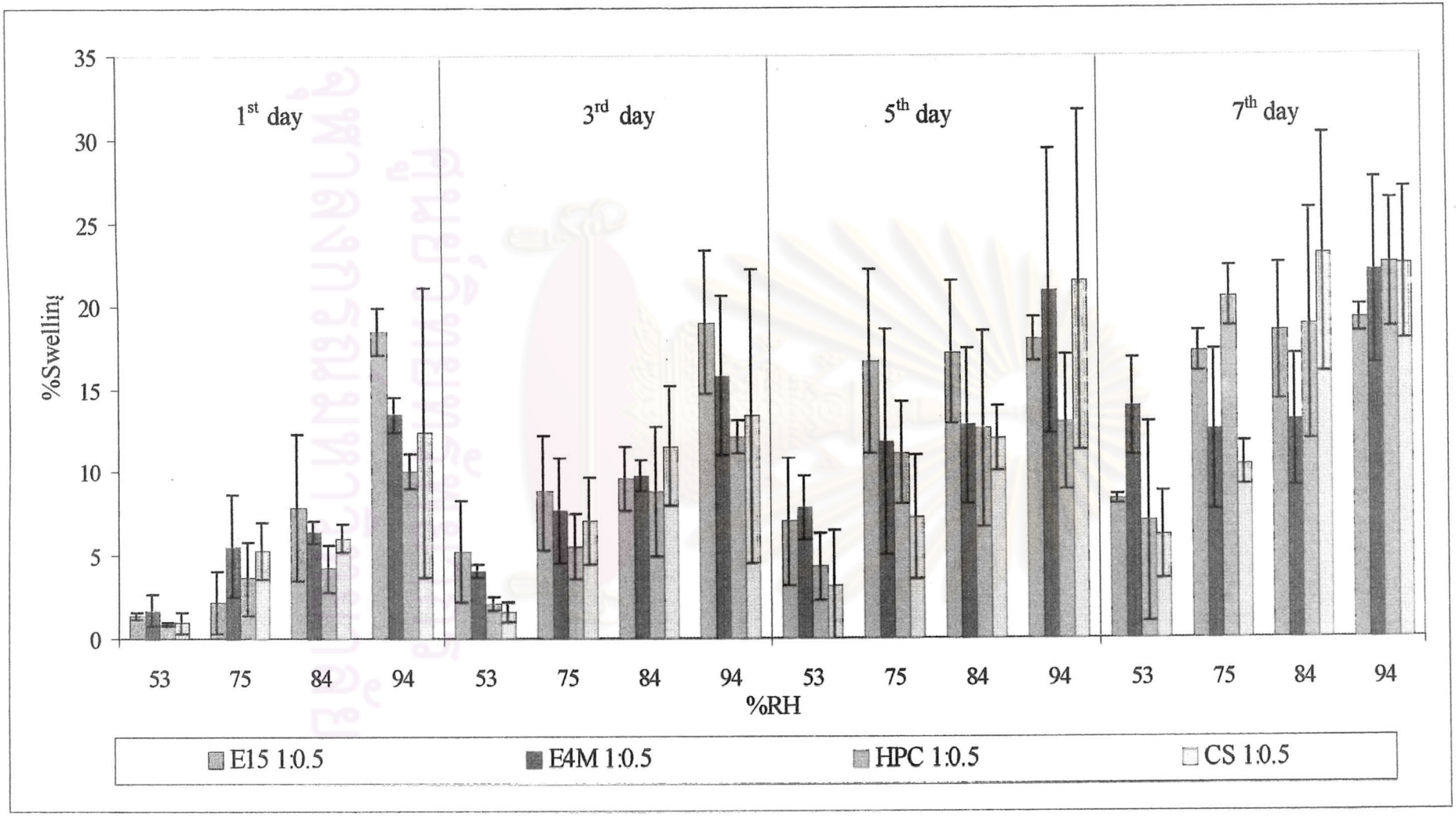

Figure 66 Percentage swelling of mucoadhesive films containing various polymers with drug to polymer ratio of 1:0.5

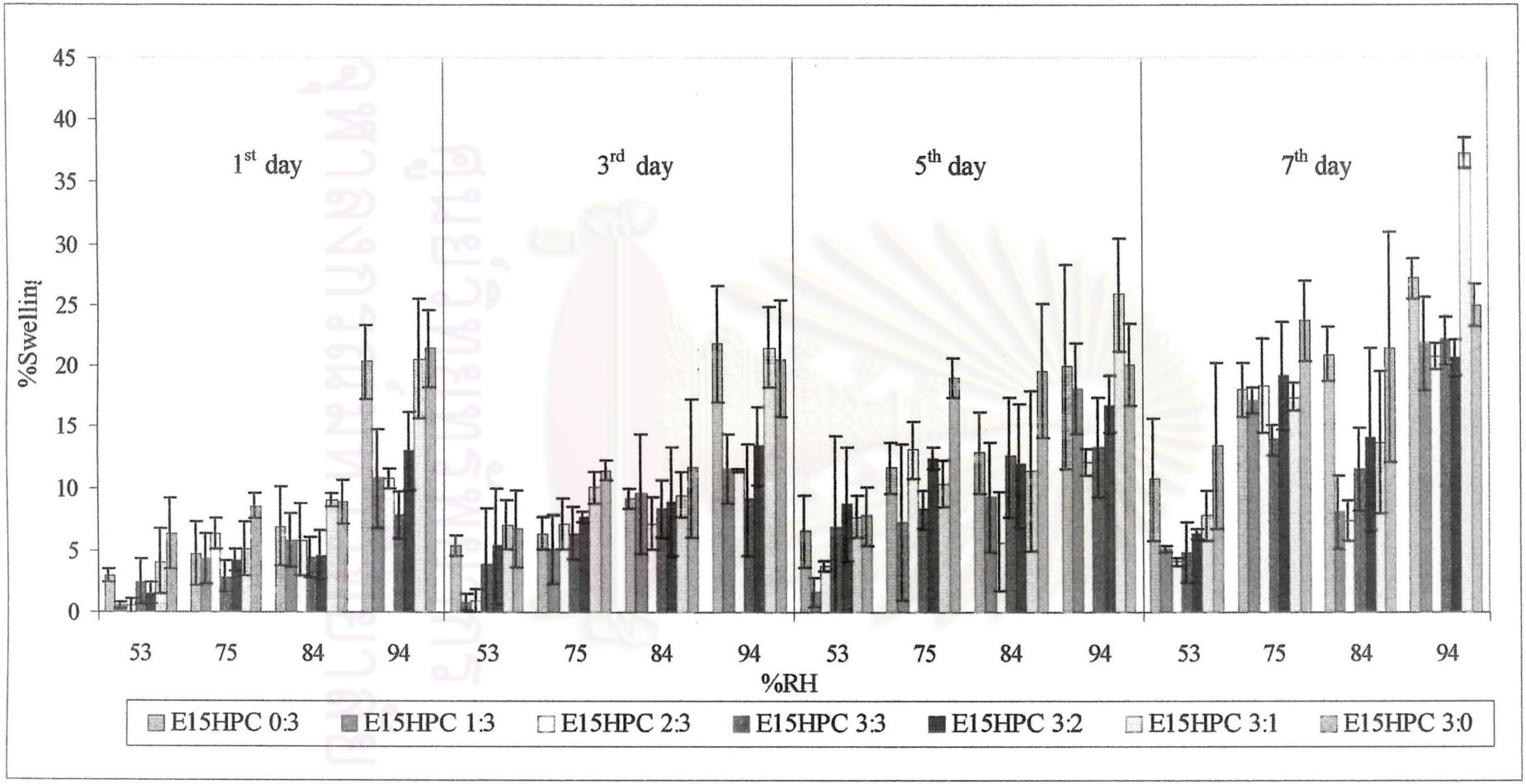

Figure 67 Percentage swelling of mucoadhesive films containing combination of HPMC E15 and HPC with drug to polymer ratio of 1:1

9. Mucoadhsive property

The mucoadhesiveness was determined in term of detachment force by measureing the force required to pull the test film, prehydrated with phosphate buffer pH 6.8 and attached on the aluminium flat surface (n=10). The detachment force results are present in Appendix C. Figure 68 shows the detachment forces of lidocaine HCl mucoadhesive films containing different polymers and ratio of drug to polymer. An increase in the drug content was associated with a corresponding decrease in detachment force. It can be inferred from Figure 68 that HPMC E15 achieved the highest value for detachment force, followed by HPMC E4M, HPC and chitosan in similar drug to polymer ratio, except for drug to polymer ratio of 1:1, chitosan film exhibited higher detachment force than HPC film.

From statistical test (Appendix D), the detachment force of HPMC E 15, HPMC E4M and HPC films, exhibited no significant difference ($p>0.05$) in every drug to polymer ratio. Chitosan film of drug to polymer ratio of 1:1, exhibited significantly different detachment force when compared with films of other drug to polymer ratios (CS 1:1 > CS 1:0.67 = CS 1:0.5) ($p<0.05$).

In the case of drug to polymer ratio of 1:1, the detachment force could be ranked as: HPMC E15 > HPMC E4M = chitosan > HPC ($p<0.05$). In the case of drug to polymer ratio of 1:0.67, the detachment force could be ranked as: HPMC E15 > HPMC E4M > HPC = chitosan ($p<0.05$). And in the case of drug to polymer ratio of 1:0.5, the detachment force could be ranked as: HPMC E15 > HPMC E4M = HPC > HPC = chitosan ($p<0.05$).

Figure 69 demonstrates that the detachment force increased with an increase in proportion of HPMC E15. The detachment force of mucoadhesive films with various ratio of HPMC E15 and HPC could be ranked as: HPMC E15 to HPC ratio of 3:0 > 3:1 > 3:2 > 3:3 > 2:3 > 1:3 > 0:3.

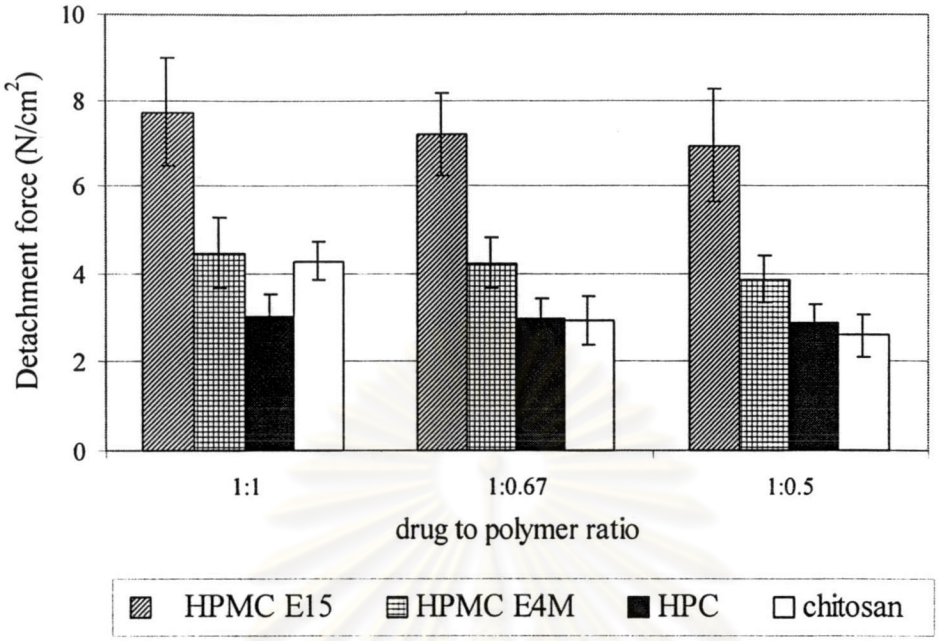

Figure 68 The detachment force of lidocaine HCl mucoadhesive films

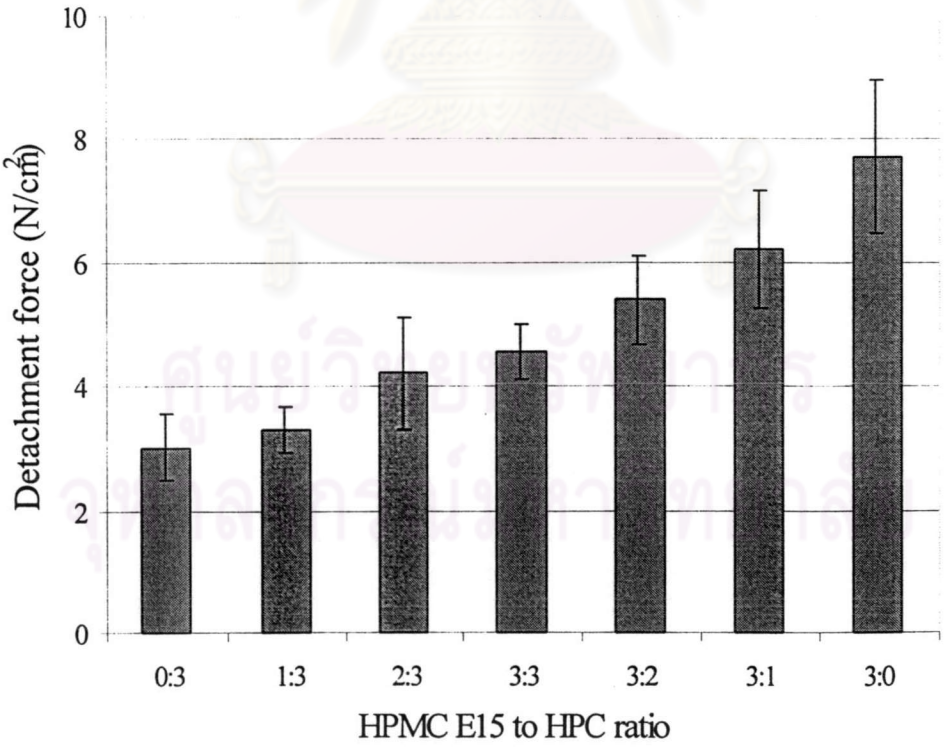

Figure 69 The detachment force of lidocaine HCl mucoadhesive films from combination of HPMC E15 and HPC at drug to polymer ratio of 1:1

10. In vitro drug release and penetration from the mucoadhesive films

In this study, five models of penetration kinetics: zero order, first order, Higuchi model, Weibull model and Korsmeyer-Peppas model (power law expression model) were used to assess the drug penetration model (Brazel and Peppas, 2000, Costa and Lobo, 2001 and Siepmann and Pappas, 2001). The equations for the drug penetration model are shown in Table 12.

Table 13 The penetration kinetic models

Model	Equation
Zero order	$Q_t = Q_0 + kt$
First order	$\mathrm{Ln}Q_t = \ln Q_0 + kt$
Higuchi	$Q_t = kt^{1/2}$
Weibull	$\log[-\ln(1 - Q_t/Q_\infty) = b \times \log t - \log a$
Power law expression (Korsmeyer-Peppas)	$Q_t/Q_\infty = kt^n$ $\ln Q_t/Q_\infty = \ln k + n \ln t$

Q_t was the amount of drug released in time t, Q_0 was the initial amount of drug in the solution (most times, $Q_0 = 0$), Q_∞ was the amount of drug penetrated at infinite time (which should be equal to the drug incorporated within the pharmaceutical dosage form at time $t = 0$).

The plots of these kinetic models of each preparation were constructed. The higher coefficient of determination (R^2) was accepted as the model for drug penetration.

The concentration of lidocaine hydrochloride saturated solution used in drug penetration study was 691.04 mg/ml. The drug was rapidly penetrated through dialysis membrane into pH 6.8 phosphate buffer. About 6.4 mg of the drug, equal to 80% of the drug loading in the mucoadhesive films (8 mg/cm^2), was penetrated within 27 minutes. The penetration-time profile of lidocaine hydrochloride saturated solution is shown in Figure 70. However, it was found

that the drug penetration rate from saturated solution was fast. Its penetration kinetic was fitted to both zero order ($R^2 = 0.9988$) and the power expression model ($R^2 = 0.9988$).

The drug penetration data in this study are presented in Appendix C. The penetration-time profiles of lidocaine HCl mucoadhesive films are shown in Figures 71-75. Eighty percent of drug loaded in the films was released from HPMC E15, HPMC E4M and HPC within 60 minutes. While release of drug from chitosan films were more sustained. Figures 71-74 shows the penetration-time profiles of mucoadhesive films with different drug loading which were prepared from different polymers, HPMC E15, HPMC E4M, HPC and chitosan, respectively. As shown in Figures 71-74, the release and penetration of the drug through dialysis membrane slightly increased with the increasing of drug to polymer ratios. When tested with two-way ANOVA, statistical significant difference of penetration-time profile was not observed between the same polymer in various ratio of drug and polymer except chitosan films which were significantly different between Formulas CS1:1, CS1:0.67 and CS 1:0.5.

The influence of the ratio of combination polymers on the in vitro penetration of drug through dialysis membrane was carried out. The drug penetration data were presented in Appendix C. Formula E15HPC 3:3 exhibited higher drug penetration than the HPMC E15 to HPC ratios of 1:3, 2:3, 3:2, 3:1 and 3:0 but showed no significantly different when compared upon the ratio of 0:3 ($p < 0.05$) as shown in Figure 75.

As shown in Figures 76-78, the penetration-time profiles of mucoadhesive films of different polymers at the same drug to polymer ratio were observed. HPC films exhibited the highest drug release and penetration. And chitosan films showed the slowest. When test with two-way ANOVA, statistical significant differences were observed ($p < 0.05$) except between the penetration from Formulas E15 1:1 and HPC 1:1.

As shown in Figures 79 and 80, the penetration-time profiles of the HPMC E4M mucoadhesive films of different drug loading at the same drug to polymer ratio were observed. About 7.10 mg/cm^2 and 13.43 mg/cm^2 of the drug were

penetrated through dialysis membrane within 60 minutes from the Formula E4M 1:0.5 and E4M 2:1, respectively. Figure 80 revealed that Formula E4M 2:1 displayed slower release and penetration through dialysis membrane than E4M 1:0.5 in term of percentage of cumulative amount.

The release of lidocaine HCl mucoadhesive films without dialysis membrane is shown in Figure 81. Statistically significant difference was observed by two-way ANOVA ($p < 0.05$) that the release-time profiles of the drug from chitosan films were significant different when compared with other formulas. The influence of various grades of HPMC also showed significant difference in release of the drug when tested with two-way ANOVA. HPMC E15 films showed higher drug release profile than films of HPMC E4M. Therefore, higher drug release profile was observed with lower viscosity grade of HPMC.

Coefficient of determinations and kinetic constants of the penetration kinetic models of lidocaine HCl through dialysis membrane are summarized in Tables 13 and 14. The highest correlation of determination of linear regression relationship, except Weibull model, were observed when plotted as amount of drug penetrated versus square root time, or Higuchi model indicating a linear penetration profile, a behavior typical of a homogeneous matrix system. When treated with power law equation to all formulas, anomalous penetration profiles were observed ($0.5 < n < 1$).

When treated with Weibull model to all formulas, the highest coefficients of determination were observed. The results indicated that there was not any single parameter related with the intrinsic penetration rate of drug.

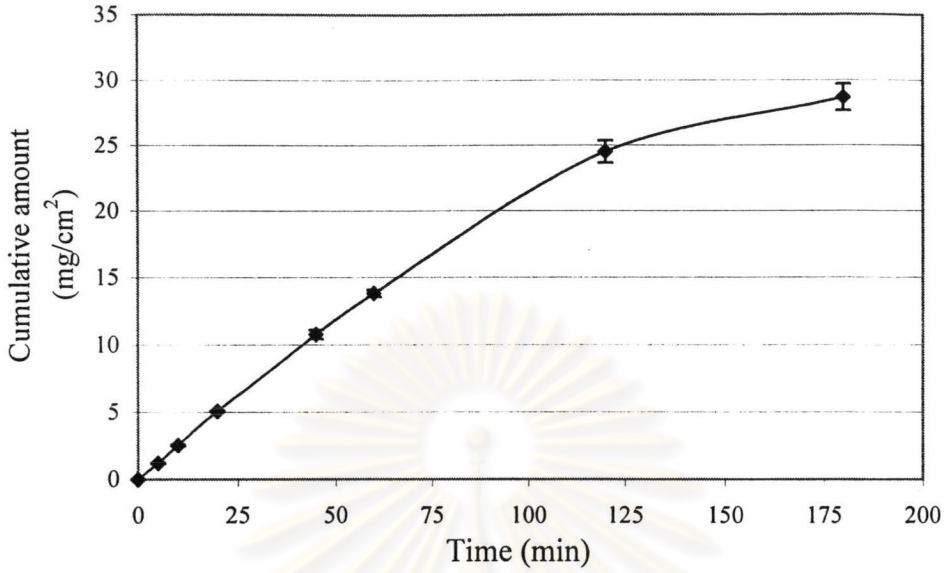

Figure 70 The penetration-time profile of lidocaine HCl saturated solution through dialysis membrane

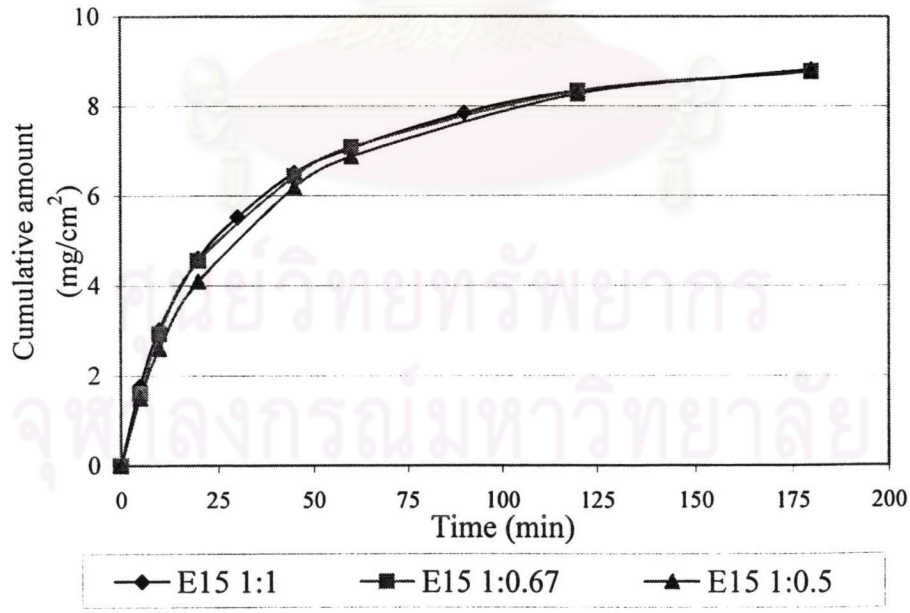

Figure 71 Effect of drug concentration on penetration of lidocaine HCl from HPMC E15 films through dialysis membrane (n=3)

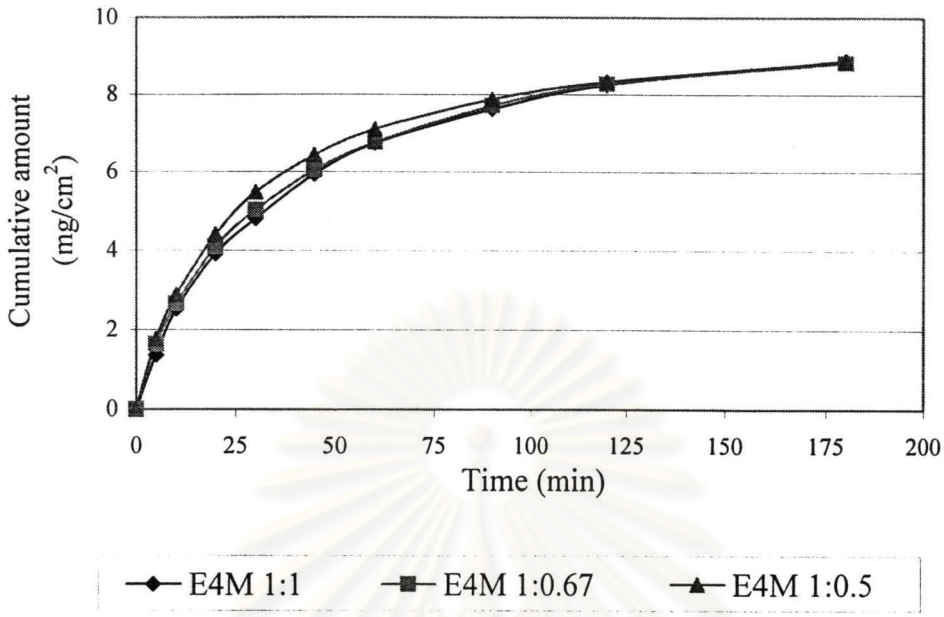

Figure 72 Effect of drug concentration on penetration of lidocaine HCl from HPMC E4M films through dialysis membrane (n=3)

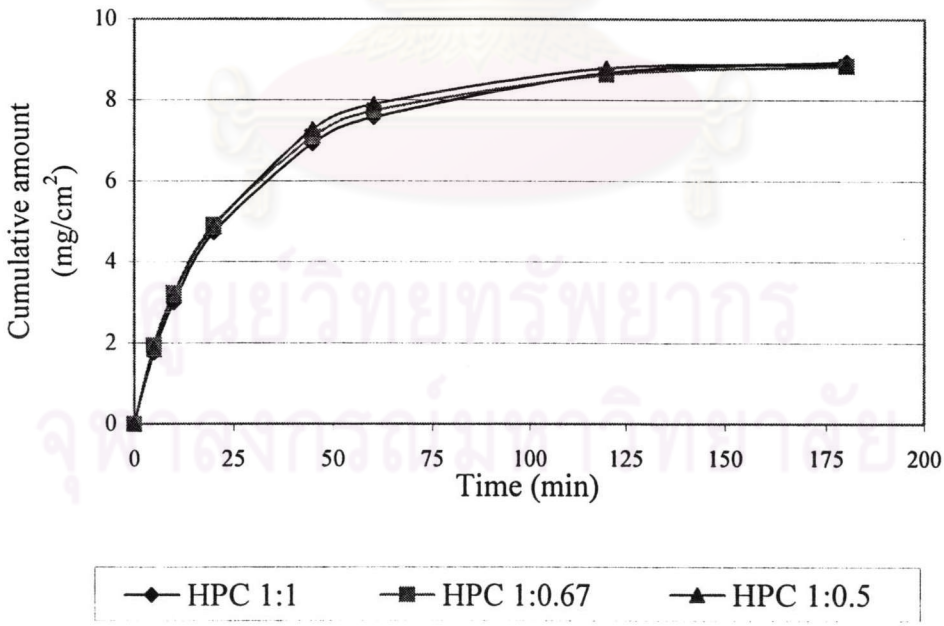

Figure 73 Effect of drug concentration on penetration of lidocaine HCl from HPC films through dialysis membrane (n=3)

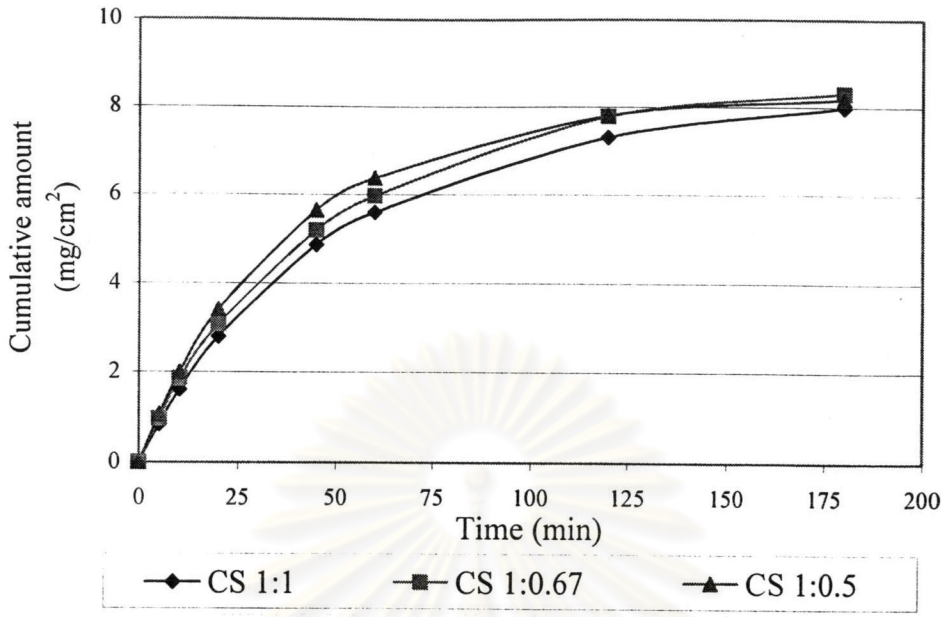

Figure 74 Effect of drug concentration on penetration of lidocaine HCl from chitosan films through dialysis membrane (n=3)

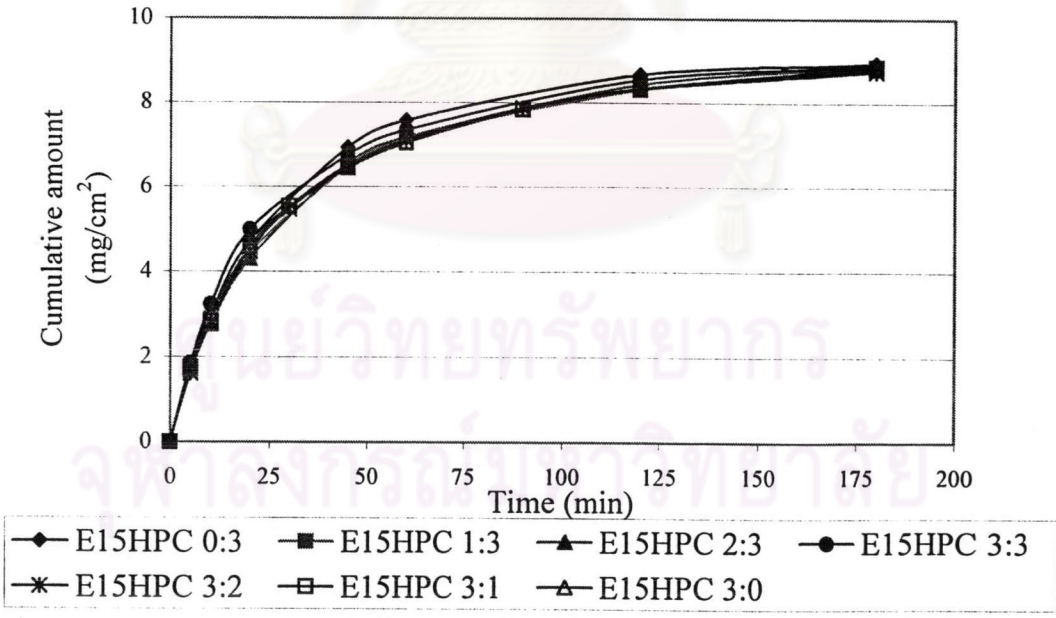

Figure 75 Effect of various ratio of polymer on penetration of lidocaine HCl from combination of HPMC E15 and HPC films through dialysis membrane (n=3)

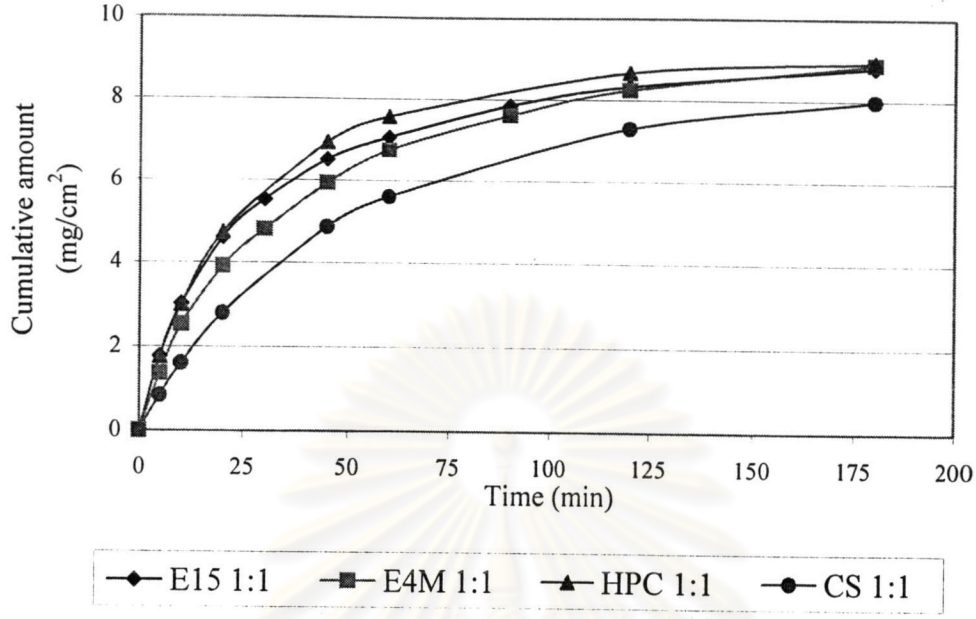

Figure 76 Effect of various polymer on penetration of lidocaine HCl through dialysis membrane at drug to polymer ratio of 1:1 (n=3)

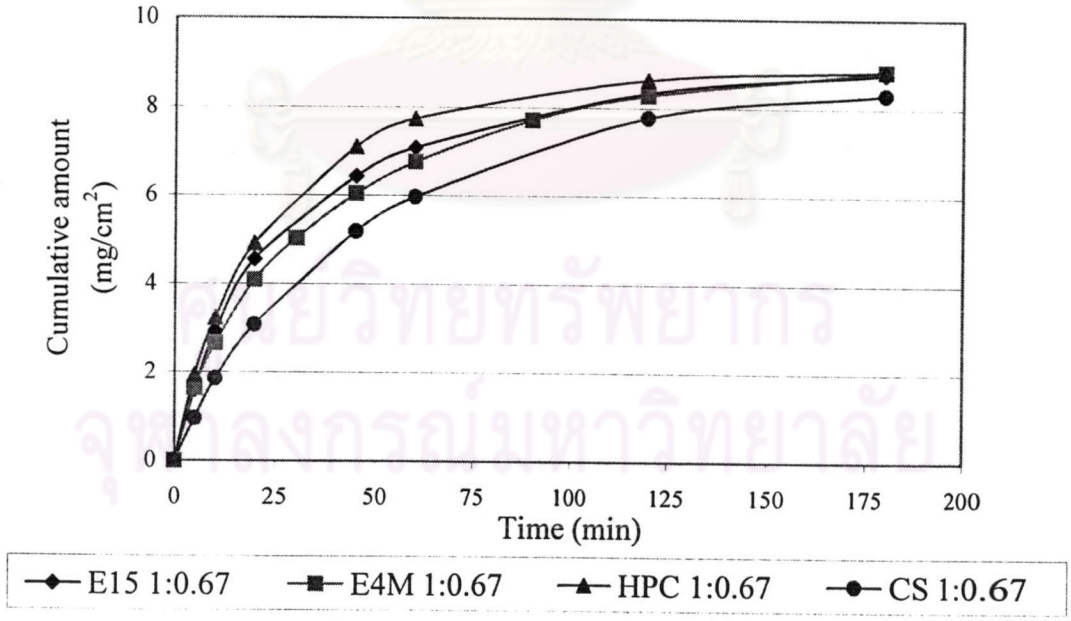

Figure 77 Effect of various polymer on penetration of lidocaine HCl through dialysis membrane at drug to polymer ratio of 1:0.67 (n=3)

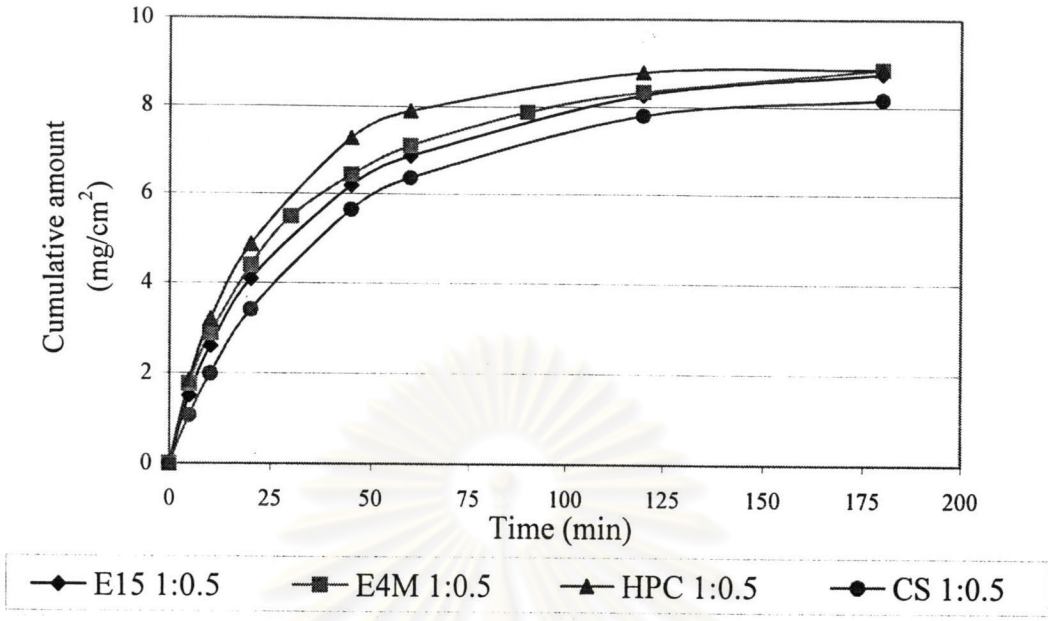

Figure 78 Effect of various polymer on penetration of lidocaine HCl through dialysis membrane at drug to polymer ratio of 1:0.5 (n=3)

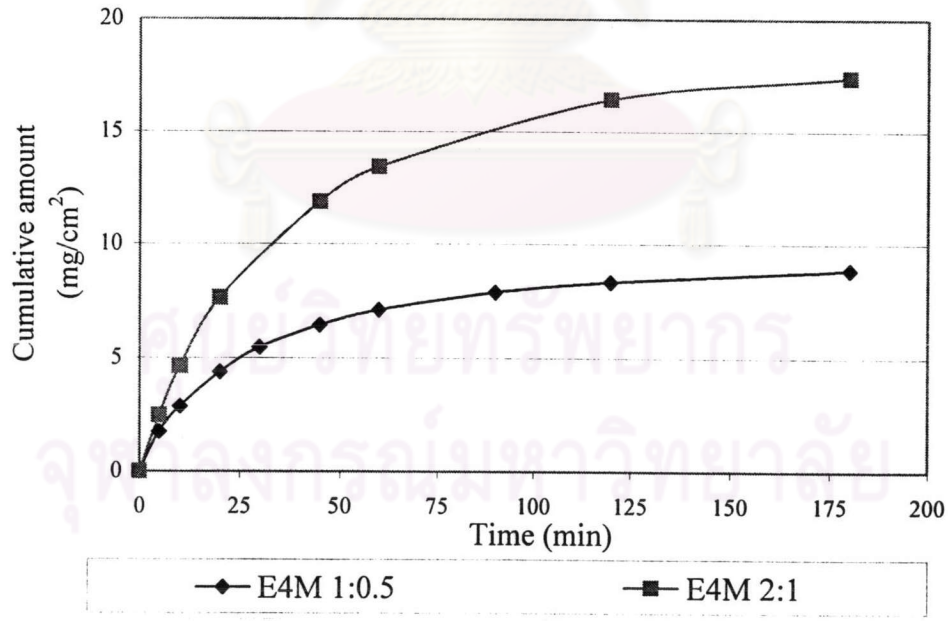

Figure 79 Effect of various drug loading in HPMC E4M mucoadhesive films on penetration of lidocaine HCl (n=3)

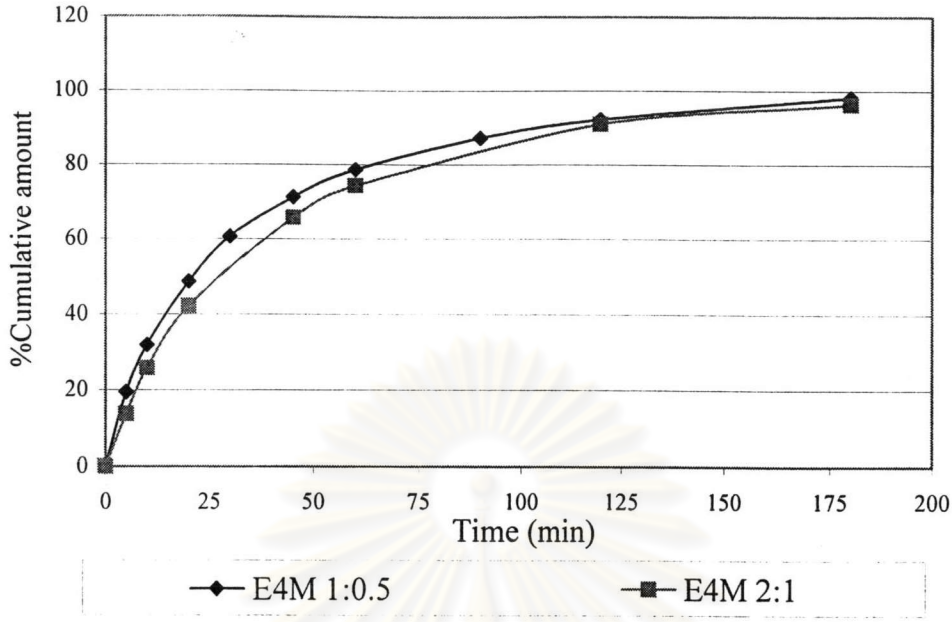

Figure 80 Effect of various drug loading in HPMC E4M mucoadhesive films on penetration of lidocaine HCl (n=3)

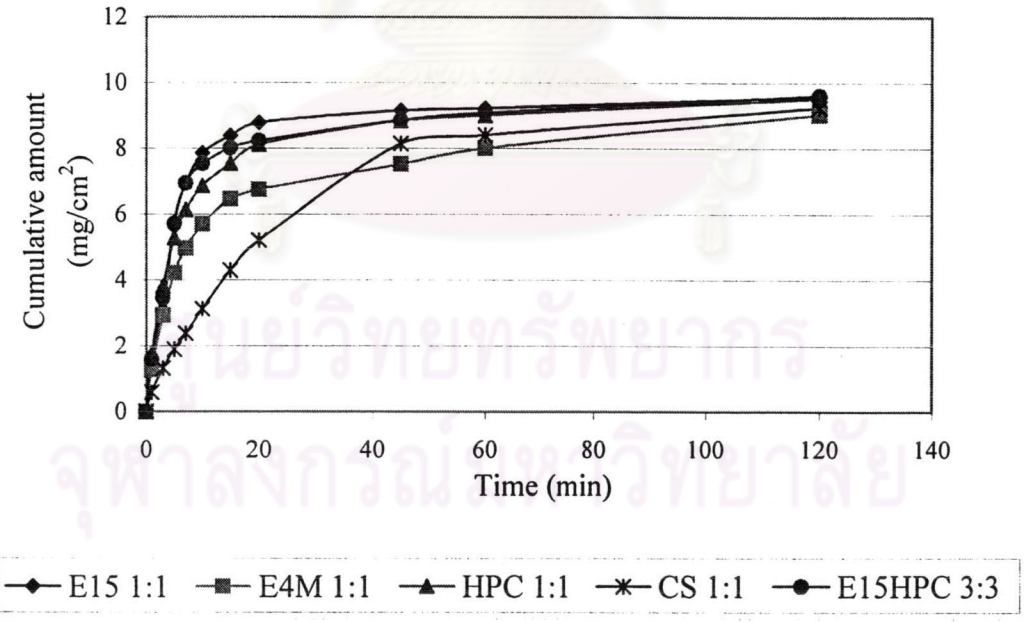

Figure 81 The release-time profiles of lidocaine HCl (without dialysis membrane)

Table 14 The coefficients of determination, kinetic constants and diffusion exponent of lidocaine HCl penetrated through dialysis membrane from mucoadhesive films

Formula	Zero order		First order		Higuchi model		Weibull model	
	R^2	k	R^2	k	R^2	k	R^2	k
saturated solution	0.9989	718.33	0.9988	0.9934	0.9885	6799.3	0.9997	1.0490
E15 1:1	0.9380	0.2314	0.9848	0.5935	0.9886	2.1384	0.9977	0.8016
E15 1:0.67	0.9315	0.2276	0.9750	0.6282	0.9844	2.1465	0.9937	0.8396
E15 1:0.5	0.9613	0.2249	0.9899	0.6431	0.9965	2.1009	0.9992	0.8401
E4M 1:1	0.9568	0.2221	0.9854	0.6626	0.9955	2.0397	0.9962	0.8421
E4M 1:0.67	0.9579	0.2174	0.9939	0.5966	0.9961	1.9956	0.9998	0.7773
E4M 1:0.5	0.9499	0.2315	0.9917	0.5960	0.9932	2.1309	0.9996	0.8000
E4M 2:1	0.9631	0.4514	0.9862	0.7111	0.9971	4.2140	0.9976	0.8996
HPC 1:1	0.9528	0.2473	0.9880	0.6235	0.9935	2.3168	0.9997	0.8670
HPC 1:0.67	0.9505	0.2456	0.9882	0.5887	0.9928	2.3027	0.9999	0.8404
HPC 1:0.5	0.9583	0.2588	0.9882	0.6199	0.9956	2.4202	0.9994	0.8895
CS 1:1	0.9776	0.1726	0.9928	0.7615	0.9990	1.7707	0.9991	0.9230
CS 1:0.67	0.9747	0.1796	0.9906	0.7268	0.9990	1.8451	0.9956	0.9030
CS 1:0.5	0.9682	0.1914	0.9901	0.7142	0.9974	1.9710	0.9991	0.9162
E15HPC 1:3	0.9502	0.2274	0.9866	0.6084	0.9927	2.1324	0.9987	0.8187
E15HPC 2:3	0.9677	0.2355	0.9941	0.6210	0.9983	2.1941	0.9999	0.8377
E15HPC 3:3	0.9155	0.2296	0.9722	0.5858	0.9759	2.1744	0.9933	0.8138
E15HPC 3:2	0.9422	0.5390	0.9858	0.6355	0.9904	2.2060	0.9980	0.8463
E15HPC 3:1	0.9356	0.2331	0.9856	0.6047	0.9866	2.1548	0.9976	0.8119

calculate from time range of 5-45 minutes

R^2 was coefficient of determination and k was correlation constant.

Table 14 The coefficients of determination, kinetic constants and diffusion exponent of lidocaine HCl penetrated through dialysis membrane from mucoadhesive films (Cont.)

Formula	Power law expression model		
	R^2	n	k
saturated solution	0.9988	0.9934	0.9934
E15 1:1	0.9904	0.6378	0.0731
E15 1:0.67	0.9925	0.7514	0.0545
E15 1:0.5	0.9970	0.7236	0.0527
E4M 1:1	0.9868	0.7026	0.0514
E4M 1:0.67	0.9971	0.6275	0.0677
E4M 1:0.5	0.9970	0.6342	0.0718
E4M 2:1	0.9951	0.9121	0.0315
HPC 1:1	0.9980	0.7114	0.0629
HPC 1:0.67	0.9969	0.6690	0.0744
HPC 1:0.5	0.9939	0.6986	0.0679
CS 1:1	0.9946	0.7969	0.0271
CS 1:0.67	0.9916	0.7611	0.0333
CS 1:0.5	0.9981	0.8368	0.0312
E15HPC 1:3	0.9961	0.6961	0.0622
E15HPC 2:3	0.9985	0.6808	0.0627
E15HPC 3:3	0.9949	0.7110	0.0670
E15HPC 3:2	0.9926	0.6846	0.0618
E15HPC 3:1	0.9959	0.6525	0.0691

Calculate from $Q_t/Q_\infty < 0.6$

R^2 was coefficient of determination, k was correlation constant, and n was diffusion exponent.